ANL-6695

This is applicable to EBR II

mu

Argonne National Laboratory

TIME-OPTIMUM CONTROL OF NUCLEAR REACTORS WITH VELOCITY-LIMITED CONTROL DEVICES

by

Thomas P. Mulcahey

ANL-6695
Reactor Technology
(TID-4500, 26th Ed.)
AEC Research and
Development Report

ARGONNE NATIONAL LABORATORY
9700 South Cass Avenue
Argonne, Illinois 60440

TIME-OPTIMUM CONTROL OF NUCLEAR REACTORS WITH VELOCITY-LIMITED CONTROL DEVICES

by

Thomas P. Mulcahey

Reactor Engineering Division

Based on a thesis submitted to the
Faculty of Purdue University
in partial fulfillment of the
requirements for the degree of
Doctor of Philosophy

October 1963

Operated by The University of Chicago
under
Contract W-31-109-eng-38
with the
U.S. Atomic Energy Commission

TABLE OF CONTENTS

TABLE OF CONTENTS

LIST OF FIGURES

LIST OF FIGURES

LIST OF TABLES

LIST OF TABLES

TIME-OPTIMUM CONTROL OF NUCLEAR REACTORS WITH VELOCITY-LIMITED CONTROL DEVICES

by

Thomas P. Mulcahey

ABSTRACT

In today's world of bigger and better mouse traps, the trend toward complete automation is brought about by several factors, three of which are economics, safety, and speed of response. The problem undertaken here is to devise a time-optimum automatic controller for a nuclear power reactor which should be consistent with the safety policies of the Atomic Energy Commission.

An automatic controller designed to be "fail-safe" and time optimum in its response is then justified as being economic if its presence manages to eliminate one serious accident which might otherwise have occurred or if better utilization of the power plant is obtained.

Since there is no single controller that will give optimum response to all reactor systems, a particular model of a reactor is established. It is based on the power system of the fast reactor EBR-II. In the model used, the coolant flow rate is assumed to be approximately linear with power. The resultant power reactivity feedback then assumes the approximate form of the natural logarithm of the power. The model of the control devices assumes a ramp rate of reactivity insertion for changes of power level.

In order to establish the method of operation of the desired controller, three main methods of analysis were used. The first involved the analytical solution of the fast reactor kinetics equations with one group of delayed neutrons and a feedback proportional to the natural logarithm of the power. In the general development of the analytical solution, a stage is reached where other solutions are possible for reactivity feedback expressions other than the natural logarithm of the power. One such possibility involves the logarithm plus the square root of the logarithm of the power, but since it was not of direct interest, it was not fully developed. Another possibility reduces to a form which can be found in the literature.

The second method involved the analog computer simulation of the six-group delayed-neutron kinetics equations with feedback. The effects of feedback delay time constants were investigated with this method.

The third method consisted of the solution of the one-group and six-group delayed-neutron kinetics equations with feedback by use of a digital

computer. This method was used as a measure of the range of validity of the analytical solution and as a means of improved accuracy over results obtained with the analog computer.

The results that are obtained from the analyses indicate that the one-group analytical solution can predict the final power levels for a particular transient and, as such, could be used to obtain design information for an optimum controller which uses as its basis of operation the measurement of elapsed time.

The six-group solution methods not only enable a prediction of the final powers but the transients, and, as such, should be the methods used in producing the information necessary for a design of an optimum controller which uses as its basis of operation the measurement of power level.

For reasons of safety, it is concluded that the power level based controller is the one that should be adopted; thus, the methods involving the six-group delayed neutrons were used to establish characteristic percent overshoot values. During a transient, these percent overshoot values are applied to the new desired power level to determine when reversal of the control element should take place. In the model of the proposed controller, the generated percent overshoot values are added to the new power level reference value to give a fictitious power level reference for the controller. Upon attaining the new fictitious power level value, the overshoot generator is switched off and the controller then converges on the new desired power level value.

I. INTRODUCTION

The design of control systems for nuclear reactors is a large and everchanging subject in which the best methods of control for a particular reactor may be dictated by the type and use of the reactor. But any method chosen for control must meet the overall governing philosophy of "super-safe operation" as established and enforced by regulations of the U. S. Atomic Energy Commission.

Even for reactors of the same type and use, there may be differences in methods and types of control. Information from earlier models or prototypes is used in improving the design characteristics of later models so that better economy or better performance is achieved.

At the present time, the development of reactor control systems is in the "semi-automatic" stage, in that some functions of reactor control are completely automatic while others are strictly manual. This is especially true for research reactors, training reactors, and small power reactors, for which there is some degree of automation in maintaining a power level once

it has been reached by manual control procedures. For most of the larger, high-power reactors under construction, plans require complete automatic control during power-level changes. Although the controls will be automatic, the usual plans call for rates of response that are slow in comparison to the rates at which the reactors are capable of performing, thus allowing errors to exist in the desired output for short periods of time. The exceptions to these slow response rates in the high-power reactors are the power plants associated with the nuclear rocket propulsion systems. Although these projects are of a classified nature, it is apparent by their very nature that in these systems, the propellant utilization factors must be taken into account; any waste of propellant while increasing the power up to the operating point must be paid for by decreased operating time or performance.

In still another class of reactors, such as for military purposes, the economy of operation is not as important a factor as the performance characteristics of the system. In military reactors, the full power output may be demanded on a very short notice. As a result, a military reactor may be operated at full power at all times and the excess power above that actually needed dumped by a bypass system. A control system capable of very rapid changes might be very useful, not only for performance reasons as in the case of rockets, but for economic reasons, such as increasing the core lifetime in a nuclear submarine.

The only conceivable control system that would be acceptable for controlling a fast-response reactor system such as for a rocket or properly utilized military power plant would be a completely automated one. Complete automation of control systems is desirable also in other fields not connected with the military or space applications. In the operation of modern electric-power-generating plants, both conventional and nuclear, the trend is to automate all of the controls that are necessary for normal operations. The automation serves several functions, one of which is the removal of the plant operation from human error by the inclusion of fail-safe automatic controls. This is a safety feature as well as an economic feature in that under fail-safe automatic operation, any potentially dangerous situation can be rapidly recognized and avoided.

Any down time caused by human error or failure of a control component can be very expensive; damaged equipment due to human error may cause long periods of inactivity. Thus, on an economic level, complete automation may pay for itself many-fold during the periods of operation.

In order to perform the task of complete automation, the dynamic characteristics of the particular system under study must be known. Since the only way to "know" a nuclear system is through actual operation and measurement of the necessary parameters, any work performed on an automatic control system for an untried reactor power plant system is based only on an educated guess. In the case of a reactor, the unknown quantity is the mechanism of reactivity feedback. This mechanism and the kinetics equations will determine the dynamic response of the reactor.

In general, two basic approaches are used to obtain the desired reactor responses for changing power-level demands. The first is to design into the reactor, itself, feedback characteristics which accomplish the desired control. An example of such a system would be the molten-salt Aircraft Reactor Experiment, for which the reactor temperature coefficient was such that the reactor maintained essentially a constant outlet temperature regardless of the power demand. Here, more power could be obtained simply by increasing the extraction of heat from the circulating molten salts.

The second method, the one most generally used, consists of the insertion or extraction of reactivity by means of control devices that either contain nuclear poisons or fuel, or that change the geometry factors of the reactor.

The first method of control, although highly desirable, has not been put into general use because of the difficulty in obtaining design feedback characteristics and because of the conflict in purposes of reactor design. The second method allows more flexibility in the design and operation of the reactor and, as a result, is considered the conventional one.

Most power reactors use either the insertion of fuel or poisons as the main source of control. The control devices move in or out of the core area to establish a power change within the reactor.

Based on the physics calculations alone, reactors are capable of changing power levels extremely rapidly if sufficient excess reactivity is available. Thus, the control of reactors during transients is based on control of the excess reactivity present within the core. The excess reactivity is dependent on the difference between the reactivity inserted by the control device and the feedback reactivity generated by internal changes within the core. The faster the control device moves, the more excess reactivity there will be in the core and the faster the power will change.

One of the main safety difficulties in changing the power level of a reactor by a large factor in a short time is the generation of thermal stresses within the core. If the rate of change of power is restricted to values below which the generation of thermal stress is no longer a problem, then the only other major safety problem is that of maintaining the power level below the maximum permissible level.

As long as a reactor controller (manual or automatic) operates within the range of the safety limitations, the control problem in changing operating power levels from one desired level to another is one of establishing the two following items:

1. the rates of reactivity insertion;
2. the time integral of these rates or the total reactivity that must be added to achieve the desired change.

Since the rates or the range of rates of reactivity insertion are fixed during the design and construction stage, the problem of achieving power level changes is in knowing when to start and stop the reactivity changes. These start and stop times are called switching points. If, in the design of an automatic controller, the switching points can be selected to obtain a minimum time between the leaving of one steady-state power level and the arrival at another, the controller will be a form of optimum controller.

In this investigation, an attempt was made to combine the ideas of fully automatic control and time-optimum control to a power reactor. The Experimental Breeder Reactor-II (EBR-II), presently being completed at a National Reactor Testing Station Site in Idaho, was chosen as a model. A reactivity-feedback model of the reactor under normal planned operation (see Appendix C) was developed and combined with the fast reactor kinetics equations to produce a method of operation and the requirements for a minimum time controller. Since the model is that of the EBR-II, the on-off characteristic of the control rod drive motors (see Appendix B) restricts the method of operation of the proposed optimum controller to that of the on-off type. The method proposed for achieving the desired optimum response is not proven mathematically to give the time minimum trajectory between operating power levels, but since it utilizes the principal of applying the maximum available acceleration and then the maximum available deceleration to the rate of change in power, it can intuitively be considered the optimum. Since the controller will be of the on-off type, the inherent dead zone may allow an error in power level to occur, but this error can be adjusted by control of the dead-zone bandwidth to achieve any desired degree of accuracy.

An example of the operation of the proposed controller is as follows.

Assume a reactor is operating at a steady-state power level and a signal is received to increase the power level of operation to a new, higher value. The controller then starts inserting reactivity at a ramp rate by control of one or a sequence of single control elements. The reactivity continues to increase until the criteria set up for the reversal time of the control element have been reached. The controller will then reverse the control element and thus decrease the excess reactivity until the criteria for the shut-off point have been reached. (The process could conceivably continue for more than two switch points, but for simplicity, it will be assumed that two are sufficient.) At the end of the reactivity-reversal period (time of the second switch point), the control element will be stopped and the reactor should be within a fixed percentage error of the new desired power level. Figure 1 illustrates this action.

Two main bases can be used as the criteria for the switching points. The first is a time base whereby the movements of the control elements would be based on a specified time interval for reactivity insertion and a

specified time interval for reactivity withdrawal to achieve the desired power level change. The main disadvantage of this basis is that the controller loses contact with the actual changes taking place within the reactor, and any slight change in reactor parameters may cause large errors in the final power.

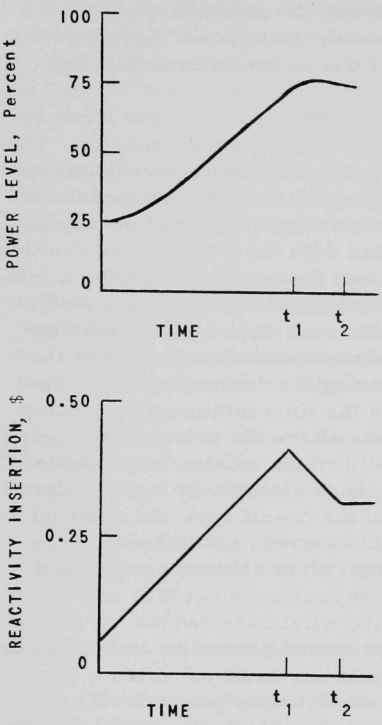

Fig. 1. Optimum Controller Action

The second basis that could be utilized for the switching criteria is that of measurement of power level. For this basis, the reactivity would be inserted for the length of time necessary to achieve a predetermined power level and then reversed until the power level has attained the new, desired state. The predetermined power level at which the reactivity reversal occurs may, and in all probability will, be different than the new, desired steady-state power level.

The purposes of this investigation will be to determine which of the bases for switching should be used and try to establish the relationships between (1) the switch times and the changes of power level; and (2) the switching power levels and the changes of power level.

To acquire the design information for the minimum time controller, three main methods of analysis were used. The first was to obtain an analytical expression for the one-group fast-reactor kinetics equations with feedback. This method is basically limited to the range of conditions or restrictions for which any one-group solution is valid. This procedure also involves other assumptions and simplifications which must, of necessity, be checked by other means. The second method consisted of an analog computer simulation of the kinetics equations to establish the effects of feedback-delay time constants and to investigate the relationship between the switching conditions and the initial and final conditions. (The analog computer presents a graphic representation of the operation of the reactor under varying conditions.) The third method was used as both a form of verification and definition of the range of validity of the assumptions made in the analytical solution, and as a method for accurate computation of the six-group delayed-neutron reactor kinetics equations with feedback. It consists of the use of

an existing digital computer program for the solution of the general kinetics equations. The accuracy capability of the digital computer are needed in the investigation of the relationships involved between the switching-point power levels and the initial and final power levels.

This investigation, although applicable to other reactors, was originally an outgrowth of a preliminary analysis of the EBR-II power-plant system (see Appendix A) to determine the control parameters and their approximate values at different power levels, and the sequence of control of the different power transfer loops involved.

The next section of this report is devoted to a survey of the literature dealing with the kinetics equations with feedback and their possible analytical solutions.

The following three sections consist of the solutions to the kinetics equations by the three principal methods outlined previously and an adaptation of the analytical solution to take into account the switching of the reactivity at the designated switching points.

Each of the solution methods assumes a ramp input of reactivity and a "logarithm of the power level" feedback except for two subsections under the analytical derivation. One of these is a solution to the zero-power kinetics, and the other assumes essentially a step input to the "log" feedback model.

The last two sections consist of the conclusions and the proposed controller design, and the generalized results.

II. REVIEW OF THE LITERATURE

The reactor transient equations were published for the first time by L. W. Nordheim[1] in 1946. Since then many more elegant approaches have been presented, such as that by Harry Soodak.[2] Also, since their origin, the usefulness of these equations has been improved by the accurate measurement of the delayed-neutron parameters. The first of these improvements was made in 1948 by D. J. Hughes[3] and the second in 1958 by G. R. Keepin and T. F. Wimett.[4] The data presented by G. R. Keepin and T. F. Wimett also indicated that there were only six important delay groups that needed to be considered for normal transients. But, due to the complexities involved in using these six groups, the one-group simplifying approximation is still in common usage and in all probability will continue to be used.

There is another simplifying maneuver which can be performed that in some respects is comparable to the one-group approximation. It consists of averaging the lifetimes of the delayed neutrons with those of the prompt neutrons. The averaged lifetime is then used as a method of eliminating the need for carrying the delayed-neutron fraction terms in the basic differential equation governing the growth and decay of the neutron population. This simplification, however, can only be used for slow transients where there would be enough time for all the delayed neutrons to contribute to the average lifetime.[5]

Many analytical solutions and approximations to the six-group and simplified forms of the kinetics equations have appeared. The large majority of these have been prepared from the linearized equations and, as a result, do not consider any feedback-reactivity mechanisms that might be present during power range transients.

Of the publications that consider feedback mechanisms in conjunction with the kinetic equations, the large majority involve the use of either an analog or a digital computer for simulation or analysis. Under the present "state of the art," these forms of analysis are justified in that they are the only ones that give answers in a reasonable time. It must be pointed out that there is no general feedback mechanism applicable to all reactors. In fact, very little work has been done in correlating feedback mechanisms between reactors of the same type; the exception to this deals with Boiling Water Reactors.[6] There are many reactor kinetics codes available. Most of these are listed in the various computer code abstracting publications.

Since one of the main approaches used in developing a solution to the problem of the design of a minimum time controller for a power range reactor is an analytical one and since the methods of analog and digital computer simulation are well documented elsewhere, only those few publications considering analytical developments of the kinetics equations

involving feedback-reactivity mechanisms are of interest and will be reviewed. For a summary of the other aspects in the analytical development of the kinetics equations, including a discussion on stability, the reader is referred to H. B. Smets.[7]

The reactor models considered up to this time in conjunction with analytical treatments of the kinetics equations fall into four categories depending upon the postulated scheme for power extraction. Each scheme is based on the assumption that the reactivity feedback is proportional to the temperature of the reactor.* The four possibilities for power extraction are as follows:

1. adiabatic, i.e., no power removal;
2. Newton's Law of Cooling, i.e., power removal is proportional to the temperature difference between coolant and fuel and assuming no flow changes;
3. constant-power extraction;
4. circulating-fuel reactors.

The adiabatic model is usually considered as a separate entity, but it could be considered as a special case of both the Newton's Law of Cooling model and the constant-power extraction model in which the flow is zero. Fuchs and Nordheim developed the model independently for rapid transients. A law that was also stated in connection with this model requires that the temperature feedback reactivity generated in an excursion be twice that required to cancel the added reactivity.

In 1949 H. Soodak[8] obtained an approximate solution assuming that the feedback reactivity was a linear function of temperature and that cooling was proportional to the reactor temperature. The input reactivity assumed was a step function, and the solution was obtained by linearization of the kinetics equations. J. Chernick[9] also used Newton's Law of Cooling, but neglected to specify as to whether he was including the effect of the delayed neutrons in the average lifetime. R. S. Margulies[10] expanded on the work of J. Chernick by considering the delayed neutrons. He also applied what amounts to an initial step increase in reactivity at time zero.

W. K. Ergen[11] and later J. MacPhee[12] presented an analysis of a circulating-fuel reactor. J. M. Stein[13] worked on the constant-power extraction model.

---

*The models utilizing other forms of feedback such as fuel element bowing and void or bubble formation are again only solvable by computers. Early work in this realm by J. M. Stein and later work by J. A. Thie[6] may be found in the literature.

In 1959 H. B. Smets[14,15] presented a topological method for attacking the adiabatic, constant-power-removal, and Newton's Law of Cooling models, using step and linear reactivity variations.

An analytical approach which holds promise for design of control systems in which a particular power-level trajectory is desired was presented by C. R. Bingham[16] in 1961. The approach used here was to find an expression for the reactivity difference between that injected by a controller and that removed by reactivity feedback to obtain the desired response.

Another review of the nonlinear reactor dynamics problems is presented in Reference 17.

A close look at the four models presented indicates that a fifth model exists and could be considered as a modification of the Newton's Law of Cooling model. In this it is assumed, not only that the heat transfer is proportional to the temperature, but that the coolant flow is varied as a function of the existing power level. For this model, which is the model to be investigated, no literature has appeared to indicate an analytical investigation. This literature study indicates that the solutions to the reactor-transient equations with feedback and in terms of well-known elementary functions are limited to a very few physical situations. In order to gain a more thorough understanding of reactor kinetics under varying conditions and to attempt to fill existing gaps in present day knowledge, more work in this field is needed.

III. ANALYTICAL SOLUTION

A. Solutions of the Fast Reactor Kinetics Equations with Feedback

1. Solution for a Step Plus Ramp Reactivity Input

This section consists of the analytical development of the fast reactor kinetics equations with feedback and a step and ramp input. A general feedback expression is utilized until the development can proceed no further without a specific expression. At this point, two specific functions are substituted. One corresponds to the zero-power kinetics and results in the same expression as that obtained by J. J. Syrett[18] with his source term set equal to zero. The other uses the natural logarithm feedback expression developed in Appendix C.

The space-independent reactor kinetics equations in the absence of an external source and under the assumption of one average group of delayed neutrons may be written as follows:

$$\frac{dn}{dt} = \frac{\rho - \beta}{\ell^*} n + \lambda D \quad ; \tag{1}$$

$$\frac{dD}{dt} = \frac{\beta}{\ell^*} n - \lambda D \quad , \tag{2}$$

where n is the neutron density; D the delayed-neutron precursor density, λ the decay constant of the delayed neutrons, and

$$\ell^* = \ell / k_{eff} \quad ,$$

where ℓ is the prompt-neutron lifetime, β the fraction of delayed neutrons, and k_{eff} the ratio of the number of neutrons in one generation divided by the number of neutrons in the previous generation. But

$$\rho = \frac{k_{eff} - 1}{k_{eff}} = \frac{k_{exs}}{k_{eff}} \quad ,$$

where k_{exs} is $(k_{eff} - 1)$. Now, with the assumption that the excess multiplication factor k_{exs} be much less than one, k_{eff} is approximately one, and k_{exs} and the reactivity ρ may be used interchangeably.

The simultaneous solution of Equations (1) and (2) gives the following result:

$$\ell^* \frac{d^2n}{dt^2} + (\ell^*\lambda + \beta - \rho) \frac{dn}{dt} - \left(\lambda\rho + \frac{d\rho}{dt}\right) n = 0 \quad . \tag{3}$$

If we divide ρ into its two components, ρ_1, the reactivity input and ρ_2, the reactivity feedback (i.e., $\rho = \rho_1 - \rho_2$), Equation (3) becomes

$$\ell^* \frac{d^2n}{dt^2} + [\ell^*\lambda + \beta - (\rho_1 - \rho_2)] \frac{dn}{dt} - \left[\lambda(\rho_1 - \rho_2) + \frac{d\rho_1}{dt} - \frac{d\rho_2}{dt}\right] n = 0 \quad . \tag{4}$$

For a fast reactor with a constant-speed "control rod" and a reactivity feedback which is a function of the power level, the following approximate values may be inserted into Equation (4). Equation (5a) is the representation used for the reactivity input as a function of time for a constant speed "control rod."

$$\rho_1 = \alpha + \gamma t \quad ; \tag{5a}$$

$$\rho_2 = \rho_2(n) \quad ; \tag{5b}$$

$\ell^* = 8 \times 10^{-8}$ sec ;

$\lambda = 0.081$ sec^{-1} ;

$\beta = 0.00735$;

$\gamma = 3 \times 10^{-5}$ $\Delta k/k/$sec ;

α = a constant equivalent to a step input; α at $t = 0$ will equal $\rho_2(n)$ at $t = 0$;

$\ell^*\lambda = 6.48 \times 10^{-9}$;

and

$$8 \times 10^{-8} \frac{d^2n}{dt^2} + \{6.48 \times 10^{-9} + 7.35 \times 10^{-3} - [\alpha + \gamma t - \rho_2(n)]\} \frac{dn}{dt}$$

$$- \left\{0.081 [\alpha + \gamma t - \rho_2(n)] + \gamma - \frac{d\rho_2(n)}{dt}\right\} n = 0 \quad . \tag{6}$$

Noting that the value of $\ell^*\lambda$ is 6 orders of magnitude less than β, it can be neglected. Also, for $t \leq 0$, the reactor has been operating at a steady state, the excess reactivity equals zero, i.e., $\rho_1 - \rho_2 = 0 = \alpha + \gamma t - \rho_2(n)$, and the following equation results:

$$8 \times 10^{-8} \frac{d^2n}{dt^2} + 7.35 \times 10^{-3} \frac{dn}{dt} + \left[-3 \times 10^{-5} + \frac{d\rho_2(n)}{dt}\right] n = 0 \quad . \tag{7}$$

It will be noted that if $\frac{d\rho_2(n)}{dt}$ is small compared with 3×10^{-5}, the value of the coefficient of the second derivative term is several orders of magnitudes less than the coefficients of the other terms. Then if the value of the second derivative is small, the second-order term may be neglected.

By neglecting the very small terms above, the equation is simplified to the following:

$$\{\beta - [\alpha + \gamma t - \rho_2(n)]\} \frac{dn}{dt} - n \left\{\lambda[\alpha + \gamma t - \rho_2(n)] + \gamma - \frac{d\rho_2(n)}{dt}\right\} = 0 \quad . \tag{8}$$

In a reactor, the power level is directly proportional to the average neutron concentration n, i.e.,

$$\text{Power} = \bar{\alpha} n \quad .$$

For simplicity, a new variable A will be defined as the fraction of power level of operation of the reactor, i.e., $A = n/n_{100\% \text{ power}}$. The feedback term ρ_2 is now a function of the fractional power level, and Equation (8) can be reduced to the following form:

$$[\beta - \alpha - \gamma t + \rho(A)]\, \dot{A} = A\{\lambda[\alpha + \gamma t - \rho(A)] + \gamma - \dot{\rho}(A)\} \quad . \tag{*9}$$

Since

$$\dot{\rho}(A) = \frac{d\rho(A)}{dt} = \frac{d\rho(A)}{dA} \frac{dA}{dt} = \rho'(A)\, \dot{A} \quad , \tag{10}$$

and if $A\dot{A} \neq 0$, it is possible to multiply Equation (9) by $1/A\dot{A}$, which becomes the following:

$$\frac{\beta - \alpha + \rho(A)}{A} - \frac{\gamma}{A} t + \rho'(A) = [\lambda\alpha + \gamma - \lambda\rho(A) + \lambda\gamma t] \frac{dt}{dA} \quad . \tag{11}$$

Division by $\lambda\gamma$ and defining

$$t = y \; ; \qquad A = x \quad , \tag{12}$$

gives the following equation:

$$\frac{1}{\lambda\gamma x}[\beta - \alpha + \rho(x)] + \frac{1}{\lambda\gamma} \frac{d[\rho(x)]}{dx} - \frac{1}{\lambda x} y = \left[y + \frac{\alpha}{\gamma} + \frac{1}{\lambda} - \frac{\rho(x)}{\gamma}\right] \frac{dy}{dx} \quad . \tag{13}$$

The equation will be recognized as a linear first-order equation in y with variable coefficients.

If the following substitutions are made, Equation (13) can be recognized as that of Abel's differential equation of the second type:[19]

---

*The dot ($\cdot$) notation refers to a derivative with respect to time only. The symbol (') will be used to denote the derivative with respect to the function variable, i.e., $\eta'(\xi) = \frac{d\eta(\xi)}{d\xi}$ or $\xi'(\eta) = \frac{d\xi(\eta)}{d\eta}$.

$$f_0(x) = \frac{1}{\lambda\gamma x}\left[\beta - \alpha + \rho(x)\right] + \frac{1}{\lambda\gamma}\frac{d\rho(x)}{dx} \tag{14}$$

$$f_1(x) = \frac{-1}{\lambda x} \tag{15}$$

$$g(x) = \left[\frac{\alpha}{\gamma} + \frac{1}{\lambda}\frac{-\rho(x)}{\gamma}\right] \tag{16}$$

$$[y + g(x)]\, y' = f_1(x)y + f_0(x) \tag{17}$$

(Abel's differential equation of the second type).

To solve this equation, the procedures listed in Reference 19 are followed. Substituting

$$y(x) + g(x) = 1/U(x) \tag{18}$$

into Equation (17), Equation (19) is obtained:

$$U' = [h_2(x)]U^2 + [h_3(x)]U^3 \tag{19}$$

where

$$h_2(x) = -g'(x) - f_1(x) \tag{20a}$$

and

$$h_3(x) = f_1(x)\, g(x) - f_0(x) \quad . \tag{20b}$$

Equation (19) is now Abel's differential equation of the first type as found in Reference 19, p. 25, part d. If the substitution of Equations (21) and (22) into Equation (19):

$$U(x) = \eta(\xi) \tag{21}$$

where

$$\xi = \int h_2(x)\, dx \tag{22}$$

is made, Equation (23) is obtained:

$$\eta'(\xi) = \frac{h_3}{h_2}(\xi)\, \eta^3(\xi) + \eta^2(\xi) \quad . \tag{23}$$

Another substitution is then made: Equation (24) into Equation (23),

$$\eta(\xi) = -\frac{1}{\hat{t}\ \xi'(\hat{t})} \quad , \qquad *(24)$$

so that Equation (25) obtained:

$$\hat{t}^2\ \xi''(\hat{t}) + \frac{h_3}{h_2}(\xi) = 0 \quad , \qquad (25)$$

where

$$\frac{h_3}{h_2}(x) = -\frac{1}{\lambda} - \frac{\beta}{\gamma + \lambda x\, \rho'(x)} \qquad (26)$$

and where

$$\xi = \int [-g'(x) - f_1(x)]\, dx = -g(x) + \frac{\ln x}{\lambda} = -\frac{\alpha}{\gamma} - \frac{1}{\gamma} + \frac{\rho(x)}{\gamma} + \frac{\ln x}{\lambda} \quad . \qquad (27)$$

It will be noted that if $\rho(x)$ = a constant or $\rho(x) = \hat{C} \ln \delta x$,

$$\frac{h_3}{h_2}(x) = \frac{h_3}{h_2}(\xi) = \text{a constant} = K_i \quad , \qquad (28)$$

and Equation (25) can readily be solved:

$$\xi = K_i \ln \hat{t} + C_1 \hat{t} + C_2 \quad . \qquad (29)$$

There are several forms of $\frac{h_3}{h_2}(x)$ which give Equation (25) a form for which a solution can be found. Two of these forms will be discussed.

Case I and Case II are the already mentioned solutions of Equation (25) when $\frac{h_3}{h_2}(x) = K_i$ (a constant).

For Case I, $\rho(x) = C_0$, the constant K_i is found to be as follows:

$$K_1 = -\frac{1}{\lambda} - \frac{\beta}{\lambda} \quad . \qquad (30)$$

---

*This $\hat{t}$ variable is not the time variable t in the initial stages of this derivation, but a dummy variable used to maintain a correspondence to the derivation found in Kamke.[19]

And for Case II, $\rho(x) = \hat{C} \ln \delta x$,

$$K_2 = -\frac{1}{\lambda} - \frac{\beta}{\gamma + \lambda \hat{C}} \quad . \tag{31}$$

Equation (29) is the solution of Equation (25) obtained by substitution of Equation (28), i.e.,

$$\hat{t}^2 \, \xi''(\hat{t}) + K_i = 0 \quad .$$

It is now necessary to perform the previous substitutions in the reverse order to obtain the answer in terms of x and y. During these substitutions, it will be noted that Equations (24), (21), and (18) can be combined to form the following:

$$\eta(\xi) = -\frac{1}{\hat{t}\, \xi'(\hat{t})} = U(x) = \frac{1}{y(x) + g(x)} \tag{32}$$

or

$$-\hat{t}\, \xi'(\hat{t}) = y(x) + g(x) \quad ; \tag{33}$$

$$-\hat{t} = \frac{y(x) + g(x)}{\xi'(\hat{t})} \quad . \tag{34}$$

From Equation (29),

$$\xi'(\hat{t}) = \frac{+K_i}{\hat{t}} + C_1 \quad . \tag{35}$$

If $\xi'(\hat{t})$ is eliminated from Equations (34) and (35) and the result solved for $\hat{t}$, the following result is obtained:

$$\hat{t} = \frac{-1}{C_1} [K_i + g(x) + y(x)] \quad . \tag{36}$$

If this value of $\hat{t}$ is substituted into Equation (29) and the value of ξ from Equation (27) used, the following answer is obtained:

$$+K_i \ln \left\{ \frac{1}{C_1} \left[-K_i - y(x) - \frac{\alpha}{\gamma} - \frac{1}{\lambda} + \frac{\rho(x)}{\gamma} \right] \right\} - K_i - y(x) + C_2 = \frac{\ln x}{\lambda} \quad . \tag{37}$$

This result can be reduced to simpler forms for the two cases under study. By means of the reverse substitutions and rearrangement of the resultant equation, the result for Case I is expressed as Equation (38b):

Case I:

$$\rho(x) = C_0 \quad ; \tag{38a}$$

$$A = \left\{ \exp\left[\frac{\lambda}{\gamma} \left(\beta + \frac{\gamma}{\lambda} + \gamma C_2 - \gamma t \right) \right] \right\} \left(\frac{\gamma C_1}{\beta - \alpha + C_0 - \gamma t} \right)^{\left(1 + \frac{\beta\lambda}{\gamma}\right)} . \tag{38b}$$

This equation can be further simplified by combining the terms involving the constants into one term, C_3, i.e.,

$$A = C_3 \left[\exp(-\lambda t) \right] \left(\frac{1}{\beta - \alpha + C_0 - \gamma t} \right)^{\left(1 + \frac{\beta\lambda}{\gamma}\right)} \tag{*39}$$

where

$$C_3 = \left[\exp\left(1 + \frac{\beta\lambda}{\gamma} + \alpha\lambda C_2 \right) \right] \left(\gamma C_1 \right)^{\left(1 + \frac{\beta\lambda}{\gamma}\right)}$$

For Case II, the final result is similar in form:

$$A = C_4 \left[\exp(-\lambda t) \right] \left(\frac{1}{\frac{\gamma\beta}{\gamma + \lambda\hat{C}} - \alpha - \gamma t + \hat{C} \ln \delta A} \right)^{\left(1 + \frac{\beta\lambda}{\gamma + \lambda\hat{C}}\right)} , \tag{40}$$

where

$$C_4 = \left[\exp\left(\lambda C_2 + 1 + \frac{\lambda\beta}{\gamma + \lambda\hat{C}} \right) \right] \left(\gamma C_1 \right)^{\left(1 + \frac{\lambda\beta}{\gamma + \lambda\hat{C}}\right)}$$

2. Solution for a Step Reactivity Input

In obtaining the solutions (39) and (40), we have assumed a positive ramp reactivity input as a result of assuming γ to be positive, but the equations should hold if γ is negative. In fact, if a positive ramp input is used until time t and then the control element is reversed to put in a

*This is the same equation as that developed by J. J. Syrett,[18] where his source term is set equal to zero.

negative ramp of reactivity, the solutions (39) and (40) should still be valid, but the sign of γ should be changed. Should the rod be stopped, the value of γ will be zero, and another solution must be found. The derivation of this solution is much simpler and proceeds as follows:

In Equation (9), the value of γ is set equal to zero and Equation (41) is the result:

$$[\beta - \alpha + \rho(A)]\dot{A} = A\{\lambda[\alpha - \rho(A)] - \dot{\rho}(A)\} \quad . \tag{41}$$

Since $\dot{\rho}(A) = \frac{d\rho(A)}{dA}\frac{dA}{dt} = \rho'(A)\dot{A}$, it can be moved to the left side of Equation (41). Then, dividing by $\dot{A}A$, we obtain Equation (42):

$$\frac{1}{A}[\beta - \alpha + \rho(A)] + \rho'(A) = \frac{dt}{dA}[\lambda\alpha - \lambda\rho(A)] \quad . \tag{42}$$

Rearrangement of Equation (42) shows it to be a first-order linear equation in t:

$$\frac{dt}{dA} = \frac{\beta - \alpha + \rho(A) + A\rho'(A)}{A[\lambda\alpha - \lambda\rho(A)]} \quad . \tag{43}$$

This equation can be partially solved by direct integration:

$$t = \int \frac{-1}{\lambda A}\, dA + \int \frac{\beta + A\rho'(A)}{\lambda A[\alpha - \rho(A)]}\, dA \tag{44}$$

$$= -\frac{1}{\lambda}\ln A + \frac{\beta}{\lambda}\int \frac{1}{A[\alpha - \rho(A)]}\, dA + \frac{1}{\lambda}\int \frac{\rho'(A)\, dA}{[\alpha - \rho(A)]} \quad , \tag{45}$$

where

$$\frac{1}{\lambda}\int \frac{\rho'(A)}{[\alpha - \rho(A)]}\, dA = \frac{1}{\lambda}\int \frac{d\rho}{\alpha - \rho} = \frac{-1}{\lambda}\ln[\alpha - \rho(A)] \quad . \tag{46}$$

Thus,

$$t = -\frac{1}{\lambda}\ln\{A[\alpha - \rho(A)]\} + \frac{\beta}{\lambda}\int \frac{dA}{A[\alpha - \rho(A)]} \quad . \tag{47}$$

The last integral can be evaluated only for a given function of $\rho(A)$. Since the function of prime interest is $\rho(A) = \hat{C}\ln\delta A$, the value of the integral is as follows:

$$\int \frac{dA}{A[\alpha - \hat{C}\ln\delta A]} = -\frac{1}{\hat{C}}\ln(\alpha - \hat{C}\ln\delta A) - \frac{1}{\beta}\ln K_{Z_3} \quad , \tag{48}$$

where K_{Z_3} is the constant of integration. The resultant value of t is as follows:

$$t = \frac{-1}{\lambda}\left\{\ln[A(\alpha - \hat{C}\ln\delta A)] + \frac{\beta}{\hat{C}}\ln(\alpha - \hat{C}\ln\delta A)\right\} - \frac{1}{\lambda}\ln K_{Z_3} \quad . \tag{49}$$

Multiplying by $-\lambda$ and taking the antilog of both sides of the equation gives Equation (50):

$$e^{-\lambda t} = K_{Z_3} A[\alpha - \hat{C}\ln\delta A]^{\left[1 + \frac{\beta}{\hat{C}}\right]} \quad . \tag{50}$$

Equation (50) indicates that in the limit as t approaches infinity, the value of A will be determined by the equation

$$\hat{C}\ln\delta A = \alpha \quad , \tag{51}$$

where α is determined by the initial condition at the beginning of the time period under analysis.

Another form for Equation (51) is

$$A = \frac{\exp(\alpha/\hat{C})}{\delta} \quad . \tag{52}$$

In summary, in this section the step and ramp input fast reactor kinetics equations with feedback were developed to the point at which specific functions had to be inserted to achieve a solution in terms of elementary functions [Equation (26)]. Two elementary feedback expressions were used. The result corresponding to the zero-power kinetics case is represented by Equation (39). The result with a natural logarithm of the power (Case II) is represented by Equation (40). The result with only a step input with a "log" feedback is found in Equation (50).

B. Evaluation of the Switching Points

In the preceding section, a solution to the fast reactor kinetic equations has been obtained with use of the natural logarithm of the power level (see Appendix C) as the feedback reactivity expression.

It is planned to use the solution presented to determine a switching criterion whereupon a time-optimum transient would occur in the changing of steady-state power levels in reactors. In the equations, the switching is accomplished by changing the sign of γ from positive to negative and will occur when a desired time has elapsed or a specific power level has

been reached. A second switching will occur at the designation of a time duration or power-level attainment or when the excess reactivity reaches a value of zero. The control mechanism is then temporarily deactivated, allowing the reactor to "steady out" at the new steady-state condition.

In the practical use of Equations (40) and (50) to solve the problem of reactor kinetics involving switching, three or more time zones of interest occur. For the case of increasing power level, the first zone is from $t = 0$ to $t = t_1$, i.e., the period when γ is positive. The second zone consists of the time from $t = t_1$ to $t = t_2$, i.e., the time while γ is negative. The third zone (if only 3 zones are considered) is for t greater than t_2, i.e., when the rod motion has been stopped altogether and the γ of rod motion is zero.

During each of these time zones, the constants involved in the utilization of Equations (40) and (50) must be changed. The first constant to be discussed is α.

1. Evaluation of the Constants for the Three Main Time Zones of Interest

The symbol α in the original analytical derivation was included as a matter of course to give a solution for a more general input situation. In the physical sense, α in Equation (5) represents a step reactivity input occurring at time equal to zero. In the mathematical sense, it is a parameter specifically evaluated in terms of the initial conditions for each time zone of interest involved in this kinetics problem. The purpose of α and its method of evaluation concern the value of excess reactivity ρ in the reactor kinetics equations. The restriction that will be used for switching between time zones is that ρ must remain constant at the switching junction. Prior to the first time zone, the reactor has been in the steady-state condition, i.e.,

$$\rho = 0 = \rho_1 - \rho_2 = \alpha + \gamma t - [\rho_2(n)]_{t=0} \quad , \tag{53}$$

so that

$$\alpha = [\rho_2(n)]_{t=0} \tag{54}$$

or, when applied to the specific model used,

$$\alpha_{Z_1} = \hat{C} \ln \delta A_0 \quad , \tag{55}$$

thus giving ρ the form

$$\rho_{Z_1} = \hat{C} \ln (\delta A_0) + \gamma t - \hat{C} \ln \delta A \tag{56}$$

for Zone 1. In a more simplified form,

$$\rho_{Z_1} = \gamma t - \hat{C} \ln (A/A_0) \quad . \tag{57}$$

At the first reactivity reversal time, i.e., the time when γ changes sign from + to -, the value of α is changed to include another term. This is necessary in the mathematics in order to maintain the value of the excess reactivity constant while transforming to the new equation in which γ is negative.

The term which is added is obtained in the following manner:

The reactivity added to the reactor (above 10% power) results from two main sources: the initial power level of operation,

$$\rho(t = 0) = \hat{C} \ln \delta A_0 \quad , \tag{58}$$

and that added due to control rod motion, γt, thus making the excess reactivity at switch time t_1

$$\rho_{Z_1} = \hat{C} \ln (\delta A_0) + \gamma t_1 - \hat{C} \ln \delta A_1 \quad , \tag{59}$$

where $\hat{C} \ln \delta A_1$ is the reactivity subtracted due to the present power level of the reactor. Thus, the value of α for the second time zone is

$$\alpha_{Z_2} = \hat{C} \ln (\delta A_0) + 2\gamma t_1 \quad . \tag{60}$$

The value of the reactivity subtracted at any time t during the second time zone due to the control rod motion is $\gamma(t - t_1)$, thus making the total reactivity expression during the second time zone

$$\rho_{Z_2} = \hat{C} \ln (\delta A_0) + \gamma t_1 - \gamma(t - t_1) - \hat{C} \ln \delta A \quad . \tag{61}$$

If the terms involving t_1 are combined, and also the terms involving the log functions, the following simplified form is obtained:

$$\rho_{Z_2} = \gamma(2t_1 - t) - \hat{C} \ln (A/A_0) \quad . \tag{62}$$

The same criterion holds true for the evaluation of α for the third zone as for the second and first. Thus, the value of the excess reactivity at the beginning of the third zone should be the same as that at the end of the second, i.e.,

$$\rho_{Z_2} = \hat{C} \ln (\delta A_0) + \gamma t_1 - \gamma(t_2 - t_1) - \hat{C} \ln \delta A_2 \quad , \tag{63}$$

where t_2 is the time at which all rod motion will cease. Since the rods will be stationary in this zone (3), the only reactivity changes occurring will be due to the changes in the power level. Thus, the values of ρ_{Z3} and α_{Z3} are

$$\rho_{Z3} = 2\gamma t_1 - \gamma t_2 - \hat{C} \ln (A/A_0) \tag{64}$$

and

$$\alpha_{Z3} = \hat{C} \ln (\delta A_0) + 2\gamma t_1 - \gamma t_2 \quad . \tag{65}$$

A summary of the expressions for ρ and α for the three time zones of interest can be found in Table 1.

Table 1

TABLE OF VALUES OF α AND ρ FOR THE THREE TIME ZONES OF INTEREST

Time Zone	Rod Reactivity Insertion Rate	α	$\rho(A)$ throughout Time Zone
1	$+\gamma$	$\hat{C} \ln \delta A_0$	$\gamma t - \hat{C} \ln (A/A_0)$
2	$-\gamma$	$\hat{C} \ln (\delta A_0) + 2\gamma t_1$	$2\gamma t_1 - \gamma t - \hat{C} \ln (A/A_0)$
3	0	$\hat{C} \ln (\delta A_0) + 2\gamma t_1 - \gamma t_2$	$2\gamma t_1 - \gamma t_2 - \hat{C} \ln (A/A_0)$

The second constant involved in the practical kinetics solutions (40) and (50) is C_4. Since Equation (40) is used for solutions in both time zone 1 and time zone 2, there will be two principal values of C_4 of interest. A look at Equation (40) indicates that it can be simplified for numerical computations by removing γ from the denominator and combining it with C_4 to form a single constant K_Z:

$$K_Z = C_4 [\gamma]^{-\left[1 + \frac{\lambda\beta}{\gamma + \lambda\hat{C}}\right]} \quad , \tag{66}$$

which must then be evaluated for both zones 1 and 2. The value of K_{Z1} can then be found from Equation (40):

K_{Z1} = K_Z in Time Zone 1 (before first reversal time);

K_{Z2} = K_Z in Time Zone 2 (after first reversal time);

$$K_{Z_1} = A[\exp\ \lambda t]\ \{[\ \beta/(\gamma + \lambda\hat{C})] - (\alpha/\gamma) - t + (\hat{C}/\gamma)\ \ln \delta A\}^{\left[1 + \frac{\beta\lambda}{\gamma + \lambda\hat{C}}\right]} \quad . \tag{67}$$

By use of the following substitutions in the evaluation of K_{Z_1}:

$$t = 0 \quad ; \tag{68}$$

$$A = A_0 \quad ; \tag{69}$$

$$\alpha = \hat{C}\ \ln \delta A_0 \quad ; \tag{70}$$

$$\hat{\xi} = \beta/(\gamma + \lambda\hat{C}) \quad , \tag{71}$$

a simplified form can be obtained:

$$K_{Z_1} = A_0[\hat{\xi}]^{[1 + \lambda\hat{\xi}]} \quad . \tag{72}$$

Similarly, the value of K_{Z_2} can be obtained:

$$\alpha = \hat{C}\ \ln\ (\delta A_0) + \gamma t_1 \quad ; \tag{73}$$

$$t = t_1 \quad ; \tag{74}$$

$$\bar{\hat{\xi}} = \beta/(\lambda\hat{C} - \gamma) \quad ; \tag{75}$$

$$K_{Z_2} = [A_1 \exp(\lambda t_1)]\ [\bar{\hat{\xi}} + t_1 - (\hat{C}/\gamma)\ \ln\ (A_1/A_0)]^{[1 + \lambda\bar{\hat{\xi}}]} \quad . \tag{76}$$

The value of the constant K_{Z_3} for the third time zone can be evaluated similarly. Equation (80) is obtained by substituting Equations (77), (78), and (79) into Equation (50) and solving for K_{Z_3}:

$$t = t_2 \quad ; \tag{77}$$

$$A = A_2 \quad ; \tag{78}$$

$$\alpha = \hat{C}\ \ln\ (\delta A_0) + 2\gamma t_1 - \gamma t_2 \quad ; \tag{79}$$

$$K_{Z_3} = \frac{e^{-\lambda t_2}}{A_2\left(2\gamma t_1 - \gamma t_2 - \hat{C}\ \ln \frac{A_2}{A_0}\right)^{\left(1 + \frac{\beta}{\hat{C}}\right)}} \quad . \tag{80}$$

*Note: This is not the same ξ as appeared in an earlier derivation.

2. Results

Substituting the values of the different constants back into the kinetics equation and evaluating the "power level" vs "time" curves for many different initial power levels and switching times would be very time consuming if done by hand. As a result, a computer program was written to perform the evaluation in the first and second time zones. The program, written for the LGP-30, used the Act III compiling code. The program code name used is "KEEPWOLF" (see Appendix E).

The results produced by the digital program are plotted in Figures 2 and 3 for only one numerical value of ramp rate of reactivity and one value of the feedback reactivity coefficient $\hat{C}$. It was noted that the values of the power levels at any fixed time were a consistent ratio to the initial values regardless of what the initial value was. Thus, for any set fractional change in power, a specific switching time and final time could be determined to perform the change. Also, as a result, the amount of computer time needed to obtain a new series of curves for different parameters could be shortened by running only one initial value and obtaining the fractional changes from it.

The results of other series are given in Table 2. These results indicated what was to be expected: for lower reactivity input rates or larger feedback coefficients, a longer time was required to perform a given change.

From the results obtained by the analytical approach, the switching power level could be determined as a function of the final power, and the control element reversal time could be computed. Representative results appear in Figure 4.

In computing the relationships of the switching power to the final power, the difference between the two power levels is taken and then divided by the switching power to obtain a percentage error at the switch time. This percentage error varies from negative to positive, indicating that for short switch times, the corresponding indicated switching power was less than the final power. For longer switching times, the switching power was higher than the final power.

These values will later be compared with the values obtained by the other two major methods of analysis.

Graphs of the final power levels as a function of the switching times are represented in Figures 5, 6, 7, and 8 for two values of reactivity input and one coefficient of the feedback reactivity, the information being taken from Table 2. The other curves represent the comparable results by the other two major methods and will be referred to in later sections.

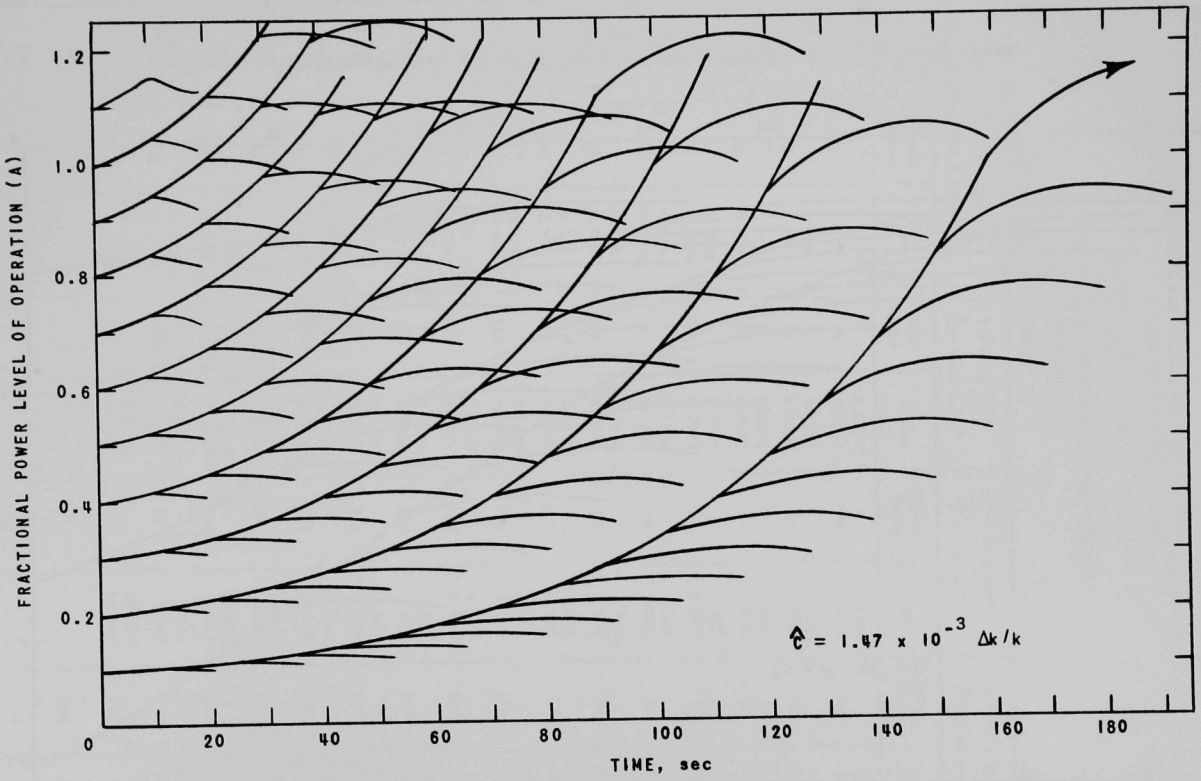

Fig. 2. "Rising Power Level" Trajectories for $\gamma = +3 \times 10^{-5}$ Δk/k/sec

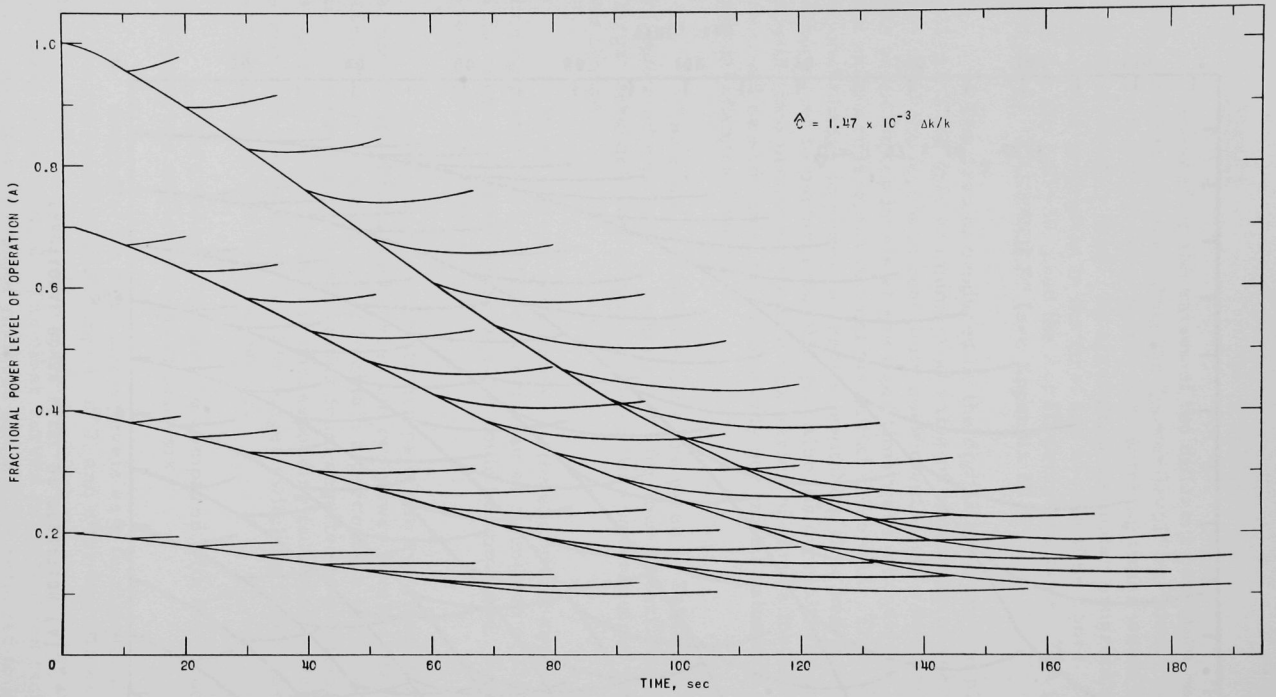

Fig. 3. "Falling Power Level" Trajectories for $\gamma = -3 \times 10^{-5}$ Δk/k/sec

Table 2

SWITCHING AND FINAL POWER LEVELS PREDICTED
BY ANALYTICAL RESULTS

Time - sec

Value - Fractional Change from Initial

γ - $\Delta k/k/sec$

$\hat{C}$ - $\Delta k/k$

Switch Time	$\gamma = -3 \times 10^{-5}$ $\hat{C} = 1.47 \times 10^{-3}$		$\gamma = -3 \times 10^{-5}$ $\hat{C} = 2.05 \times 10^{-3}$		$\gamma = +3 \times 10^{-5}$ $\hat{C} = 1.47 \times 10^{-3}$		$\gamma = +3 \times 10^{-5}$ $\hat{C} = 2.05 \times 10^{-3}$	
	Final Time	Value	Final Time	Value	Final Time	Value	Final Time	Value
10		0.9567		0.9599		1.047		1.042
	19	0.9770	19	0.9802	19	1.024	19	1.020
20		0.8986		0.9070		1.120		1.107
	35	0.9164	35	0.9282	35	1.097	35	1.080
30		0.8309		0.8459		1.222		1.194
	52	0.8440	50	0.8621	51	1.201	50	1.168
40		0.7580		0.7805		1.357		1.305
	67	0.7598	64	0.7892	65	1.355	63	1.287
50		0.6836		0.7136		1.529		1.443
	80	0.6713	77	0.7141	79	1.545	75	1.438
60		0.6104		0.6476		1.748		1.609
	95	0.5913	90	0.6421	92	1.792	88	1.610
70		0.5401		0.5838		2.019		1.807
	108	0.5133	102	0.5726	104	2.103	99	1.825
80		0.4743		0.5235		2.358		2.043
	120	0.4411	114	0.5087	115	2.496	110	2.078
90		0.4135		0.4672		2.775		2.320
	133	0.3784	125	0.4490	127	2.967	121	2.371
100		0.3583		0.4152		3.290		2.645
	145	0.3219	137	0.3965	138	3.557	132	2.714
110		0.3090		0.3676		3.924		3.025
	157	0.2730	148	0.3482	149	4.279	143	3.110
120		0.2650		0.3246		4.702		3.468
	168	0.2298	159	0.3053	160	5.164	153	3.582
130		0.2262		0.2858		5.658		3.985
	180	0.1935	170	0.2671	170	6.267	164	4.116
140		0.1924		0.2510		6.832		4.585
	190	0.1615	180	0.2328	180	7.621	174	4.750
150		0.1629		0.2201		8.271		5.282
	202	0.1353	192	0.2040	191	9.249	184	5.485
160		0.1377		0.1926		10.038		6.092
	213	0.1128	202	0.1773	202	11.240	194	6.336
170								7.031
							204	7.324
180								8.120
							214	8.467

Table 2 (Contd.)

Switch Time	$\gamma = -2.35 \times 10^{-5}$, $\hat{C} = 1.47 \times 10^{-3}$		$\gamma = -2.35 \times 10^{-5}$, $\hat{C} = 2.05 \times 10^{-3}$		$\gamma = 2.35 \times 10^{-5}$, $\hat{C} = 1.47 \times 10^{-3}$		$\gamma = 2.35 \times 10^{-5}$, $\hat{C} = 2.05 \times 10^{-3}$	
	Final Time	Value	Final Time	Value	Final Time	Value	Final Time	Value
10		0.9659		0.9684		1.036		1.033
	19	0.9820	19	0.9844	19	1.018	19	1.016
20		0.9192		0.9260		1.092		1.083
	35	0.9336	35	0.9430	35	1.074	35	1.062
30		0.8637		0.8764		1.168		1.148
	52	0.8748	50	0.8897	51	1.154	50	1.129
40		0.8029		0.8222		1.266		1.230
	67	0.8050	64	0.8298	65	1.265	63	1.217
50		0.7394		0.7659		1.389		1.329
	80	0.7296	77	0.7669	79	1.402	75	1.327
60		0.6754		0.7091		1.539		1.446
	94	0.6579	90	0.7051	92	1.572	88	1.449
70		0.6126		0.6532		1.721		1.583
	107	0.5881	102	0.6443	104	1.780	100	1.594
80		0.5522		0.5990		1.939		1.740
	120	0.5229	114	0.5868	115	2.034	110	1.767
90		0.4949		0.5472		2.198		1.920
	132	0.4619	125	0.5317	128	2.319	122	1.953
100		0.4413		0.4983		2.506		2.126
	144	0.4062	137	0.4821	139	2.668	133	2.169
110		0.3917		0.4525		2.871		2.360
	155	0.3554	148	0.4352	150	3.083	143	2.419
120		0.3465		0.4099		3.301		2.624
	167	0.3109	159	0.3924	160	3.577	154	2.694
130		0.3053		0.3705		3.809		2.923
	179	0.2714	169	0.3524	171	4.145	164	3.011
140		0.2684		0.3344		4.407		3.261
	190	0.2359	180	0.3169	182	4.814	175	3.360
150		0.2350		0.3013		5.110		3.641
	200	0.2040	190	0.2841	193	5.598	185	3.759
160		0.2053		0.2711		5.938		4.069
	212	0.1771	200	0.2545	203	6.534	195	4.208
170				0.2436		6.911		4.552
			212	0.2290	213	7.634	205	4.713
180				0.2188		8.055		5.093
			222	0.2049	223	8.926	215	5.280
190				0.1963		9.399		5.702
			232	0.1833	234	10.410	225	5.915
200								6.385
							235	6.629
210								7.152
							245	7.429
220								8.014
							255	8.327
230								8.980
							265	9.335
240								10.070
							275	10.470

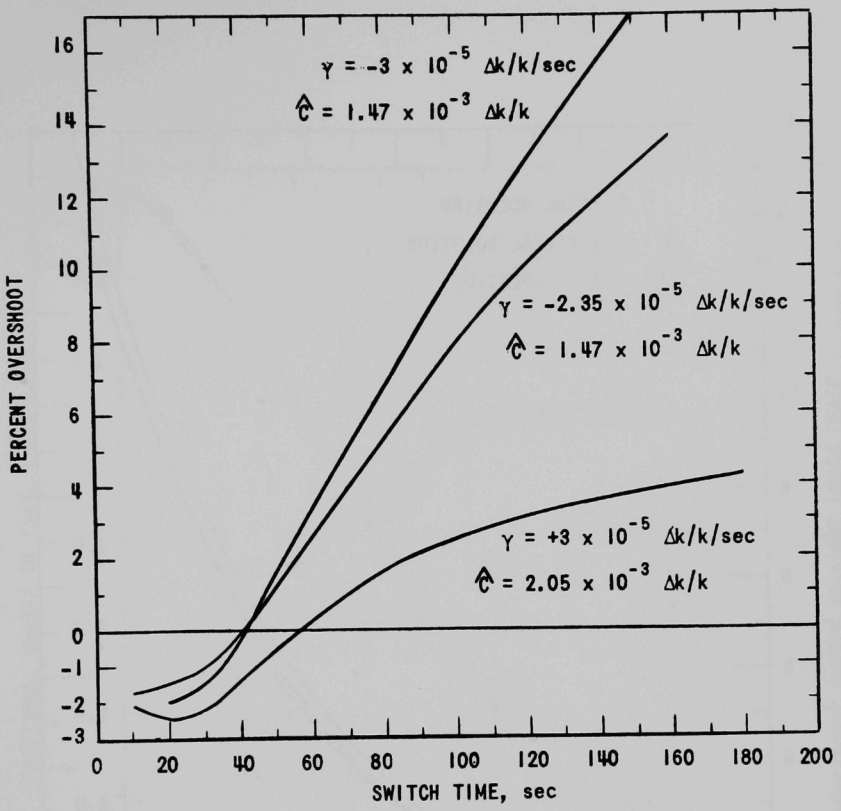

Fig. 4. Percent Overshoot by Analytical Method

Other values of reactivity input were tried but some trouble was experienced with the computer program (see Appendix E). Results were obtained, however, for values of 1 x 10^{-3} $\Delta k/k$/sec and 3 x 10^{-3} $\Delta k/k$/sec. These can be found in Tables 3 and 4. The asymptotic period calculated for the results in Table 4 was 0.49 sec. This period was compared with the period obtained from ANL-5800[20] for pure U^{235} and a comparable asymptotic Δk_{exs} of 91.6¢; there was a difference of a factor of five.

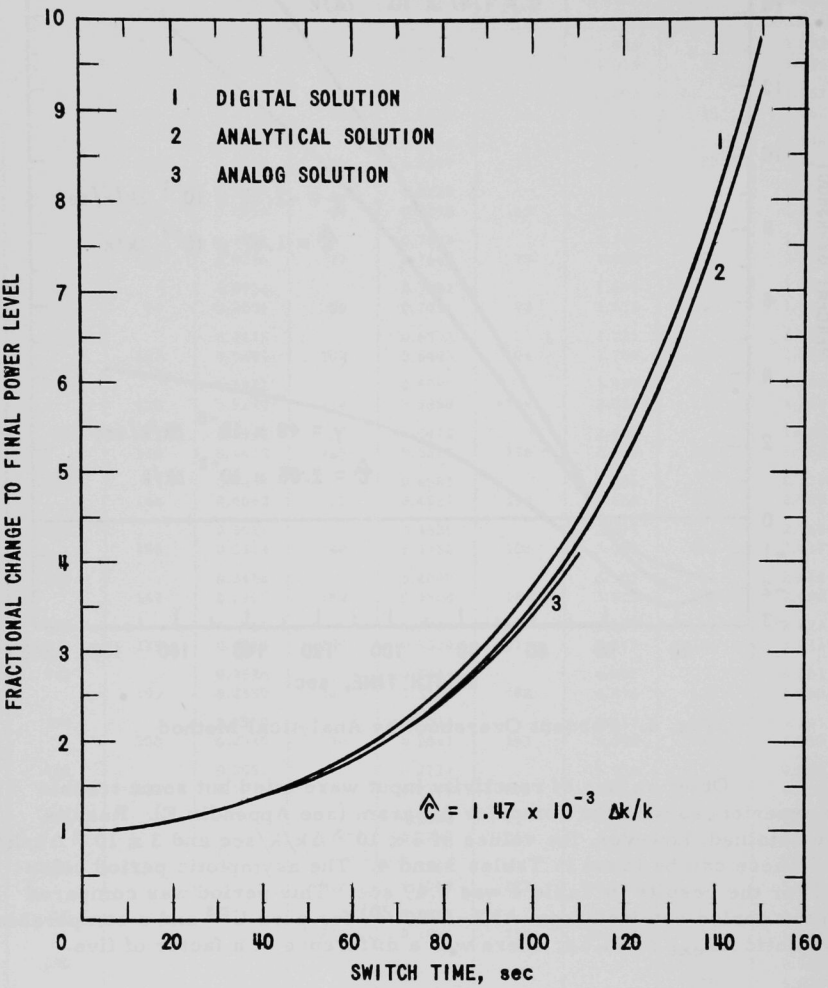

Fig. 5. Fractional Change to Final Power for $\gamma = 3 \times 10^{-5}$ Δk/k/sec

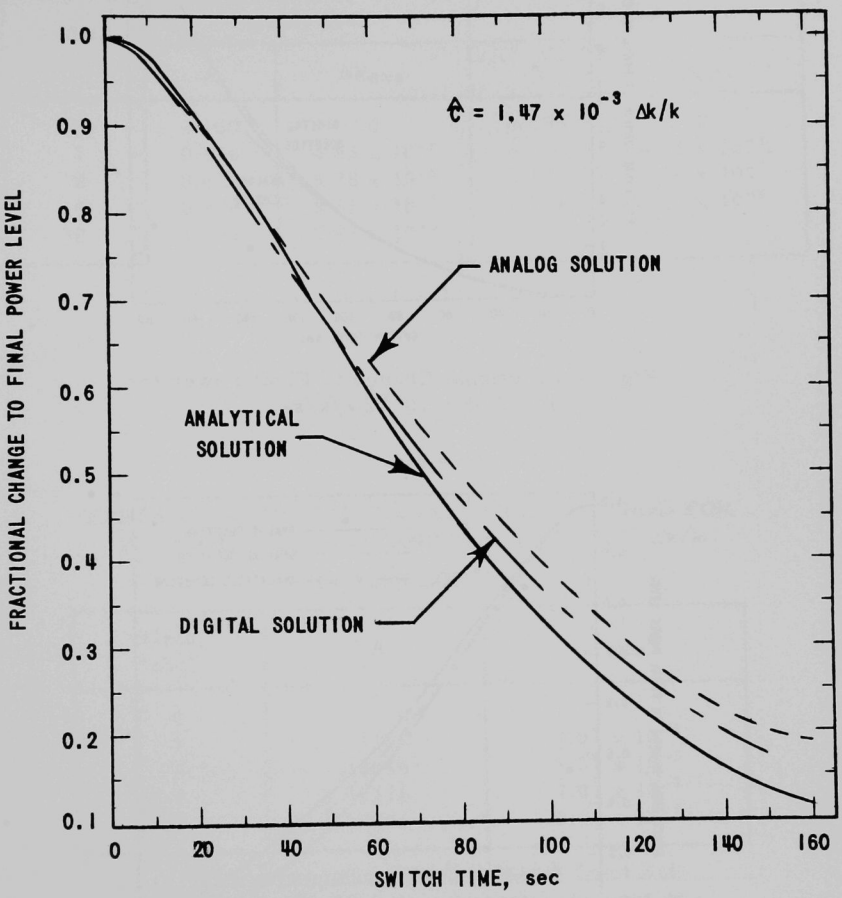

Fig. 6. Fractional Change to Final Power for $\gamma = -3 \times 10^{-5}$ Δk/k/sec

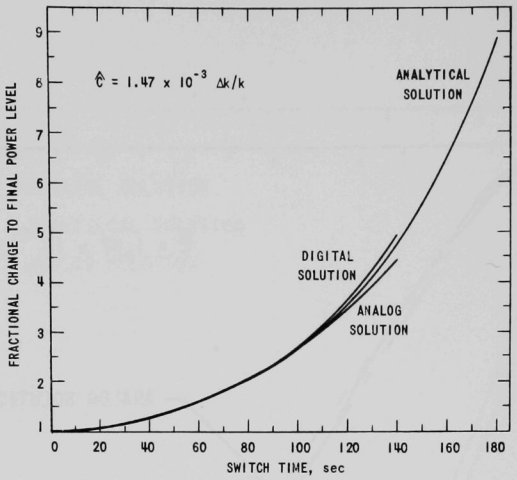

Fig. 7. Fractional Change to Final Power for $\gamma = 2.35 \times 10^{-5}$ Δk/k/sec

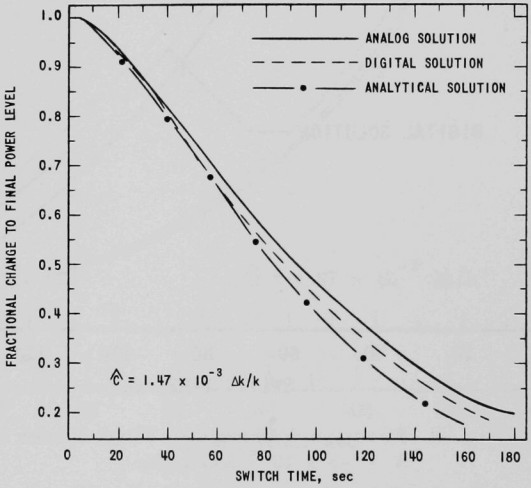

Fig. 8. Fractional Change to Final Power for $\gamma = -2.35 \times 10^{-5}$ Δk/k/sec

Table 3

COMPARISON OF ONE-GROUP SOLUTIONS FOR
$\gamma = 1 \times 10^{-3}$ $\Delta k/k/sec$ AND $\hat{C} = 1.47 \times 10^{-3}$ $\Delta k/k$

Time, sec	Analytical		Digital	
	A	Δk_{exs}	A	Δk_{exs}
0	0.100	0	0.100	0
7	0.436	4.83×10^{-3}	0.433	4.85×10^{-3}
8	0.636	5.28×10^{-3}	0.630	5.30×10^{-3}
9	0.978	5.65×10^{-3}	0.968	5.67×10^{-3}
10	1.591	5.93×10^{-3}	-	-

Table 4

TABLE OF RESULTS OF ANALYTICAL METHOD FOR
$\gamma = 3 \times 10^{-3}$ $\Delta k/k/sec$ AND $\hat{C} = 1.47 \times 10^{-3}$ $\Delta k/k$

1-Group LGP-30

Time, sec	A	Δk_{exs}*
0	0.1	
7	1306	7.07×10^{-3}
8	10046	7.07×10^{-3}
9	77316	7.07×10^{-3}
10	595083	7.07×10^{-3}

*The asymptotic period obtained from Reference 20 using the same excess reactivity is 0.1 sec.

IV. ANALOG SIMULATION STUDIES

A. With Feedback-delay Time Constants

The analog simulator of the zero-power kinetics with "natural logarithm of the power" feedback was constructed as indicated in Appendix D. This method of representation allows different feedback-delay time constants to be tried for their effect on the power-level trajectories. Several different ramp rates of reactivity input were tried with and without any feedback-delay time constants.

The criterion of operation of the analog computer was similar to that used in establishing the switching points for the results from the analytical study. A ramp rate of reactivity was inserted for a specified period of time and then reversed for the length of time necessary for the excess reactivity to return to zero. The power level at which the ramp rate was stopped should be the final steady-state value.

Figure 9a shows the effects of placing 2.5-sec and 5.0-sec delay time constants in the feedback path. The switching power level which corresponds to 120 sec of elapsed time since initiation of the ramp does vary by as much as 4% of power for a 5-sec time constant, but the final differences are only about half of that amount, i.e., approximately 2% of power. It should also be pointed out that the 5-sec time constant represents a value which is over five times the value of the largest time constant expected to occur in a small, high-power fast reactor (see Appendix C). The largest time constant that is expected is inversely proportional to the flow and, as a result, attains its largest value at the lower powers. Thus, a time constant of 5 sec at high powers is somewhere close to 50 times the expected time constant. The resultant error of 2% of power can, therefore, be considered as a maximum that might be expected to occur with a ramp rate of 2.34×10^{-5} $\Delta k/k/sec$.

Figure 9b also represents the results of delay time constants in the feedback path, but as to be expected, the effects of faster ramp rates are larger errors in the switching power levels and final power levels. The final steady-state power level in this case was 3% of power higher than the point at which the ramp reactivity rate simulator was finally stopped. Here the effect of the delay feedback reactivity would have to be overcome by an additional switching cycle or movement of the control element.

Figure 10 shows the results of feedback-delay time constants in a decreasing power-level trajectory. Here it will be noticed that the apparent effect of delay time constants is reduced for decreasing power levels, that is, the error in power is less, but nothing can be said about the percentage error of the final low-power level as a 2% error of 20% is difficult to read.

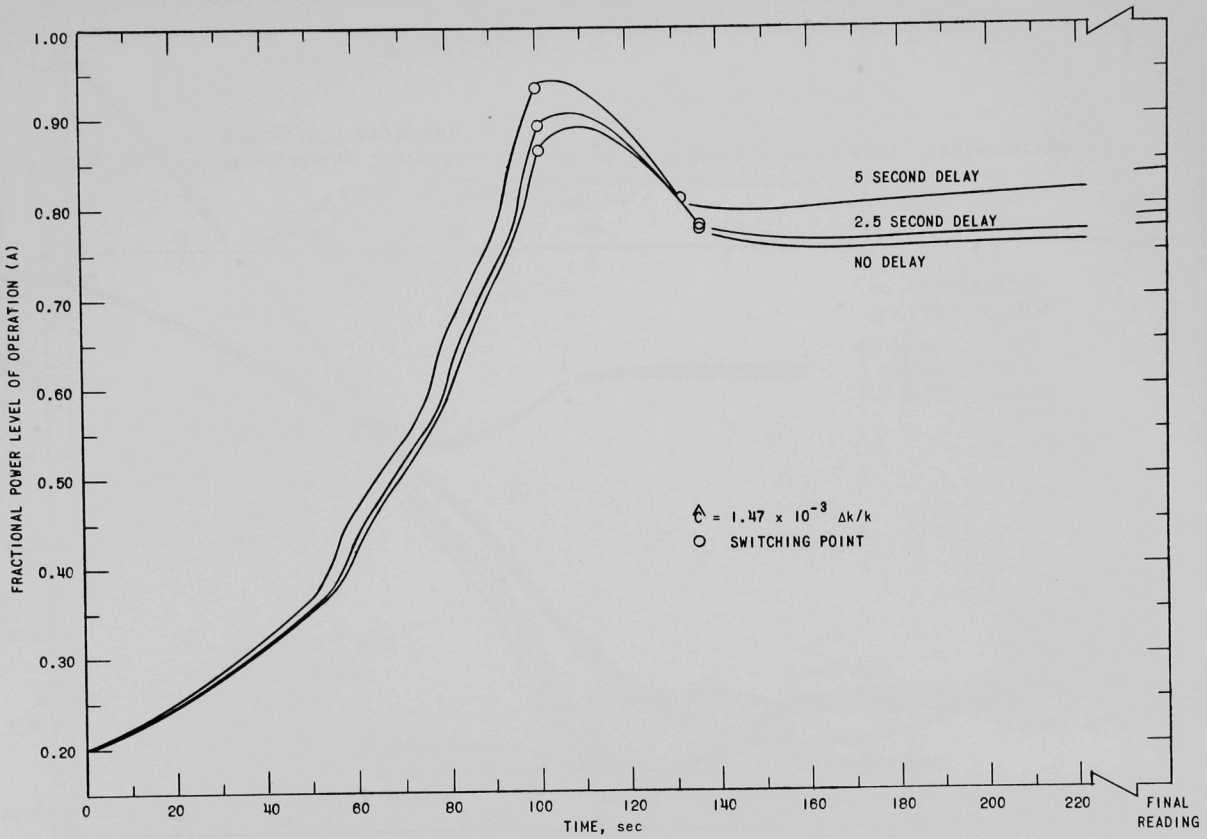

Fig. 9a. Feedback-delay Time Constant Effect on "Rising Power Level" Trajectories for $\gamma = 2.34 \times 10^{-5}$ $\Delta k/k/sec$

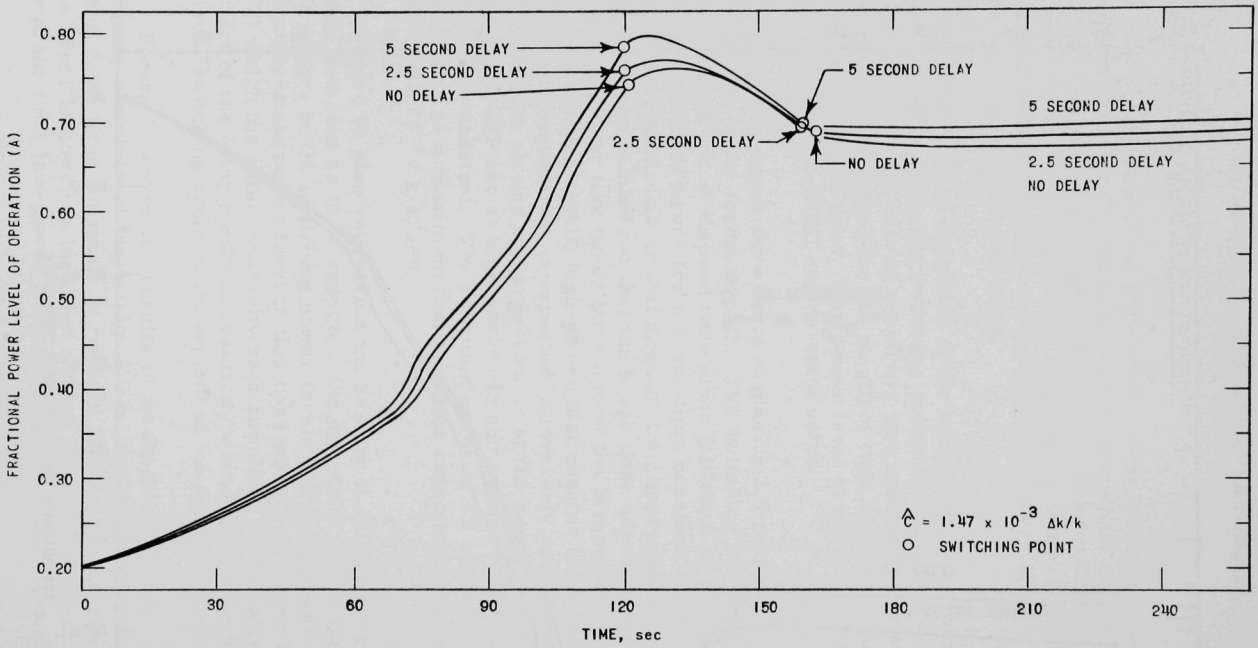

Fig. 9b. Feedback-delay Time Constant Effect on "Rising Power Level" Trajectories for $\gamma = 3.09 \times 10^{-5}$ $\Delta k/k/sec$

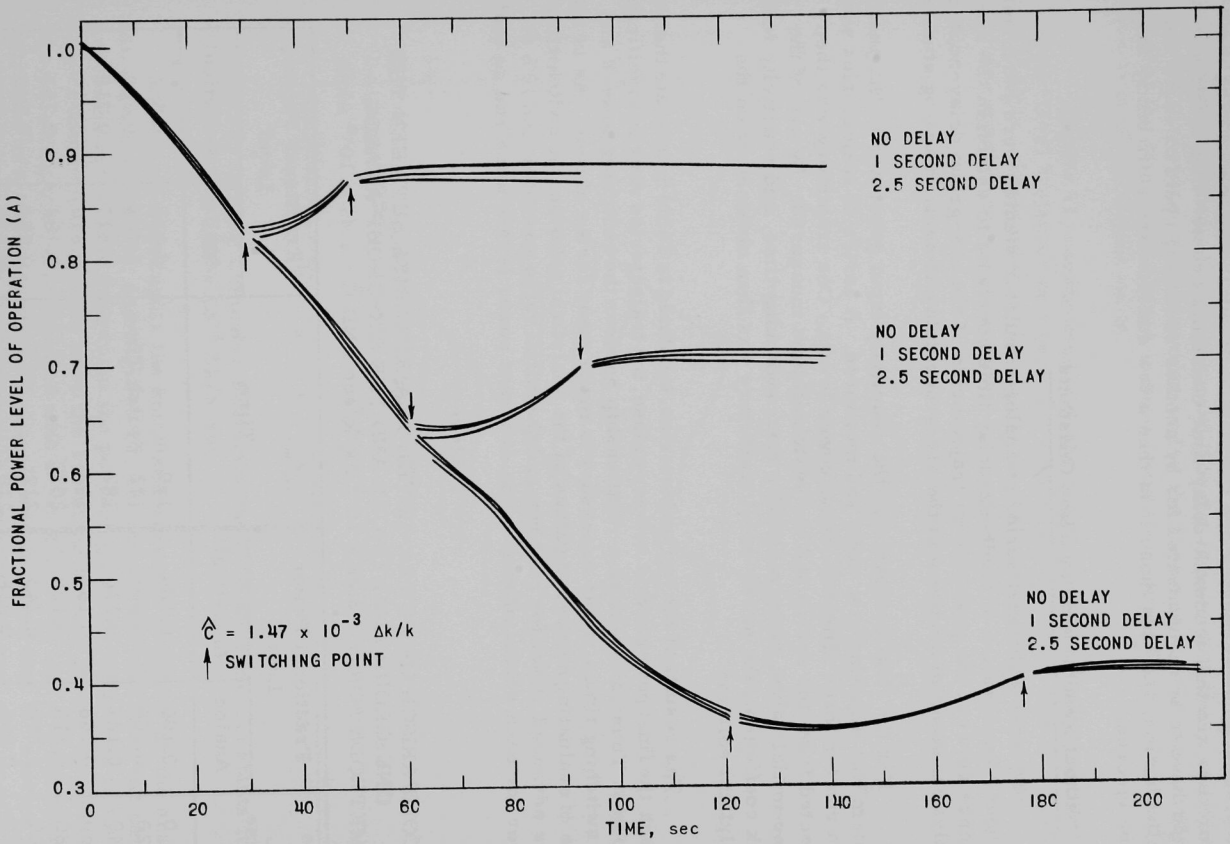

Fig. 10. Feedback-delay Time Constant Effect on "Falling Power Level" Trajectories for $\gamma = -2.34 \times 10^{-5}$ Δk/k/sec

The general conclusions that can be drawn from these analog simulator runs are that feedback-delay time constants greater than a few seconds might have to be compensated for by another switching cycle or more controller action, and thus those less than a few seconds are sufficiently small to be ignored.

B. Without Feedback-delay Time Constants

Several additional series of analog simulator studies were performed without consideration of feedback-delay time constants to establish the difference between the power-level trajectories of the one-group delay-neutron analytical solution studies and the six-group delayed-neutron analog studies.

For the first comparison, the reactivity input generator to the analog system was adjusted to a value and measured. A series of trajectories was then run for three different initial power levels. One trajectory was then selected from the series and the switching time measured. By use of the same initial value, ramp reactivity rate, switching time, and reactivity feedback coefficient, the power-level trajectory was then obtained from the analytical solution.

The results of the two trajectories, tabulated in Table 5, indicate that, although the final power levels are very close, the trajectories vary by significant amounts. Thus, to establish a relationship between the switching powers and the switching times, it was necessary to make many series of runs. As in the case of evaluating numerical values of the analytical solution, the switch times were advanced 10 sec for each run and the initial value was advanced 10% of power for each series of runs. The different power levels were run so that

Table 5

COMPARISON OF POWER-LEVEL TRAJECTORIES BETWEEN THE ONE-GROUP ANALYTICAL AND THE SIX-GROUP ANALOG METHODS FOR $\gamma = 2.28 \times 10^{-5}$ $\Delta k/k/sec$ AND $\hat{C} = 1.47 \times 10^{-3}$ $\Delta k/k$

Time	Fractional Power Level		Time	Fractional Power Level	
	Analog	Analytical		Analog	Analytical
0	0.100	0.100	160	0.685	0.562
20	0.105	0.109	172 Switch Time	0.784	0.670
40	0.127	0.126	182	0.817	0.718
60	0.148	0.152	192	0.810	0.745
80	0.215	0.190	202	0.788	0.753
100	0.290	0.243	212	0.754	0.745
120	0.365	0.318	215	0.735	0.739
140	0.515	0.421	216	0.730	

an average numerical gain or loss figure could be obtained as a function of the switching time. It was assumed that the same relationship would hold for the six-group representation as for the analytical one-group solution in that the fractional change in power was time-dependent only and not a function of the initial value.

Figure 11, constructed with the analog simulator, represents the power-level trajectories where $\gamma = 2.35 \times 10^{-5}$ $\Delta k/k/sec$ and $\hat{C} = 1.47 \times 10^{-3}$ $\Delta k/k$. The center of the circles on the trajectories represents a 10-sec marker or a switch time.

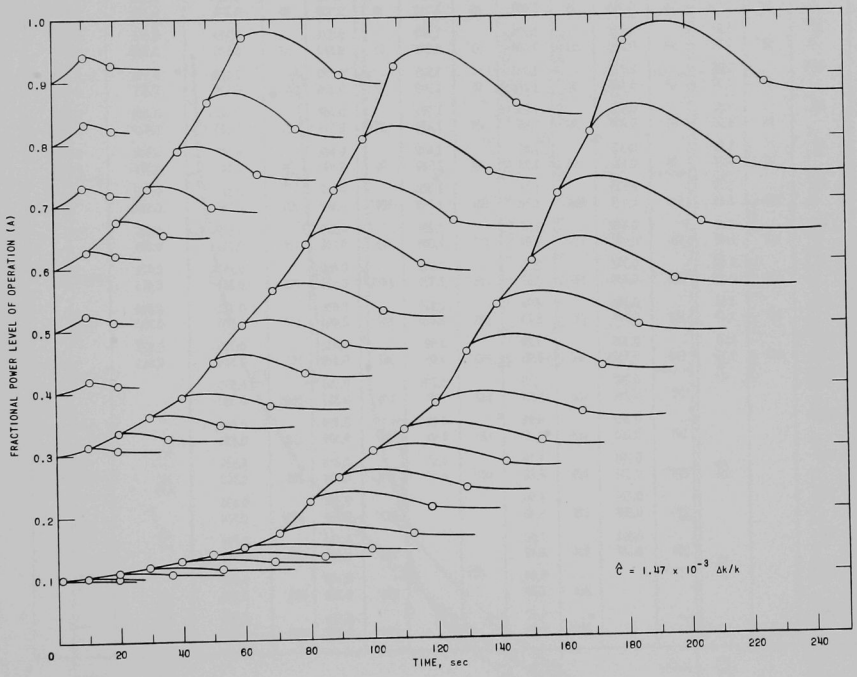

Fig. 11. Analog Computer Results without Delay Time Constants for $\gamma = 2.35 \times 10^{-5}$ $\Delta k/k/sec$

Table 6 represents the combined averages produced by the analog simulation technique, and Figures 12, 13, and 14, derived from the data contained in Table 6, represent the percentage of the difference in the final and switching powers over the switching power. It was discovered when plotting the curve labelled with □, in Figure 12 that a discontinuity occurred at a switch time of 70 sec. It was believed that the system parameters must have been disturbed in some manner and, as a result, the series was repeated and is plotted as the curve labelled with △.

Table 6

AVERAGED VALUES FOR FRACTIONAL CHANGE IN POWER LEVEL OBTAINED BY ANALOG SIMULATOR TECHNIQUE

Time - sec
Value - Fractional Change from Initial
$\hat{\gamma}$ - $\Delta k/k/sec$
$\hat{C}$ - $\Delta k/k$

Switch Time	$\hat{\gamma} = +3 \times 10^{-5}$ $\hat{C} = 1.47 \times 10^{-3}$		$\hat{\gamma} = -3 \times 10^{-5}$ $\hat{C} = 1.47 \times 10^{-3}$		$\hat{\gamma} = 2.28 \times 10^{-5}$ $\hat{C} = 1.47 \times 10^{-3}$		$\hat{\gamma} = 2.35 \times 10^{-5}$ $\hat{C} = 1.47 \times 10^{-3}$		$\hat{\gamma} = -2.35 \times 10^{-5}$ $\hat{C} = 1.47 \times 10^{-3}$		Final Time	Rerun Values for Different Initial Conditions for $\hat{\gamma} = 2.35 \times 10^{-5}$ and $\hat{C} = 1.47 \times 10^{-3}$		
	Final Time	Value	Final Time	Value	Final Time	Value	Final Time	Value	Final Time	Value		$A_0 = 0.100$	$A_0 = 0.300$	$A_0 = 0.600$
10		1.063		0.945		1.054		1.060		0.954		0.1045	0.314	0.629
	19⁻	1.039	19	0.967	19	1.036	19⁻	1.035	19	0.973	19	0.1025	0.308	0.620
20		1.163		0.870		1.120		1.155		0.902		0.109	0.335	0.675
	35⁻	1.116	36	0.908	35	1.094	35	1.110	35	0.930	36	0.106	0.326	0.654
30		1.21		0.793		1.224		1.270		0.831		0.123	0.361	0.729
	50⁺	1.22	52	0.842	51	1.174	51⁻	1.205	51	0.872	52	0.120	0.348	0.698
40		1.46		0.712		1.344		1.385		0.770		0.128	0.392	0.790
	64⁺	1.37	67	0.768	66	1.274	65	1.305	67⁻	0.816	67	0.125	0.377	0.751
50		1.67		0.637		1.43		1.525		0.707		0.1425	0.449	0.869
	78	1.55	81	0.697	80	1.35	79	1.435	81⁺	0.754	81	0.133	0.429	0.824
60		1.92		0.565		1.62		1.680		0.642		0.149	0.507	0.972
	91	1.77	96	0.628	91	1.53	93	1.580	96	0.692	94	0.145	0.475	0.908
70		2.30		0.503		1.77		1.870		0.578		0.171	0.563	
	103	2.10	110	0.561	104	1.70	106	1.760	109⁺	0.627	105	0.167	0.528	
80		2.67		0.443		1.97		2.235		0.523		0.222	0.637	
	115	2.45	125	0.497	115	1.84	117⁻	2.065	123	0.568	118	0.211	0.603	
90		3.19		0.392		2.55		2.525		0.469		0.261	0.722	
	126	2.89	138	0.439	131	2.37	128⁺	2.335	137⁻	0.513	130	0.241	0.673	
100		3.81		0.345		2.94		2.835		0.426		0.301	0.804	
	137	3.49	152	0.389	143	2.73	140	2.625	149⁺	0.466	141	0.280	0.750	
110		4.55		0.300		3.29		3.30		0.382		0.335	0.923	
	147	4.12	164	0.336	154	3.08	150	3.05	162	0.419	152	0.314	0.861	
120				0.260		3.70		3.705		0.350		0.379		
			177	0.294	166	3.50	162	3.41	176	0.383	166½	0.360		
130				0.226		4.52		4.29		0.309		0.461		
			191⁻	0.256	173	4.25	172	3.96	189⁻	0.339	174	0.436		
140				0.201		5.19		4.85		0.278		0.535		
			205	0.231	185	4.84	183⁺	4.47	199	0.304	185	0.500		
150				0.177		5.90				0.240		0.606		
			219	0.207	195	5.60			212⁻	0.266	195½	0.574		
160				0.156		7.00				0.214		0.713		
			234	0.187	204	6.48			225	0.240	205	0.663		
170						7.84				0.193		0.812		
					214	7.32			236	0.212	216	0.762		
180						9.12				0.176		0.955		
					223	8.48			250	0.197	225	0.887		

It may be observed from Figures 12 and 13 that for decreasing power levels, there appears to be an upward swing for the long switching times. This upward swing may be due to errors in the reading of power levels that are close together and then dividing the difference between them by the small number that represents the switching power level.

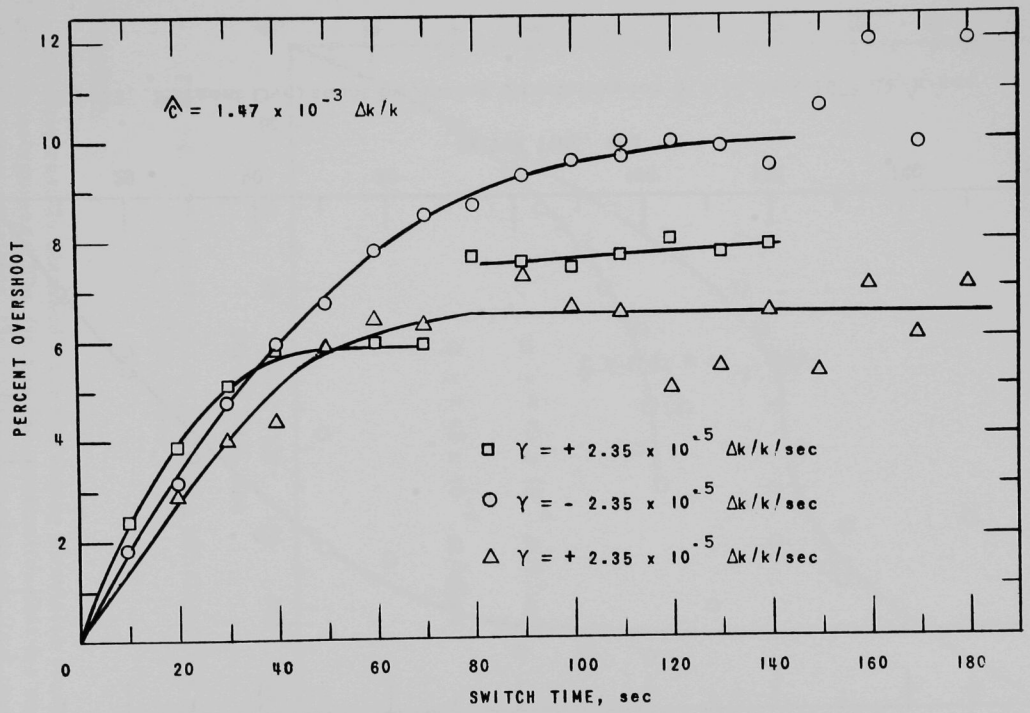

Fig. 12. Percent Overshoot by Analog Simulation for $\gamma = \pm 2.35 \times 10^{-5}$ Δk/k/sec

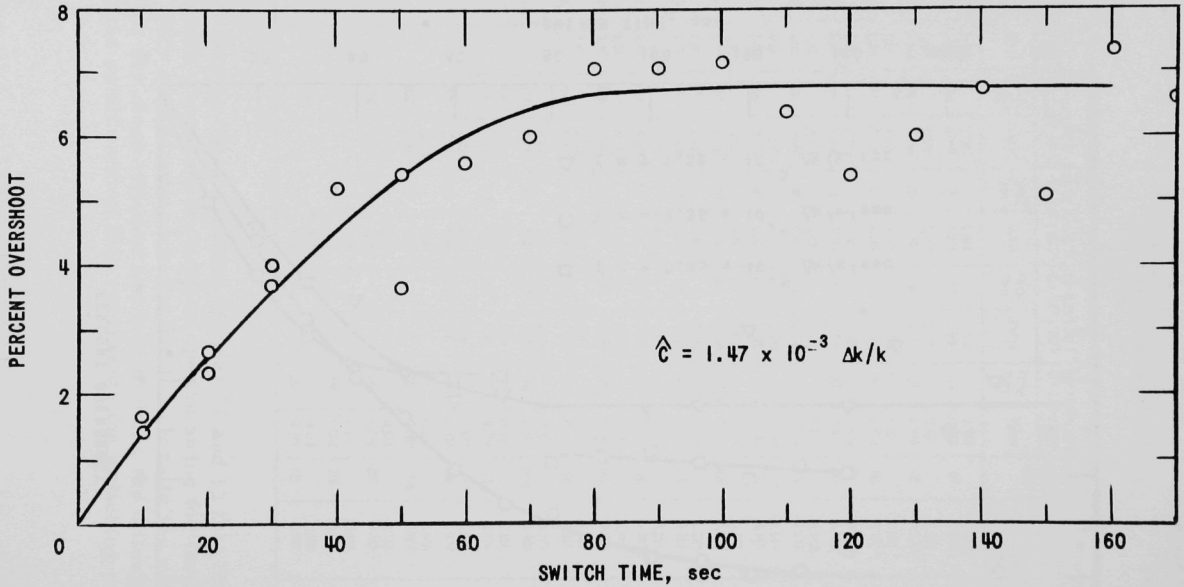

Fig. 13. Percent Overshoot by Analog Simulation for $\gamma = +2.28 \times 10^{-5}$ $\Delta k/k/sec$

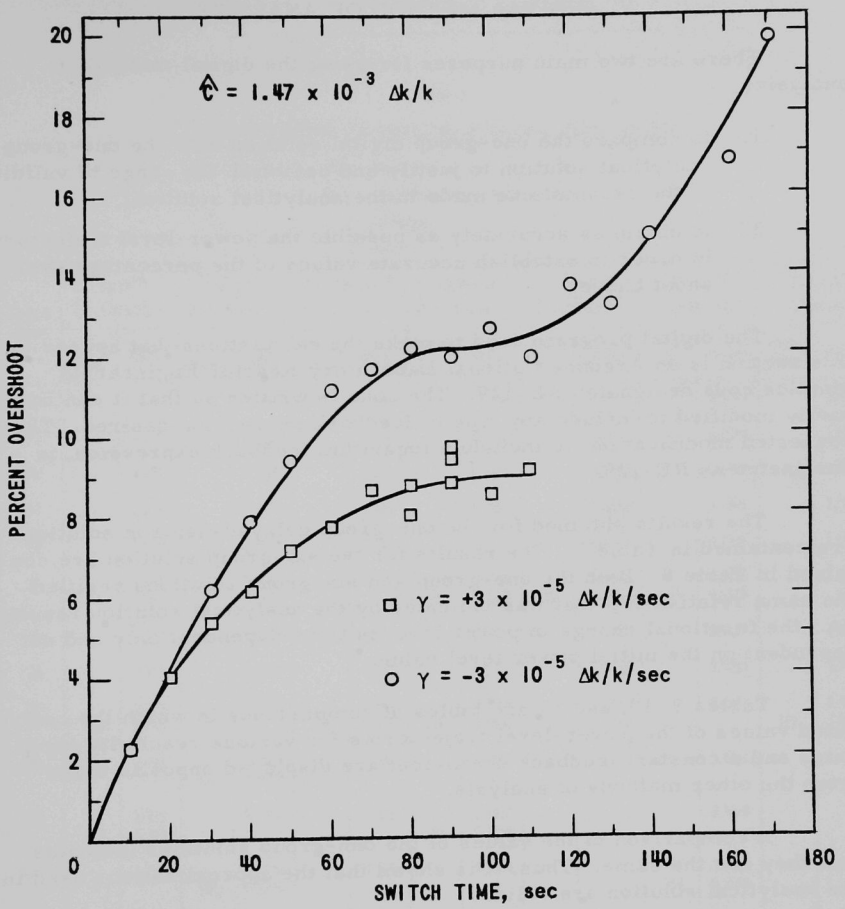

Fig. 14. Percent Overshoot by Analog Simulation for $\gamma = \pm 3 \times 10^{-5}$ Δk/k/sec

C. Conclusion

The main results obtained from the analog simulator study are divided into two categories. The first is the verification that for small feedback-delay time constants, the analytical results for final power levels are consistent with the analog simulator studies. The second is the establishing of the general shape and values of the percentage overshoot curve.

V. DIGITAL METHOD OF ANALYSIS

There are two main purposes for using the digital method of analysis:

1. to compare the one-group digital solution with the one-group analytical solution to justify and establish the range of validity of the assumptions made in the analytical solution;
2. to obtain as accurately as possible the power-level trajectories in order to establish accurate values of the percentage overshoot curves.

The digital program used to make the calculations that appear in this section is an Argonne National Laboratory Reactor Engineering kinetics code designated RE-129. The code is written so that it can be easily modified to include any type of feedback expression desired. The requested modification, to include a logarithm feedback expression, is designated as RE-129J.

The results obtained for the one-group delayed-neutron solution are contained in Table 7. The results for the six-group solution are contained in Table 8. Both the one-group and six-group solutions verified the same relationship that was indicated by the analytical solution results, i.e., the fractional change in power level is time-dependent only and not dependent on the initial power level value.

Tables 9, 10, and 11 are tables of comparisons in which the computed values of the power-level trajectories for various reactivity ramp rates and a constant feedback coefficient are displayed opposite those from the other methods of analysis.

A comparison of the values of the one-group solutions indicates that they are the same. Thus, it is shown that the approximations used in the analytical solution are valid.

Table 12 represents the results when the neutron lifetime is neglected in the analytical solution. In the investigation, the neutron lifetime was varied from that of a fast reactor to that of a thermal reactor, and it was found that no appreciable change occurs for the ramp rates used until the neutron lifetime increased to values above 1×10^{-4} sec. Thus, for the ramp rates used, the analytical solution would apply to almost any reactor with a characteristic "logarithm of the power" feedback and no appreciable feedback-delay time constants.

Table 7

RESULTS OF DIGITAL SOLUTION USING ONE GROUP OF DELAYED NEUTRONS

Time - sec

Value - Fractional Change from Initial

γ - $\Delta k/k/sec$

$\hat{C}$ - $\Delta k/k$

Switch Time	$\gamma = 3 \times 10^{-5}$ $\hat{C} = 1.47 \times 10^{-3}$		$\gamma = -3 \times 10^{-5}$ $\hat{C} = 1.47 \times 10^{-3}$		$\gamma = 2.35 \times 10^{-5}$ $\hat{C} = 1.47 \times 10^{-3}$		$\gamma = -2.35 \times 10^{-5}$ $\hat{C} = 1.47 \times 10^{-3}$		$\gamma = +3 \times 10^{-5}$ $\hat{C} = 2.05 \times 10^{-3}$		$\gamma = -3 \times 10^{-5}$ $\hat{C} = 2.05 \times 10^{-3}$		$\gamma = 2.35 \times 10^{-5}$ $\hat{C} = 2.05 \times 10^{-3}$	
	Final Time	Value	Final Time	Value	Final Time	Value	Final Time	Value	Final Time	Value	Final Time	Value	Final Time	Value
10		1.046		0.9567		1.036		0.9658		1.04274		0.9599		1.033
20		1.119		0.8985		1.092		0.9192		1.10741		0.9070		1.083
30		1.221		0.8307		1.168		0.8638		1.19463		0.8460		1.148
40		1.356		0.7578		1.266		0.8030		1.30583		0.7805		1.230
50		1.529		0.6833		1.389		0.7395		1.44316		0.7137		1.329
60		1.747		0.6099		1.539		0.6755		1.60946		0.6476		1.447
	91	1.804	94	0.5875			93	0.6550	87	1.620	89	0.6389		
70		2.020		0.5396		1.721		0.6126		1.80830		0.5838		1.583
80		2.359		0.4737		1.939		0.5521		2.04399		0.5234		1.741
90		2.777		0.4130		2.199		0.4948		2.32167		0.4671		1.921
	126	2.983			127	2.328	131	0.4604	120	2.38262			121	1.966
100		3.293		0.3578		2.507		0.4412				0.4151		
			144	0.3204										
110		3.928		0.3084		2.872		0.3917				0.3676		
	148	4.304					155	0.3554						
120		4.708		0.2644		3.304		0.3464				0.3245		
			167	0.2286							158	0.3043		
130		5.667		0.2257		3.812		0.3053						
140		6.844		0.1919		4.412		0.2682						
					181	4.838								
150		8.290		0.1626				0.2349						
	190	9.314	201	0.1347										
160								0.2053						
170								0.1789						
							222	0.1528						

Table 8

RESULTS OF DIGITAL SOLUTION USING SIX GROUPS OF DELAYED NEUTRONS

Time - sec

Value - Fractional Change from Initial

γ - $\Delta k/k/sec$

$\hat{C}$ - $\Delta k/k$

Switch Time	$\gamma = 3 \times 10^{-5}$ $\hat{C} = 2.05 \times 10^{-3}$		$\gamma = -3 \times 10^{-5}$ $\hat{C} = 2.05 \times 10^{-3}$		$\gamma = 2.35 \times 10^{-5}$ $\hat{C} = 2.05 \times 10^{-3}$		$\gamma = -2.35 \times 10^{-5}$ $\hat{C} = 2.05 \times 10^{-3}$		$\gamma = +3 \times 10^{-5}$ $\hat{C} = 1.47 \times 10^{-3}$		$\gamma = -3 \times 10^{-5}$ $\hat{C} = 1.47 \times 10^{-3}$		$\gamma = +2.35 \times 10^{-5}$ $\hat{C} = 1.47 \times 10^{-3}$		$\gamma = -2.35 \times 10^{-5}$ $\hat{C} = 1.47 \times 10^{-3}$	
	Final Time	Value	Final Time	Value	Final Time	Value	Final Time	Value	Final Time	Value	Final Time	Value	Final Time	Value	Final Time	Value
10		1.05706		0.9473		1.044		0.958357		1.064		0.9416		1.049		0.953827
															18	0.970452
20		1.14440		0.879202		1.11086		0.903604		1.16720		0.864450		1.12787		0.8915
	33	1.10612	33	0.908091	33	1.08180	33	0.926921	34	1.12606	35	0.899594	34	1.09676		
30		1.25663		0.8075		1.194		0.844759		1.306		0.7828		1.230		0.8240
40		1.39439		0.736464		1.29454		0.785180		1.485		0.7023		1.35825		0.755581
	61	1.31906	63	0.781711	61	1.24019	63	0.823280	63		66	0.7498	64	1.29577	65	0.791889
50		1.56011		0.6681		1.412		0.726596		1.711		0.6256		1.514		0.6887
60		1.75723		0.6036		1.54762		0.670004		1.99384		0.5541		1.70223		0.6246
	86	1.64337	91	0.6535	87	1.46354	90	0.710734	89	1.87495	94	0.6001	90	1.61646	94	0.6627
70		1.99002		0.5435		1.70356		0.615994		2.345		0.4886		1.927		0.5642
80		2.26362		0.4878		1.88166		0.564912		2.779		0.4290		2.195		0.5078
							116	0.605684	113							
90		2.58402		0.436795		2.08426		0.516938		3.317		0.3755		2.514		0.4556
	120	2.39651	129	0.478369	121	1.96096			124	3.114			125	2.390	135	0.4883
100		2.95828		0.3902		2.31403		0.472139		3.980		0.3276		2.890		0.4077
											149	0.3575				
110		3.39456		0.3480		2.57400		0.430501		4.796		0.2852		3.336		0.3640
									146	4.507					161	0.3904
120		3.90239		0.309746		2.86761		0.391956		5.801		0.2477		3.861		0.3242
	152	3.61001	167	0.344371	153	2.67633	165	0.424596			176	0.2717	158	3.681		
130		4.49281		0.275312		3.19876		0.356393		7.03627		0.2146		4.481		0.2883
									167	6.63282						
140		5.17862		0.244380		3.57182		0.323679		8.555		0.1857		5.210		0.255852
													180	4.951	198	0.272759
150		5.97470		0.216667		3.99173		0.293660		10.421		0.1604				0.2267
	183	5.52072	203	0.242546					188	9.817	214	0.1749				
160						4.46403		0.266176		12.713						0.2007
					195	4.18185	212	0.290533								
170								0.241061								0.1774
															235	0.1888
180								0.218149								
							234	0.237670								

Table 9

COMPARISON OF RESULTS OF ONE-GROUP AND SIX-GROUP SOLUTIONS FOR $\gamma = -3 \times 10^{-5}\ \Delta k/k/sec^{\dagger}$

Time, sec	1-group		6-group	
	Analytical*	Digital*	Digital*	Analog*
0	1.000	1.000	1.000	1.000
10	0.956	0.956	0.941	0.945
20	0.898	0.898	0.864	0.870
30	0.831	0.831	0.783	0.793
40	0.758	0.758	0.702	0.712
50	0.684	0.683	0.625	0.637
60	0.610	0.610	0.554	0.565
70	0.540	0.540	0.488	0.503
80	0.474	0.474	0.429	0.443
90	0.413	0.413	0.375	0.392
100	0.358	0.358	0.328	0.345
110	0.309	0.308	0.285	0.300
120	0.265	0.264 (switch time)	0.248	0.260
130	0.243	0.243	0.236	0.244
140	0.231	0.230	0.234	0.241
150	0.225	0.224	0.237	0.247
160	0.225	0.225	0.247	0.261
167	0.230	0.229		
170			0.261	0.278
176			0.272	
177				0.294

†Feedback coefficient $\hat{C} = 1.47 \times 10^{-3}\ \Delta k/k$

*All values are in fraction of maximum power level of operation.

Table 10

COMPARISON OF RESULTS OF ONE-GROUP AND SIX-GROUP SOLUTIONS FOR $\gamma = +3 \times 10^{-5}$ $\Delta k/k/sec^{\dagger}$

Time, sec	1-group Delayed Neutrons		6-group Delayed Neutrons	
	Analytical*	Digital*	Digital*	Analog*
0	0.100	0.100	0.100	0.100
10	0.104	0.104	0.106	0.106
20	0.111	0.111	0.116	0.116
30	0.121	0.122	0.131	0.121
40	0.134	0.135	0.148	0.146
50	0.152	0.153	0.171	0.167
60	0.174	0.174	0.199	0.192
70	0.201	0.202	0.234	0.230
80	0.235	0.236	0.278	0.267
90	0.277	0.278	0.332	0.319
100	0.328	0.329	0.398	0.381
110**	0.391	0.393	0.480	0.455
120	-	0.423	0.502	0.467
130	0.436	0.438	0.493	0.457
140	0.438	0.438	0.469	0.434
146			0.450	
148		0.430		0.412
149	0.426			

†Feedback coefficient $\hat{C} = 1.47 \times 10^{-3}$ $\Delta k/k$.

*All values are in fraction of maximum power level of operation.

**Switch time.

Table 11

COMPARISON OF RESULTS OF THE ANALYTICAL SOLUTION AND THE DIGITAL SOLUTION FOR $\gamma = +3 \times 10^{-4}$ $\Delta k/k/sec$ †

Time, sec	Analytical*	Digital*	IBM-704 $\dot{N}/N$ sec	k_{exs} Analytical	k_{exs} Digital
0	0.100	0.100			
5		0.124	19.3		1.19×10^{-3}
10	0.169	0.168	13.7	2.23×10^{-3}	2.23×10^{-3}
15		0.257	10.3		3.11×10^{-3}
20	0.444	0.442	8.3	3.81×10^{-3}	3.82×10^{-3}
25		0.858	6.9		4.34×10^{-3}
30	1.879	1.858 (switch time)	6.1	4.69×10^{-3}	4.70×10^{-3}
35		1.933	-143		3.20×10^{-3}
40		1.795	-46		1.81×10^{-3}
46		1.522	-30		2.49×10^{-4}

†Feedback coefficient $\hat{C} = 1.47 \times 10^{-3}$ $\Delta k/k$.

*All values are in fraction of maximum power level of operation.

Table 12

COMPARISON OF RESULTS FOR VARIATION OF THE NEUTRON LIFETIME†

A_0 = 10% Power Level

ℓ*, sec	A, %, at 100 sec	A, %, at 160 sec
8×10^{-8}	32.93	100.6
1×10^{-5}	32.93	100.6
1×10^{-4}	32.90	100.5
1×10^{-3}	32.65	99.48
1×10^{-2}	30.38	89.89

†Feedback coefficient $\hat{C} = 1.47 \times 10^{-3}$ $\Delta k/k$; applied reactivity, 3×10^{-5} $\Delta k/k/sec$.

The results from Tables 7 and 8 were used to calculate the percentage overshoot as was calculated for the previous methods of analysis (see Figures 15 and 16). The results of the six-group analysis agree, in general, with the shape of the curve of the analog values, but not necessarily with the values. The shape of the "percent overshoot curves" for the one-group solution as calculated from the analytical results and the digital results do not agree with the shape of those from the six-group solutions. The conclusion that can be drawn from this is that, although the one-group solutions predict the final power levels satisfactorily, they cannot be used to predict the switching powers.

Thus, if a controller were to use a time-switching base, the analytical solution would be used, but if a controller were to use a power-level-switching base, the percent overshoot curves of the six-group analog or digital calculations must be used to indicate the proper switching power level.

Table 13 contains the values of the precursors of the six groups of delayed neutrons used in the digital computer program. The values used in the one-group solutions were the same as those used in the analytical solution:

$\lambda = 0.081$; $\beta = 7.35 \times 10^{-3}$

Table 13

SIX-GROUP DELAYED-NEUTRON PRECURSORS

Group	λ_i	β_i
1	1.27×10^{-2}	2.32×10^{-4}
2	3.18×10^{-2}	1.424×10^{-3}
3	1.153×10^{-1}	1.333×10^{-3}
4	3.12×10^{-1}	2.957×10^{-3}
5	1.4	1.122×10^{-3}
6	3.87	2.82×10^{-4}

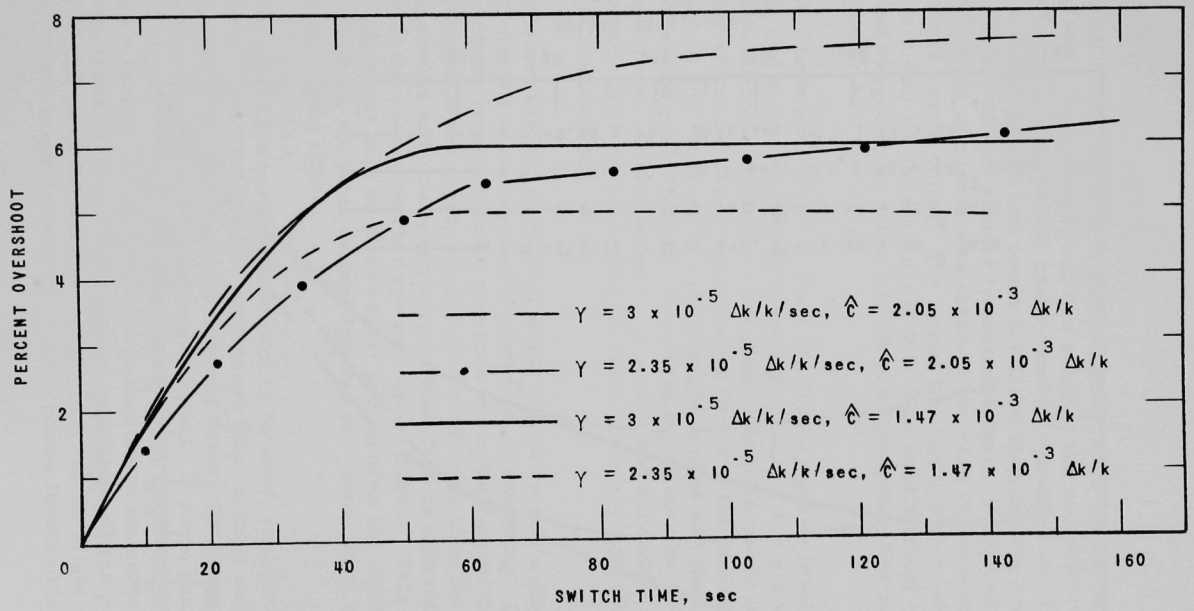

Fig. 15. Percent Overshoot from Digital Method of Analysis for Positive Reactivities

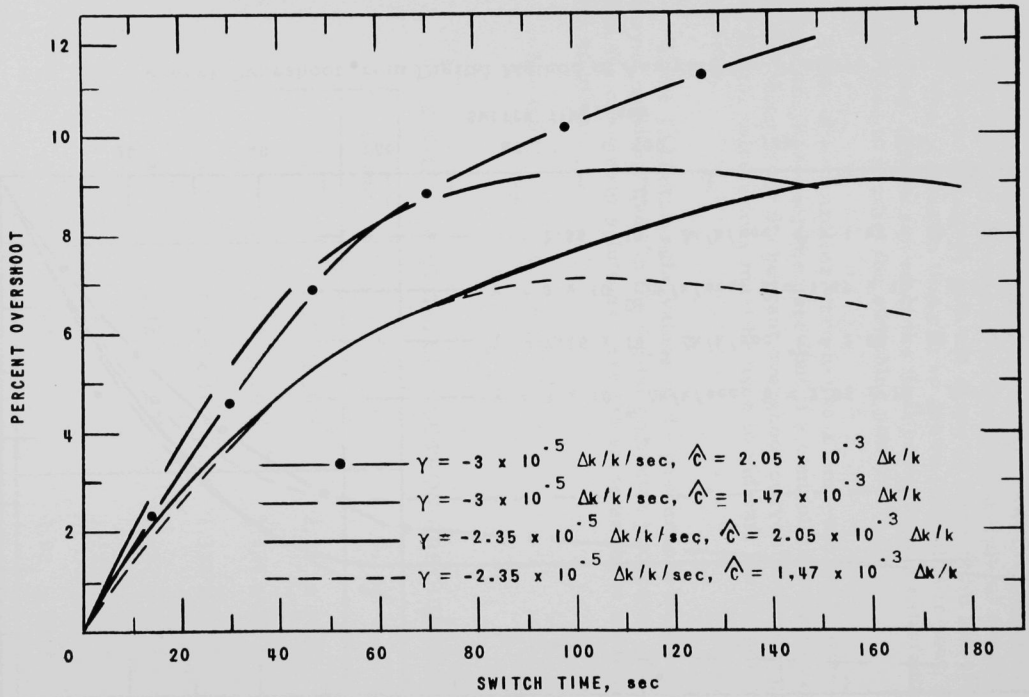

Fig. 16. Percent Overshoot from Digital Method of Analysis for Negative Reactivities

VI. CONCLUSIONS AND CONTROLLER DESIGN

A. Conclusions

For all three methods of analysis used, i.e., analytical, digital, and analog, the simplest approach to a study of the parameters involved consisted of selecting an initial power level of operation and a switching time. The final stop time and power level are then determined by the point at which the excess reactivity becomes zero. By means of this approach, a series of curves was obtained for each initial power level and for various switch times. The initial fractional power levels used ranged from 0.1 to 1.0 in intervals of 0.1. The switch times used started at 10 sec and ranged up to 240 sec in 10-sec intervals. The final power levels ranged from 0.10 to 1.10.

This "time switching" concept of changing power level could be directly applied to the reactor by means of a control system which would consult a tabulation or chart for each given change in power level and obtain the desired times. The control would then run the desired reactivity into the reactor for the first specified length of time and then reverse the rod for the second specified time, thus arriving at the new power level in the minimum time. Allowing that the primary and secondary systems are under automatic control, a reactor operator could perform the same task by means of the same tabulation.

The other method of control which allows more flexibility for parameter changes is the method of power-level switching. In this method, the reactivity ramp would be reversed when the reactor had reached a predetermined power level, which may be different than the final desired level. The second and final switchpoint would then be determined by the condition that the power reached the new desired level. This method of control is dependent only on power level and ignores the actual times for switching, whereas the first method ignores the power level and depends only on the switching times.

In selecting the method of control to be used, reactor safety must be considered. The first method considered (that of time control) completely ignores the actual transient involved during the change of power level, which could lead to a hazardous situation. If some reactor parameter should change even slightly, the power level might exceed safe limits or approach a scram condition without indication to the control system of any deviation from normal. A precise knowledge of all the parameters is necessary to end up at the desired power level. Even slight variations of parameters cause large errors in the final power levels obtained by this method.

The operation of the power-level-based controller is much more consistent with requirements of reactor safety in that the power is always monitored by the controller. Should a slight change in some parameter occur to cause the power to rise slightly faster than expected, the power controller would switch at the predetermined power level and cause less error than the time control, which might run for 5 or 10 sec past the desired switching power and create a large error in the final value. Hence, for a more accurate and safe controller, it was decided to use the power-level method for determining the switching point.

B. Controller Design

1. Use of Existing Equipment for Reactor Control

It is desirable when revising or modifying the control procedures or operation to make use of as much of the previously designed and installed equipment as possible. One such piece of equipment that might be utilized in automating the reactor for minimum time response is the automatic flux controller, which was designed to maintain a preset power level once it had been achieved by manual operation of the reactor. One such piece of equipment was designed by the Control and Instrumentation Section, Reactor Engineering Division, at Argonne National Laboratory. It is similar in the principle of operation to the CP-5 reactor automatic controller, but it contains some modifications which increase its flexibility. The main method of operation is as follows:

A reference voltage corresponding to the desired power level is compared with the voltage generated by nuclear measurement instrumentation. The "error" is positive or negative, depending upon whether the reactor power is higher or lower than the reference voltage. An adjustable dead-zone error is contained within the controller that allows an error voltage to exist, corresponding to a fixed percentage of the existing power level without causing any resultant motion of the control rods. Should the error become greater than the prescribed limits, the controller will actuate the control rods so as to reduce the error. Thus, the reactor power level will be maintained within preset limits.

2. Proposed Modifications

Contained in the actual controller is a device which limits the maximum allowable time of travel of the control rod. The limits contained in this device are such that any rod motion, in one direction, greater than that specified would cause the controller to switch out of automatic. A modification of the controller system would be necessary to cause this device to be inoperative during large power transients, thus only using it to maintain steady state.

It was noted that in changing the desired power levels of operation of the reactor in a minimum time, the desired switching power occurs at a different power level than the final desired power level. Curves were obtained, giving the percentage difference at the switching time that the reactivity should be reversed in order to arrive at the desired final value. One of the proposed modifications to the controller would be an "n_0 offset generator" which would change the reference value of n_0 by the proper percentage difference so that the controller will enter the "dead zone" at the proper switching power. The "n_0 offset generator" will be de-activated at the switch time, thus resetting the value of the reference n_0 to the desired value. This sudden change in reference n_0 will cause an error and the rods will be moved to compensate for it, thus initiating the rod reversal.

An example of what is meant is as follows:

A reactor is operating at a steady-state power level until time t = 0 when the desired power output is suddenly changed to a higher value (see Figure 17). The controller will sense a large error and attempt to compensate by increasing the actual value of the reactor power. As the reactivity is being inserted, the value of the reference n_0 will increase by the necessary percentage until at $t = t_1$, the actual power level crosses into the dead zone of the controller and the reactivity insertion is stopped. At this time, the effective value of n_0 is decreased to the desired final value of power level, thus creating an error, the sign of which will cause the controller to decrease the reactivity until the actual power level of the reactor again enters the controller dead zone. At this time (t_2), the control rod will be shut off, thus completing the power-change cycle. The reference value of n_0 is decreased at t_1 by eliminating the error offset percentage that has been added since the time t = 0. This offset error percentage is a combination of the percentage overshoot values plus one half of the dead-zone bandwidth.

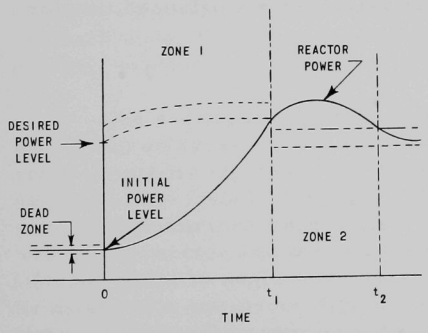

Fig. 17. Proposed Controller Operation

One method of adding the n_0 displacement voltage would be the use of a summing junction at the n_0 voltage input to the controller, thus enabling a time-controlled function generator to add its output to that of n_0, giving the new displaced value. The function generator could be reset to zero at the time the actual power entered the controller dead zone,

hence bringing the voltage at the summing junction back to n_0, the final desired value. As a safety device, the voltage polarity of the control rod motor tachometers could be used in a logic circuit to keep track of the reactivity insertion rate to determine whether the reactivity being inserted is positive or negative.

Up to this point, a positive or negative ramp rate of reactivity has been assumed to be easily obtainable. This is not necessarily the case. It is well known that the reactivity rod worth per unit length displacement is much greater near the middle of the core than it is near the edge. The reactivity worth of a control rod follows the characteristic S-curve. One such curve is shown in Figure B-3. In order to insert a continuous ramp rate of reactivity, it is necessary to have small changes in several control rods rather than to attempt to control with only one rod. In a reactor such as the EBR-II there are twelve control rods all located on the periphery of the hexagonal core; a series of these rods could be selected to be each moved a small distance. If the rods are of the same worth at about the same distance of insertion, then the reactivity ramp will be fairly constant. A logic network may have to be devised to select the control rod to be moved in order to keep all the rods at about the same insertion point. The logic network would thus assure a balanced reactor flux.

VII. RESULTS

In this dissertation there are presented three main contributions to the field of reactor technology: 1) generation of a feedback model for reactor transients; 2) solution of the fast reactor kinetics equations for step and ramp reactivity inputs and power level based feedback reactivity; 3) modification of a controller in order to perform time-optimum control of the reactor model mentioned under 1) above.

The power reactor model developed is based on the EBR-II and includes the assumption that normal operation will take place at all times, i.e., the flow rates and temperatures are maintained at the normal values for the particular power level of operation. It is further assumed that the variation in flow rate is approximately linear with power and the heat transfer is temperature-dependent.

The approach that is used is based on the concept of a transfer function with the feedback gain turning out to be a nonlinear quantity which is power- and flow-dependent. The predominant feedback-delay time constants are expected to be small, and as a result it was assumed that they could be neglected. The resultant approximate expression for reactivity feedback under the above assumptions turns out to be proportional to the natural logarithm of the power.

The second contribution consists of the analytical solution of the one-group delayed-neutron reactor kinetics equations with a step-and-ramp reactivity input and with the expression for feedback reactivity developed in the model. During the general development of the solution, several assumptions were made. One was that, since the reactor chosen was a fast reactor and the reactivity input rates were slow, the neutron lifetime could be neglected. This assumption and the others were checked by means of a one-group digital computer solution of the kinetics equations. The results confirmed that the analytical solution was as good as the digital for effective neutron lifetimes less than 1×10^{-4} sec for slow ramp rates, and for ramp rates of 1×10^{-3} $\Delta k/k/sec$ with a neutron lifetime of 1×10^{-8} sec.

Also, during the general development of the analytical solution, an expression was obtained [see Equations (25) and (26)] in which different feedback expressions could be used instead of the logarithm of the power. One of these possibilities is discussed as Case I. Here the expression for reactivity feedback is a constant. The resultant zero-power kinetics equation solution is the same as one previously published.[18] Another possibility which is not discussed involves a reactivity-feedback expression which is proportional to the logarithm and the square root of the logarithm of the power.

The third contribution is the development of possible modifications for converting an existing automatic flux controller into one that would control the reactor model on a time-optimum basis during changes in power level.

Of the two independent bases of control selected for consideration, it was found that a one-group delayed-neutron solution of the kinetics equations could be used for the time-based control system, but that the six-group delayed-neutron solutions must be used for a power-level-based control system. For reasons of safety, the time-based control was eliminated from consideration. Hence, the analog computer simulation and digital computer solution of the six-group kinetics equations were used to determine the proper switching powers to arrive at the new desired power level in minimum time. The resultant design for the power-level-based controller utilizes an offset function generator which gives a modified desired power level to the existing controller in order to cause the control-element switching to occur at the proper time.

The accuracy obtainable from the digital computer was utilized in obtaining the "percent overshoot curves." These curves represent the percent difference in the actual power and desired power at the switch time and, hence, represent the shape and magnitude of the error voltage output of the offset function generator. An additional constant offset error must also be added to the controller input in order to make the controller operate correctly. The magnitude of this error setting must be equal to one-half of the dead-zone bandwidth.

The applicability of the contributions made in this dissertation to other systems has already been touched on indirectly in the preceding paragraphs. The main restrictions on the model imply a fast or intermediate reactor with no feedback time constant and reactivity control elements which generate, in the reactor, ramp rates of reactivity insertion and withdrawal. The applicability of the one-group analytical solution to other feedback expressions is possible except when the excess reactivity is near one dollar.

The values obtained for the design of the offset generator apply primarily to the particular case in question but the control method is general and could be used with other on-off type controllers.

APPENDIX A

PRELIMINARY EBR-II ANALYSIS

1. Introduction

The analysis in this Appendix was performed with the idea of obtaining information on the variables and response limitations of the main system components of EBR-II. The results obtained indicate that the reactor, under the limitation of one control rod in motion at a time, will be the response-limiting component of the entire power plant system.

The EBR-II power plant system consists of three main subsystems: the primary sodium system, the secondary sodium system, and the steam-water loop. The primary sodium system consists of:

1. the primary sodium reservoir, a large tank containing 86,000 gal of sodium, the reactor, and the primary heat exchanger;
2. the reactor, which is a fast reactor with a design capability of 62.5-MW thermal power;
3. the primary heat exchanger, which is the energy-transfer point between the primary and secondary sodium systems;
4. the primary sodium pumps, which are two large, three-phase squirrel-cage centrifugal pumps, controlled by motor-generator sets and capable of pumping over 4,000 gal/min each.

The secondary system is an isolation and transport system whose primary purposes are to reduce radiation hazards by confining the radioactive sodium to the primary tank and to transport the energy produced in the primary systems to the steam-water loop. It consists of:

1. a three-phase linear electromagnetic pump controlled by an amplidyne;
2. the sodium side of the superheaters and evaporators;
3. lengths of stainless steel piping long enough to span the distance from the building containing the primary system to the building containing the evaporators and superheaters;
4. the secondary sodium side of the primary heat exchanger.

The steam-water loop is similar in most respects to a conventional steam-power plant in that the deaerated preheated water is evaporated in a boilier section (the evaporator) and then superheated (in the superheater)

prior to passing into the turbine of the generator. From the turbine, the "spent" steam is condensed and returned to a storage tank or to the deaerator to start the cycle again.

In the following analysis, some of the important system and component parameters have been calculated and compared to determine their importance with respect to complete automation of the power plant system. The analysis consists of three main topics:

1. Calculations of transport delay times were made to determine the possible cycling times for loop flow and an average time of energy from the reactor to the turbine of the generator.

2. Heat-transfer calculation and comparisons were made to determine the relative change in magnitudes of heat-transfer coefficients in changing power levels of operation of the system. The effects noted here are due mainly to changes in flow rates associated with the different power levels of operation.

3. Calculations of approximate response time of different system components were made to determine the slowest responding component of all the systems. This one (or more) component will limit the response rate of the entire power plant system and also determine the sequence of control used on the plant.

With respect to the approximate calculation of response time, no calculations were made to determine whether the maximum rates of power change were consistent with the maximum allowable thermal stresses of each of the individual system components.

Figure A-1 is a schematic representation of a general three-loop reactor power system. This schematic is modified slightly in Figure A-2 to represent the basic configuration of the EBR-II power plant system. The modification consists of the addition of a large reservoir in the

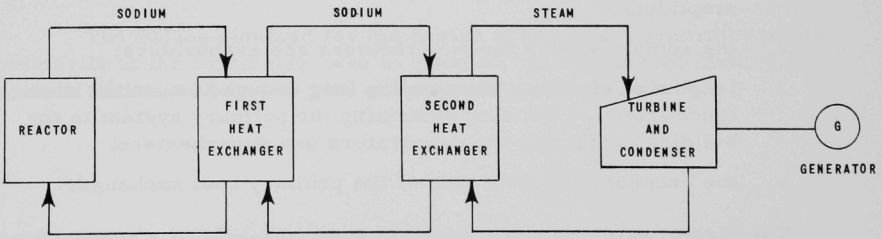

Fig. A-1. General Three-loop Nuclear Power System

primary sodium loop and the inclusion of the preheater section in the water-steam loop as a separate unit from the boiler and superheater sections. Figure A-2 also shows some of the expected operating conditions within the plant.

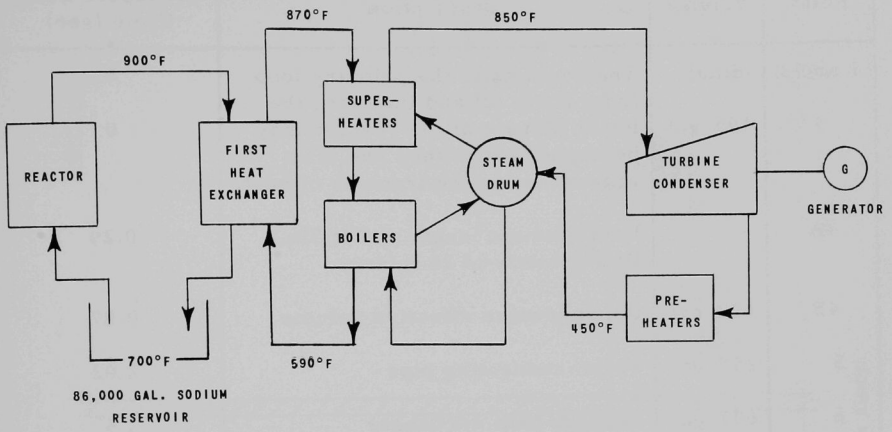

Fig. A-2. EBR-II Power System

2. Calculations of Transport Delay Times

a. Primary Sodium System

The flow through the primary system can be represented by a three-component block diagram, as in Figure A-3. The primary pumps are placed directly into the large sodium reservoir with a roughly 2-ft length of pipe on the inlet. The sodium, after passing through the inlet and the pump, goes into the lower plenum of the reactor. After passing through the reactor and into the upper plenum, the sodium then goes through a 14-in. pipe to the primary heat exchanger. The heat exchanger then empties directly back into the large reservoir. Through use of the volumes of the different components and the full-flow rate of 8840 gal/min, the individual transport delay times were calculated. The velocity through the core and the length of the core can be found in the Hazards Report,[B3] so the delay time could be calculated directly. The values of the transport times are listed in Table A-1, where the point numbers correspond to the points of Figure A-3.

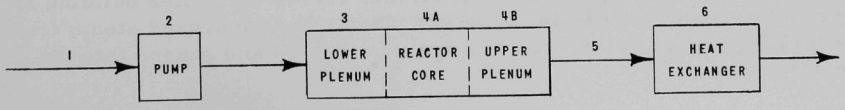

Fig. A-3. Primary Sodium System

Table A-1

TRANSPORT DELAY TIMES IN THE PRIMARY SODIUM SYSTEM

Point	Volume	Description	Transport Delay Time (sec)
1 and 2	Small	The sections of the primary loop from (1) to (3) and including the	0
3	155 gal	lower plenum of the reactor may be neglected, as they are of no importance in the transfer of heat.	0
4A		Fuel element length = 7 ft 7in.; flow velocity of 26 ft/sec.	0.29
4B	128 gal	Upper plenum effective volume	0.87
5	298 gal	14-in. connecting pipe	2.02
6	607 gal	Through heat exchanger	3.5

Of the points described in Table A-1, the only energy-transport times that are effective are those starting with the entry of the sodium to the core through to the exit of the sodium from the heat exchanger. The others can be neglected for two reasons. One, no heat transfer occurs in the excluded region. Secondly, the primary reservoir is sufficiently large to allow only very slow changes in the pump inlet temperature, thus effectively eliminating any looping effects which might occur due to changes in the exit temperature of the heat exchanger.

b. Steam-Water Loop

A schematic diagram of the main section of the steam-water loop can be found in Figure A-4. The operation of the boiler section is as follows:

Preheated water at saturation temperature is pumped into the steam drum and then passes down and through the evaporators under natural convection. The mixture of steam and water formed in the evaporators is separated in the steam drum and the steam passed to the superheaters. The superheated steam then leaves the boiler building and goes to the steam turbine in the power plant. The condensed steam from the turbine is then de-aerated and again preheated and passed into the steam drum.

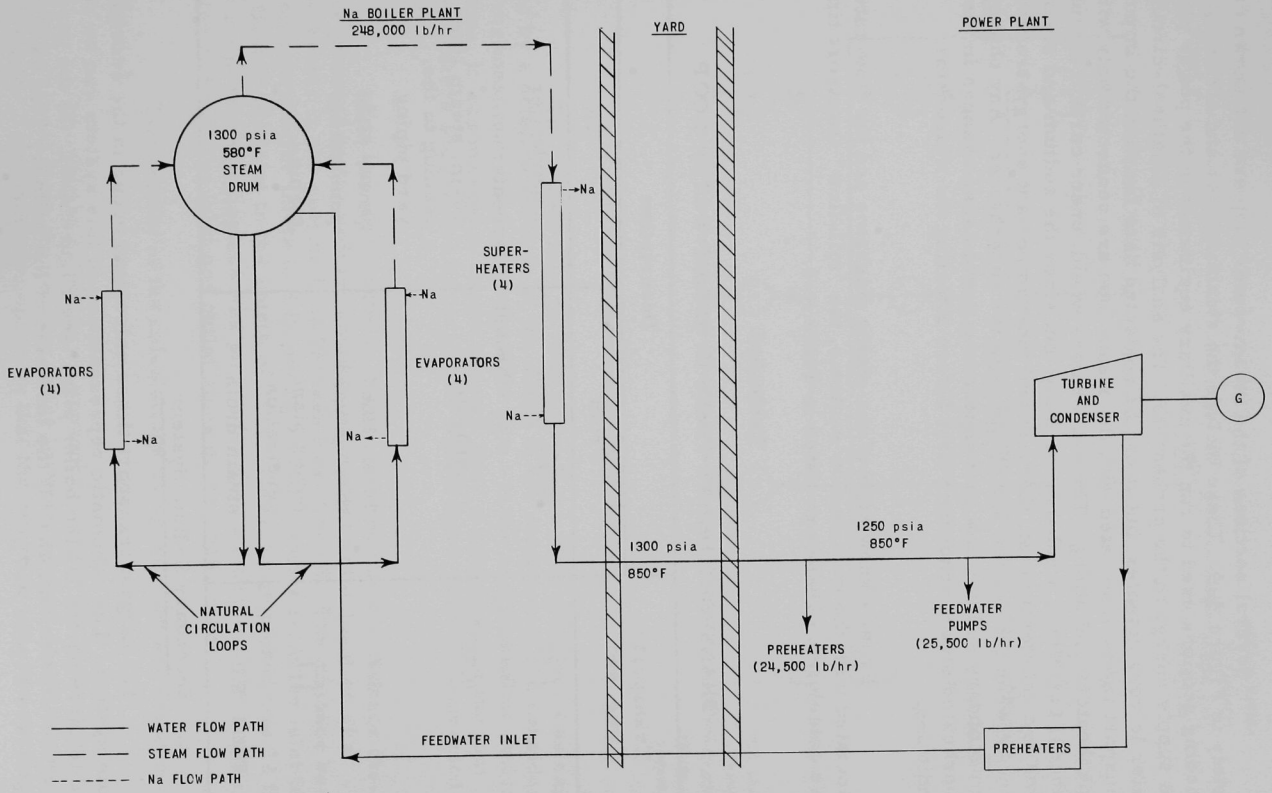

Fig. A-4. Steam Loop

Several sections of the steam-water loop are not shown completely in Figure A-4. These include the steam-bypass and steam-bleeding sections used to run the auxiliary equipment in the power plant and supply energy to the preheaters. The analysis of a natural-circulation boiler is very complex, but it can be neglected here because the important transport times associated with the steam loop are connected only with the superheaters and piping. The evaporators would, under certain circumstances, contribute a substantial delay, but since the sodium and steam flows are countercurrent, the first and most important energy-transfer point between the sodium and steam is in the superheater. Any change in the secondary sodium flow or temperature would cause changes in the superheated steam conditions first before affecting the evaporator conditions.

From a knowledge of the piping diagrams and the flow rates associated with the various flow sections, the "full-flow" transport times were calculated. These are listed in Table A-2.

Table A-2

TRANSPORT DELAY TIMES IN STEAM-WATER LOOP

Transport Time, sec	Description	
	From	To
1.41	steam drum	superheater
0.42	through superheater	
0.74	superheaters	10-in. steam line leading to the yard piping
3.7	10-in. line through yard	power plant penetration
1.7	power plant penetration	turbine
Total 8.0	steam drum	turbine

c. Secondary Sodium System

The largest transport times calculated occur in the secondary sodium system. The schematic representation of this system can be reduced to three parts: (1) the boiler plant (see Figure A-5), (2) the yard piping (not illustrated), and (3) the tube side of the primary heat exchanger (see Figure A-7).

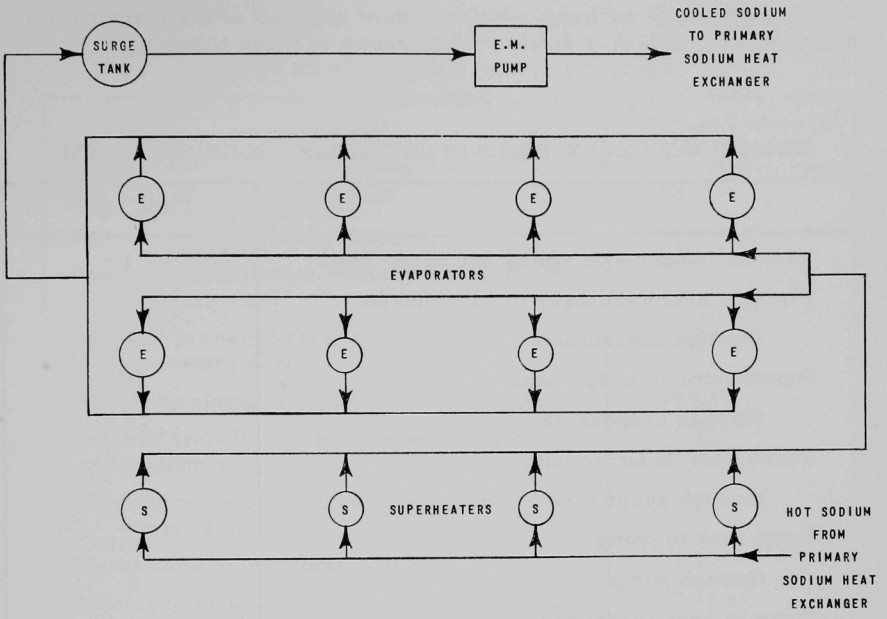

Fig. A-5. Secondary Sodium System

The transit time through these three main divisions was calculated by a detailed analysis of the sizing of the components and considering the maximum flow rate to be 6050 gpm. In the analysis of the boiler section, it was necessary to use average time of travel, since the four superheaters and the two banks of four evaporators each are connected in parallel.

For the superheaters, it was assumed that the average distance traveled by the sodium would be equivalent to the location of a superheater in the spot midway between Nos. 2 and 3. The distance between superheater inlets is 8 ft, giving a total distance from the inlet to the first to the inlet to the fourth of 24 ft. The average picked was 12 ft. The same average distance was picked for the outlet side of the superheater and both the inlet and outlet sides of the evaporators.

The results of the calculations using full flow are found in Table A-3.

In order to calculate an approximate time for a quantity of energy to travel from the reactor to the turbine, several assumptions had to be made. The main assumption is that the effective time for energy to

pass through a heat exchanger is the sum of one-half of the transit time on each side. Table A-4 gives the breakdown of these times.

Table A-3

TRANSPORT DELAY TIMES IN SECONDARY SODIUM SYSTEM

	Time, sec*
Heat exchanger exit piping and upper head	1.5
Piping - heat exchanger to superheater	18.0
through superheater	5.8
Superheater to evaporator	16.3
through evaporator	16.1
Evaporator to surge tank	16.2
through surge tank	9.9
Surge tank to pump	5.0
through pump	0
Pump to heat exchanger	11.6
Heat exchanger pipe in and lower head	3.4
shell side flow	3.4
Total Loop Transit Time	107

*At an assumed full flow of 6050 gpm.

The transport delay times previously calculated are for the full-design flow rates listed in the Hazards Report.[B3] To obtain the delay times for other power levels of operation, all that needs to be done is to divide by the fraction of maximum flow rate associated with that particular power level:

$$\text{transport delay time at any flow rate} = \frac{\text{transport delay time at maximum flow rate}}{\text{B(the fraction of maximum flow rate)}} .$$

Table A-4

TOTAL AVERAGE TRANSPORT TIMES

Condition	Average Transport Time, sec
One-half reactor transit time	0.15
Time to primary heat exchanger	2.9
One-half primary heat exchanger transit time (primary side)	1.75
One-half primary heat exchanger transit time (secondary side)	1.72
Secondary piping to superheater transit time	19.52
One-half transit time through superheater (sodium side)	2.92
One-half transit time through superheater (steam side)	.21
Superheater to turbine transit time	6.17
Reactor to turbine Total	35.34 or approx. 35

3. Heat-transfer Calculations

Calculations were made to determine the range of values which might be necessary to use if it became advisable or necessary to simulate the heat-exchange system on an analog computer. The three main classes of equipment analyzed were the superheaters, evaporators, and the primary sodium to sodium heat exchanger. Diagrams of the equipment can be found in Figures A-6 and A-7. A summary of the results are in Table A-5. These results were calculated by use of consistent data and equations to obtain relative and not necessarily precision values. The values obtained, however, do agree fairly well with the preliminary design values.(A-1)

a. Superheater* (4 units)

The superheaters are vertical, countercurrent, shell-and-tube heat exchangers with 109 duplex tubes, located in a 14-in. schedule 20 pipe shell, 30 ft in length. The sodium is passed through the shell side from bottom to top and the steam through the tubes from top to bottom.

* The design of the superheater has been changed subsequent to this analysis due to difficulties in fabrication. Two spare evaporators were modified and will be used in place of the four superheaters (Reference A-2, p. 37).

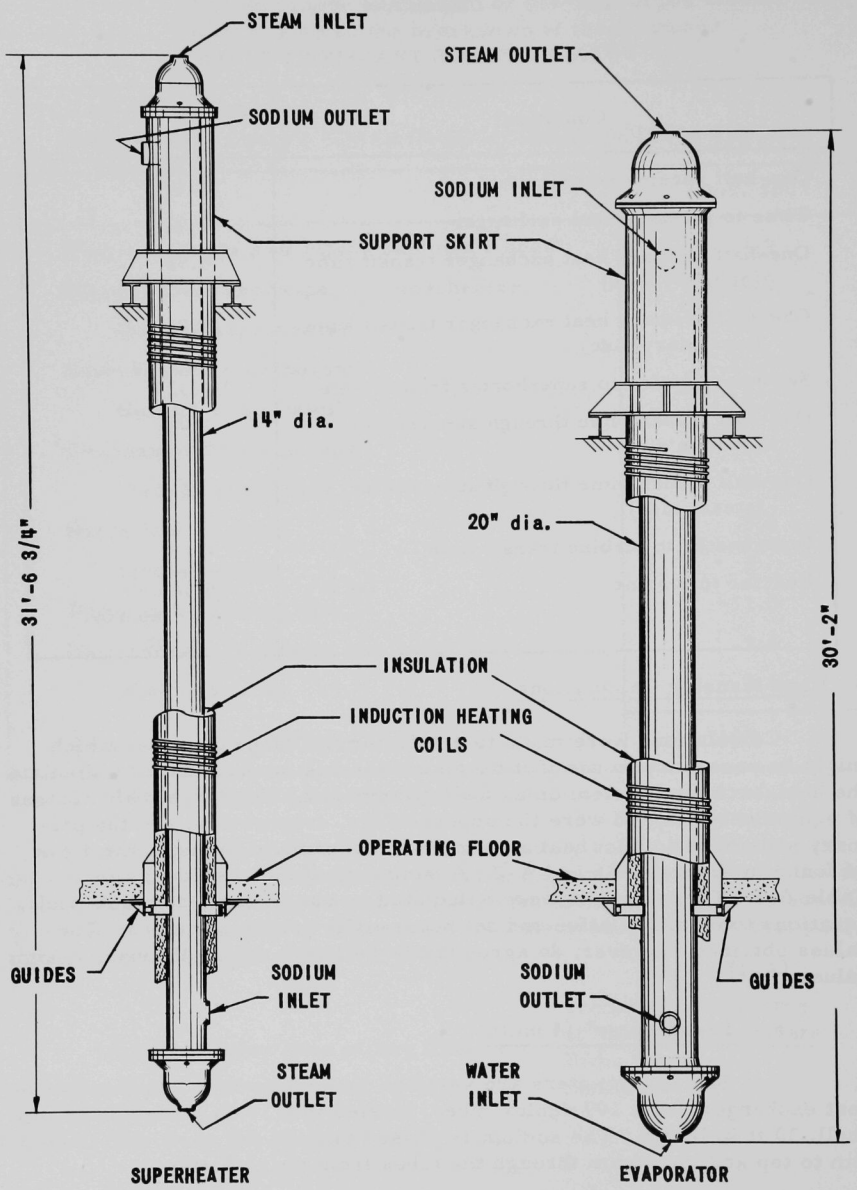

Fig. A-6. Superheater and Evaporator

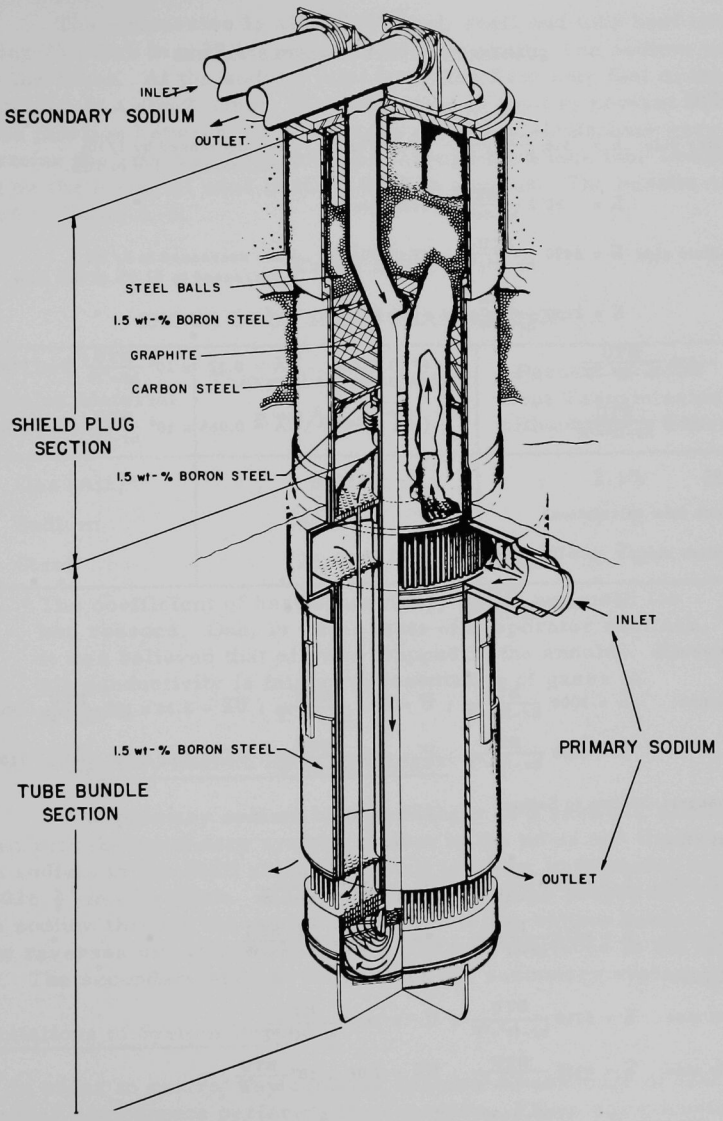

Fig. A-7. Primary Heat Exchanger

Table A-5

SUMMARY OF HEAT TRANSFER VALUES

Superheaters

1. Water side $\bar{h} = 315 \frac{BTU}{hr\text{-}ft^2\text{-}^\circ F}$ (Full Flow) Flow decreased by 1/10; $\bar{h}$ decreased to 1/6 to 16%.

   $\bar{h} = 50.2 \frac{BTU}{hr\text{-}ft^2\text{-}^\circ F}$ (10% Flow)

2. Sodium side $\bar{h} = 3470 \frac{BTU}{hr\text{-}ft^2\text{-}^\circ F}$ (Full Flow) Flow decreased to 1/10; $\bar{h}$ decreased to 61.3% of full flow

   $\bar{h} = 2130 \frac{BTU}{hr\text{-}ft^2\text{-}^\circ F}$ (10% Flow)

3. $\bar{U} = 256 \frac{BTU}{hr\text{-}ft^2\text{-}^\circ F}$ (Full Flow) $\overline{UA} = 0.32 \times 10^6 \frac{BTU}{hr\text{-}^\circ F}$ (Full Flow)

   $= 48.3 \frac{BTU}{hr\text{-}ft^2\text{-}^\circ F}$ (10% Flow) $\overline{UA} = 0.065 \times 10^6 \frac{BTU}{hr\text{-}^\circ F}$ (10% Flow)

Evaporator

1. Shock tube calculations
2. Sodium side $\bar{h} = 2670 \frac{BTU}{hr\text{-}ft^2\text{-}^\circ F}$ (Full Flow)

   $\bar{h} = 2110 \frac{BTU}{hr\text{-}ft^2\text{-}^\circ F}$ (10% Flow)

3. Water side

   Assume: $\bar{h} = 3000 \frac{BTU}{hr\text{-}ft^2\text{-}^\circ F}$; $\bar{U} = 606 \frac{BTU}{hr\text{-}ft^2\text{-}^\circ F}$; $\overline{UA} = 2.28 \times 10^6 \frac{BTU}{hr\text{-}^\circ F}$ (Full Flow)

   $\bar{h} = 1000 \frac{BTU}{hr\text{-}ft^2\text{-}^\circ F}$; $\bar{U} = 430 \frac{BTU}{hr\text{-}ft^2\text{-}^\circ F}$; $\overline{UA} = 1.62 \times 10^6 \frac{BTU}{hr\text{-}^\circ F}$ (10% Flow)

Heat Exchanger: Sodium to Sodium

A. Full Flow

   Shell side $\bar{h} = 6800 \frac{BTU}{hr\text{-}ft^2\text{-}^\circ F}$; $\bar{U} = 1790 \frac{BTU}{hr\text{-}ft^2\text{-}^\circ F}$

   Tube side $\bar{h} = 8215 \frac{BTU}{hr\text{-}ft^2\text{-}^\circ F}$; $\overline{UA} = 7.66 \times 10^6 \frac{BTU}{hr\text{-}^\circ F}$

B. 10% Flow

   Shell side $\bar{h} = 5710 \frac{BTU}{hr\text{-}ft^2\text{-}^\circ F}$; $\bar{U} = 1650 \frac{BTU}{hr\text{-}ft^2\text{-}^\circ F}$

   Tube side $\bar{h} = 6935 \frac{BTU}{hr\text{-}ft^2\text{-}^\circ F}$; $\overline{UA} = 7.06 \times 10^6 \frac{BTU}{hr\text{-}^\circ F}$

C. The change in $\bar{U}$ is $\frac{1790 - 1650}{1790} = 8\%$ change in $\bar{U}$

b. Evaporator (8 units)

The evaporator is also a vertical, shell and tube heat exchanger containing 73 tubes in a 20-in. schedule 20 pipe shell. The sodium passes through the tubes. At the sodium inlet (top), the first four feet of the tubes are contained in a shock tube. The shock tube is used to prevent overstressing of the junction between tubes and tube sheets. Calculations were made to determine the effective heat transfer through the shock tube section depending on the material used in the 0.0095 in annulus. The results are indicated in Table A-6.

Table A-6

SHOCK TUBE HEAT TRANSMISSION

Annulus Material	Thermal Conductivity BTU/hr-ft-°F	Percent of Total Heat Transmission without Shock Tubes
Gas (Air)*	0.024	2.1%
Sodium	40	57 %
Steel	25	56 %

* The coefficient of heat conductivity of air was used for two reasons. One, in water tests of evaporator sections, it was believed that air was trapped in the annulus. Two, air conductivity is fairly representative of gases in general.

c. Primary Sodium Heat Exchanger

The primary sodium heat exchanger is a vertical, shell-and-tube unit with the secondary system sodium in the tubes and the primary system sodium in the shell side. The shell is 51 in. in diameter and contains 3026 $\frac{5}{8}$-in.-OD tubes. A 12-in. schedule 20 pipe passes the secondary system sodium through the center of the unit to the bottom header, where the flow reverses direction and passes up through the tubes to the top header. The secondary sodium then enters the secondary system piping.

4. Limitations of System Response

In order to control any complex system, a knowledge of how each of its minor components performs is necessary. These components can be arranged in either series or parallel operation when serious consequences could result if any one component behaved in a widely different manner than any other. A system built of a series of components can only respond in a

manner which is consistent with the slowest responding component without abnormal changes occurring within the system. If one component is much slower in response than any of the rest, there is no need to install complex, fast-operating automatic control equipment in association with the fast components, as this fast rate of change could never be utilized. Also, under these circumstances, it might be advantageous to design a time-optimum controller for the slowest component and then derive the operating conditions for the rest of the control devices from this component.

The analysis of the equipment for the EBR-II power plant system reported in this section was made to determine performance characteristics in relation to a maximum rate of change.

a. Steam-Water Loop (see Figure A-4)

The maximum rate of flow of water through the evaporators and superheaters of the steam-water loop is about 270,000 lb/hr or 732 gal/min at 550°F. The pumps of this system are run continuously at full capacity, and a relief valve bypasses the excess flow back to the low-pressure side of the pump. All of the valve controls on the loop are pneumatically actuated, and the system as it is built contains a Leeds and Northrup three-element controller. The turbine-generator does not at the present time have an automatic control attached, but is capable of accepting a commercially available one. The turbine does, however, have a steam pressure bypass control which will bypass the excess steam directly into the condenser should the pressure become too high.(A-3) The turbine-generator is a small one (of 20-MW electrical capacity), and as a result possesses a small transient time for a change from 10% to 100% of maximum rated power.

The previous description of the steam-water loop is indicative of a fast-acting, automatic loop. As a consequence, no further analysis was made.

b. Secondary Sodium System

In the secondary system, there is only one means of control of the system sodium flow. There are no flow-controlling valves, so control is obtained by variation of the pumping power of the 3-phase linear electromagnetic pump. The power to the pump is in turn controlled by an amplidyne.

The pump input power is rated at 460 kW, and a prototype had an efficiency of 43% at the designed flow rate. Thus, the horsepower available for pumping is 265. The maximum flow rate of 6040 gpm through a 12-in. pipe gives a velocity of 16.5 ft/sec. The total system capacity is approximately 9,000 gal of sodium, as calculated from the component sizing.

The amount of energy expended in raising the 9,000 gal from "no flow" to "full flow," assuming no pressure drop, is as follows:

Kinetic Energy = $\frac{1}{2} Mv^2$;

Density of sodium at average temperature (800°F) = 53.0 lb/ft^3;

$$M \text{ (Mass)} = \frac{9{,}000\ (53)}{7.48\ (32.2)} = 1{,}980 \text{ slugs};$$

Kinetic Energy = 540,000 ft-lb.

If this energy were expended in one minute, the horsepower required is 16.4, which is only a small amount of the 265 hp available.

The maximum pressure drop through the system is expected to be 65 psi, and the work done by the pump to overcome this resistance to flow is as follows:

Flow rate - 6040 gal/min;

Density - 53 lb/ft^3;

Pressure head of sodium = 177 ft of sodium;

Mass flow - 45,300 lb/min;

1 hp = 33,000 ft-lb/min;

Required Power = 8,020,000 ft-lb/min = 243 hp.

Since this calculated maximum horsepower to overcome the pressure drop allows an extra 22 hp to store energy in the system, the maximum time to change the flow rate becomes

$$22 = 16.4/t$$

or

$$t = 45 \text{ sec} \quad ,$$

a first approximation to the transient time.

For a second (closer) approximation, it will be assumed that the initial pressure drop across the system will be zero and that the full power of 243 hp is applied. Initially, the full power will be applied to change flow rate, but it will then gradually shift until the full power is necessary to overcome the pressure drop.

Figures A-8, A-9, and A-10 are used to illustrate this. The shaded area in these figures represents the 540,000 ft-lb of stored kinetic energy.

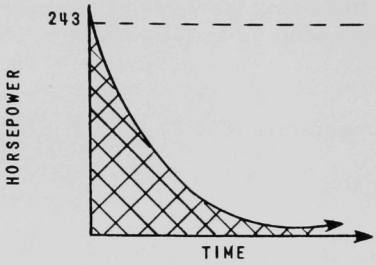

Fig. A-8. Exponential Approximation to the Kinetic Energy Storage in the Secondary System with 243 Horsepower Applied

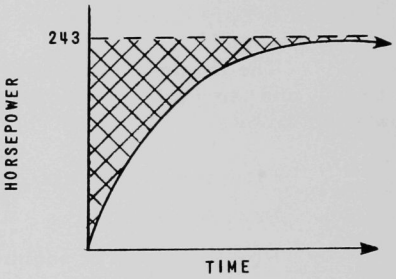

Fig. A-9. Exponential Approximation to the Secondary System Pressure Drop with 243 Horsepower Applied

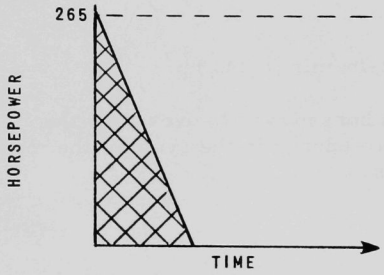

Fig. A-10. Linear Approximation to the Kinetic Energy Storage in the Secondary System with 265 Horsepower Applied

If the linear approximation (see Figure A-10) is used, the calculated time is 7.4 sec. If it is assumed that the curves have an exponential approach such that the power used to change the kinetic energy decreases exponentially to zero (see Figures A-8 and A-9), then the time calculated (equivalent to five time constants) is 20 sec.

If 265 hp is now applied, using the exponential approach (see Figure A-11), the estimated time will be 10 sec.

It is believed that the exponential approximation is the closest to what occurs, but allowing for a 100% margin of error, this pump should be able to change from zero flow to full flow in 40 sec maximum.

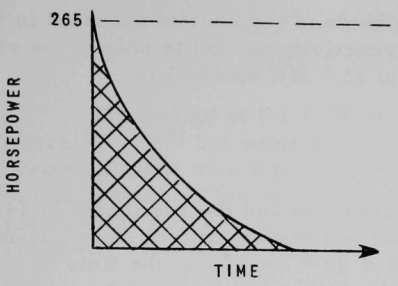

Fig. A-11. Exponential Approximation to the Kinetic Energy Storage in the Secondary System with 265 Horsepower Applied

c. Primary Sodium System

The transient analysis of the primary system pumps would be an almost impossible task since there are two basic modes of control of the squirrel-cage pump motor. The first mode, ranging from "no flow" to 18% flow, consists of the variation of frequency of a motor-generator set output through an eddy current clutch to change the speed of rotation.* The second mode of operation ranges from 18% of flow to "full flow" and consists of a constant frequency output of the motor-generator set at approximately 60 cps with a variation in the field current of the generator. As a result, only an estimate could be made. An experimental test model had been run using water as the pump fluid, but no transient studies were made. Personnel associated with the tests estimated that the time of change of flow would be about the same or less than that for the pump of the secondary sodium system.

As the system now stands, there is a rate-limit control of the pumps which limits the rate of change of flow to 0.4% flow per second. This rate is set as a safety measure in the manual adjustment of the primary system power. The operating manual for a change in power calls for, first, a small change in flow, and then a change in reactor power in small steps until the new, desired operating conditions have been reached. The limit of the rate of flow change limits the stresses induced in the heat-exchange equipment during the flow change. If the flow change and power change were coupled under automatic control, the stresses induced would be considerably reduced and the limit could be changed.

The reactor response time calculated here only considers the reactivity input necessary to overcome the feedback effects in changing the steady-state power level from 10% to 100% of maximum power. It does not allow for any transient time other than that to insert the necessary reactivity.

* In a re-evaluation of the operating procedures performed in March of 1962, the operation of the primary pumps in the first mode has been eliminated, and the flow rate below 20% of power fixed at 22% of full flow.

If the estimated power coefficients of the reactor as listed in the Hazards Report[A-3] are used, the total reactivity needed to change the reactor from a hot condition at low power to 62.5 MW thermal is

$$31.2 \times 10^{-4} \frac{\Delta k}{k} \text{ or } \$0.42 \quad .$$

If an average rod is worth 5×10^{-3} $\Delta k/k$ per rod and the rod length is 14 in., the rod is worth 3.57×10^{-4} $\Delta k/k$/in. The rod travels at 5 in./min. Thus, using the reactivity insertion rate of 2.97×10^{-5} $\Delta k/k$/sec, the time of travel is about 105 sec. The actual transient time will be much longer than this since, with the insertion rate of 0.4¢/sec, the corresponding transient will indicate an overdamped system.

Since the reactor is a fast neutron reactor, safety considerations have led to the requirement that only one rod may be in motion at any time. The resultant slow response time makes this reactor the slowest responding component in the power plant system.

NOTE: Later measurements made during the dry critical experiments with the reactor indicate that the rod-insertion rate around the control position will be even less than that used in the above calculation. The new maximum value is 2.35×10^{-5} $\Delta k/k$/sec. Most of the work was performed on this analysis prior to the dry critical experiments and so the previous value of 3×10^{-5} $\Delta k/k$/sec is used as the comparison point. See Appendix B.

APPENDIX B

EBR-II REACTOR INFORMATION

The design of the EBR-II system is discussed in detail elsewhere,[B-1,B-3] but some of the important information concerning the measurements made with the reactor and the design of the reactor will be given in this section. This information was used to establish values for important parameters in the development of the feedback model and ramp rates of reactivity insertion.

A vertical section of the reactor is shown in Figure B-1. A drawing of the core subassemblies is shown in Figure B-2. The core region of a normal subassembly contains 91 pins, each 14.22 in. long. The fuel is uranium metal approximately 50% enriched in U^{235} and containing 5 w/o simulated fission products (this alloy is referred to as fissium). The fuel pins are 0.144 in. in diameter and are surrounded by a sodium bond, 6 mils thick, and a Type 304 stainless steel cladding, 9 mils thick. The upper and lower blankets contain similar, but larger, pins, 19 to a subassembly, the uranium diameter being 0.317 in. in this case. Above and below the core are coolant header regions in which sodium is redistributed between core and blanket pins.

The following description of the subassemblies and their method of support has been reproduced from Reference B-3.

> "All core subassemblies are identical in size and shape (hexagonal). The dimension across outside flats of each subassembly is 2.290 in. The center-to-center spacing of the subassemblies is 2.320 in. The resulting nominal clearance between flats of adjacent subassemblies is 0.030 in. Each core subassembly, as well as each inner blanket subassembly, is provided with a 'button' on each of its six flats; the buttons are positioned so that they lie in a horizontal plane 1.00 in. above the core (fuel) center line. These buttons protrude a nominal 0.014 in. from the subassembly flat. The button flats are 0.375 in. in diameter. The dimension across opposite button flats of each subassembly is held to 2.318 ± 0.002 in. The resulting nominal clearance between button flats of adjacent subassemblies is 0.002 in.
>
> "The subassemblies are positioned and supported in the reactor by their lower adaptors, the ends of which pass through holes in the upper plate of the support grid and engage in the axially aligned holes in the lower plate. The portion of the adaptor which rests on the upper plate is of the shape of a truncated sphere; the upper edge of the plate hole, on which the adaptor rests, is chamfered conically. This arrangement provides a continuous line contact for subassembly support. It has been established experimentally that

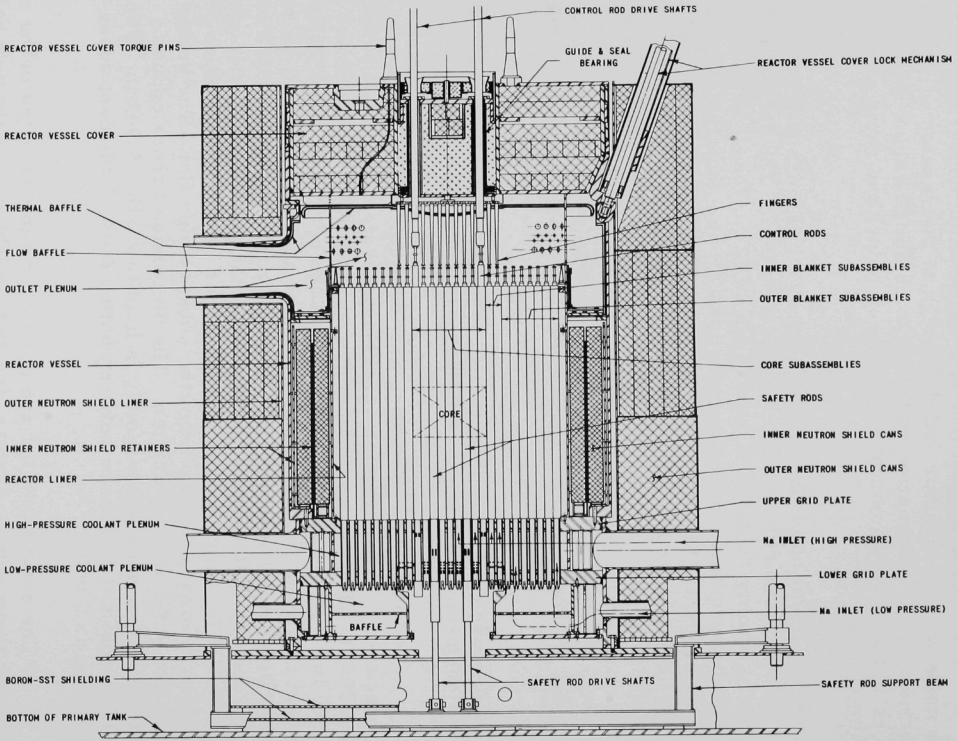

Fig. B-1. EBR-II Reactor (Vertical Section)

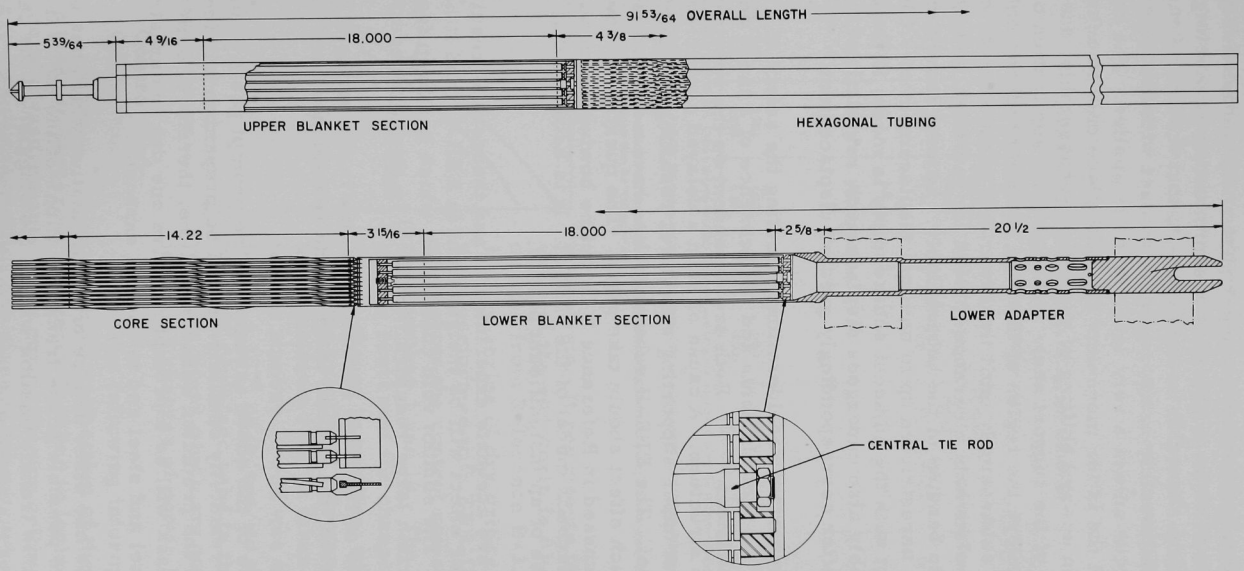

Fig. B-2. EBR-II Core Subassembly

lateral movement of the upper part of the subassembly (or of the lower end of the adapter) is accommodated by pivoting of the subassembly about this area of contact; that is, lateral movement of the subassembly in the region of contact with the upper plate does not occur unless a very large force is applied. The reason for this is that the latter movement can take place only in accompaniment with an upward shifting of the entire subassembly, due to the conical shape of the support seat. Consequently, application of lateral force in or above the region of the core section produces only a pivoting of the subassembly until the lower end of the adaptor closes the lower plate hole clearance (0.0042 in. radially), and, thereafter, results in bending of the subassembly. Lateral movement of the top end is unrestricted up to nominal displacement of 0.030 in., when contact with the adjacent subassembly is made; if the adjacent subassembly also undergoes displacement, restriction is not effected until after correspondingly greater displacement."

Two important considerations affecting the safety of a fast reactor are bowing of the fuel elements and the presence of a large delayed negative reactivity coefficient.(B-2) Both are dependent on the specific design of the core and core structure. A cause of such a delayed coefficient might be the expansion of an upper supporting structure, resulting in an outward movement of the fuel. The EBR-II subassemblies have a method of bottom support in which no such effect should take place. The question of bowing in the EBR-II is discussed in Reference B-3, but no bowing effect will be incorporated into a feedback model of the EBR-II. It is believed that these effects will prove to be of an insignificant nature.

There are adequate experimental and theoretical results to indicate that the Doppler effect will be insignificant in EBR-II, and it has, therefore, been ignored. The sodium void coefficient, which has been found to be positive in certain large reactors,(B-4,B-5) is strongly negative in EBR-II.

Because of the large sodium inventory in the primary coolant tank, the temperature of the sodium entering the reactor has been assumed to be constant.

Because of the above assumption, no prompt positive or large delayed negative reactivity coefficients will be present in any feedback model developed, and the predicted behavior will be, therefore, quite stable. The assumed feedback will be a prompt negative one due to unrestrained thermal expansion of fuel and steel and to coolant expansion.

There is one other source of nonlinearities which has not been discussed yet: the possible phase transformations of the fuel. It is believed, however, that this transformation will be too sluggish in the case of the fissium to affect the results of any transients except those associated with time constants of the order of hours or days.

To establish the value used to represent the ramp rate of reactivity change, many sources were consulted. Table B-1, reproduced from Reference B-6, represents the range of values considered. A value of 3×10^{-5} $\Delta k/k/sec$ is used as a comparison point for the different methods

Table B-1

NORMAL RATES OF REACTIVITY INSERTION BY VARIOUS DRIVE MECHANISMS

	Control Subassembly			Two Safety Subassemblies			Core Subassembly Loading Mechanism (Central Core Subassembly)		
	Predicted[1]	Measured[2]	Estimated[3] for Dry Critical	Predicted[1]	Measured[2]	Estimated[3] for Dry Critical	Predicted[1]	Measured[2]	Estimated[3] for Dry Critical
Total Reactivity Worth, % $\Delta k/k$	0.5	0.37	0.32	2.0	1.36	1.1	~2.0	1.5	1.2
Drive Speed, in./min	5.0	-	5.0	2.0	-	2.0	6.0	-	6.0
Effective Stroke, in.	14.0	14.0	14.0	14.0	14.0	14.0	-	-	-
Rate of Reactivity Addition, % $(\Delta k/k)$/sec									
Average	0.003	0.0022	0.0022	0.0050	0.0032	0.0026	0.015	0.011	0.0088
Maximum	0.005	0.0038	0.0034	0.0086	0.0055	0.0045	0.025	0.018	0.014

[1]Predicted for wet critical reactor. These reactivity insertion rates were used to specify control rod, safety rod, and fuel-handling mechanism drive speeds.

[2]Measured on EBR-II Mockup in ZPR-III. The mockup has the configuration of the wet critical reactor except that low-density aluminum represents the sodium coolant.

[3]These values are inferred from the "Measured" values. Reduced reactivity insertion rates and total reactivity worths prevail because the dry critical core is at least 20% larger than the "Measured" core.

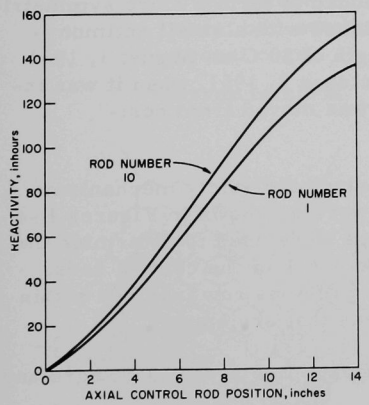

Fig. B-3. Control Rod Calibrations

of analysis. It represents the average value of the rod worth in $\Delta k/k/sec$ as calculated from Reference B-3. In the fall of 1961, a series of dry critical experiments were performed with EBR-II. Figure B-3 represents the control rod calibrations for rods number 1 and 10. The slopes of the curves represent the change in reactivity with a change in position; with a known rod rate, the reactivity rate can be calculated. The maximum rate as taken from the curve for the number 10 rod was calculated to be 2.9×10^{-5} $\Delta k/k/sec$, so that the value 3×10^{-5} $\Delta k/k/sec$ used in the calculations will give times which are too short for the indicated changes of power level.

The following information on the location and calibration of the control and safety rods is taken in part from Reference B-7 and is included to show the range of values of measurements made during the dry criticals. It will be noted that the values of reactivities are given in inhours where 415 inhours equals 1% $\Delta k/k$.

Location of Rods. The number and location of each safety and control rod can be seen in Figure B-4. The two safety rods are in the third row and the twelve control rods are in the fifth row of the core. These rods are moved into and out of the core area by 60-cycle, 3-phase synchronous motors.

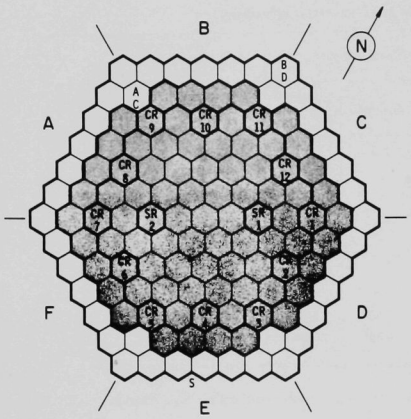

Fig. B-4

Core Configuration for Most Control and Safety Rod Measurements (Total reactivity worth and incremental calibration; 232.18 kg of U^{235} loaded into reactor)

Calibration of Control and Safety Rods. After the critical approach, the fuel subassemblies were slightly rearranged to form a more symmetric loading. The large neutron source was replaced with a small antimony-beryllium neutron source which had a strength of 30 C on August 1, 1961. It had decayed* to approximately 15 C on October 2, 1961, when it was inserted in the reactor. The source location was moved from position 7-E-3 to 8-E-5.

The measured total worths of the control and safety mechanisms are given in Table B-2. The core loadings were as shown in Figures B-4 and B-5. Two slightly different core loadings were used to determine the effect of perturbing the core boundary on the worth of the control rods. In each figure, the outer row and part of the previous row included within the outer heavy lined area contain those areas that are empty.

The area contained within the inner heavy line is the main core and control element area.

Control rods No. 1 and 10 were also calibrated over the 14 in. stroke. The calibration curves are shown in Figure B-3.

*Sb^{124} has a 60-day half-life.

Table B-2

REACTIVITY WORTHS OF CONTROL AND SAFETY RODS

Rod	Core Loading Figure Number	Reactivity Worth	
		Inhours	% $\Delta k/k$[3]
Control Rod*			
No. 10	22	154.0[1]	0.37
No. 1	22	137.0[1]	0.33
No. 7 (special)	22	239.0[2]	0.58
No. 9	22	132.5[2]	0.32
No. 6	23	163.0[1]	0.39
No. 2	23	149.5[1]	0.36
No. 2	23	150.1[2]	0.36
All 12 Control Rods	22	1854**[2]	4.37
Two Safety Rods	22	430**[2]	1.04
Two Safety Rods	22	425**[2]	1.02

[1]Period Measurement

[2]Subcritical Measurement

[3]415 inhours = 1% $\Delta k/k$

*Even-numbered control rods on "flat" of hexagonal core; odd-numbered control rods on corner of hexagonal core.

**Error is ±10%.

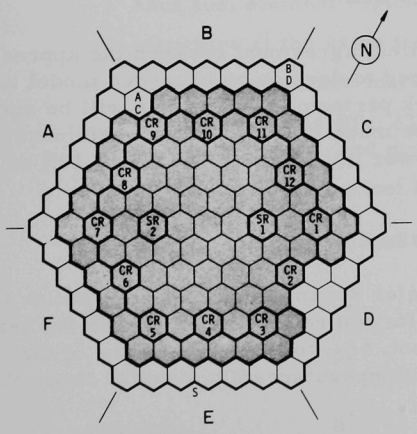

Fig. B-5

Core Configuration for Reactivity Worth Determination (Control rods 2 and 6; 235.00 kg of U^{235} loaded into reactor)

APPENDIX C

FEEDBACK MODEL DEVELOPMENT

As was stated in the literature review of Section II, the model to be developed here is comparable with Newton's Law of Cooling model with the flow rate as an additional variable.

In the following analysis, the transfer-function approach will be used to develop a reactivity-feedback gain constant to be used to evaluate the total reactivity insertion above a base power level. The gain constant developed is dependent on the coolant flow rate as well as the power level. There are several restrictions placed on the developed model; these will be discussed throughout the development.

The physical construction of the EBR-II reactor is such that under normal operation no feedback effects are expected to occur as a result of changes in the secondary or steam systems.(A-3) This is primarily due to the large sodium reservoir which essentially maintains the inlet sodium temperature at a constant level. Thus, the only existent power feedback effects will be due to the temperature changes necessary for, or as a result of, power changes.

Several analyses have been performed to predict the dynamic behavior of the EBR-II reactor. References C-1, C-2, C-3, and C-4 present the predicted results of models of varying degrees of complexity. The models used by Bump and Hummel involved extensive digital calculations of the blanket regions as well as of the core. The model used by Pezuela is much simpler, as it only involves the core region. The results produced by both approaches, however, agree quite well.

Since there existed such excellent agreement between the approaches, Pezuela's simplified approach was used to develop an expanded model of the EBR-II reactivity feedback. The work performed by Pezuela will be summarized and further adaptation will be made to increase the usefulness of the model over the entire range of power levels of interest, i.e., 10% to 100% power.

Figure C-1 shows Pezuela's simplified model.

The approach to the heat transfer dynamic equations is similar to that used in References C-5 and C-6 for the relationship between the heat generation in the averaged fuel element, δq_q, to the temperature of the fuel element, δT_F, and to the coolant temperature, δT_C.

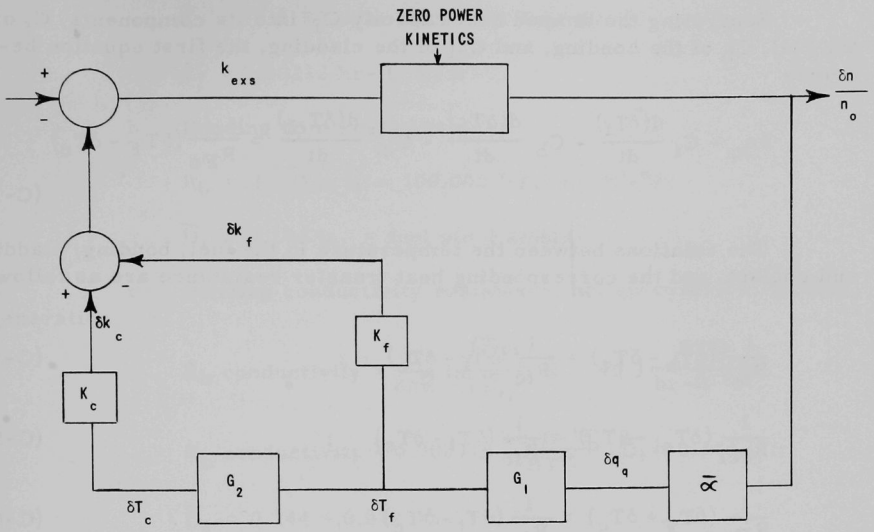

Fig. C-1. Simplified EBR-II Model

Some of the basic assumptions for this model are:

a. uniform heat generation in the core, δq_q;

b. no axial heat transfer;

c. lumped heat capacities and heat transfer resistances for each fuel element region;

d. structure at the same temperature as that of the coolant;

e. linear temperature increase in the coolant channel;

f. small deviations δT_f, δT_c, and δq_q around the steady-state values of T_f, T_c, and q_q, respectively;

g. temperature-dependent heat transfer.

The heat balance in the fuel is given by the following equation:

$$\delta q_q - C_F \frac{d(\delta T_F)}{dt} = \frac{1}{R_{Fc}} (\delta T_F - \delta T_c) \quad . \tag{C-1}$$

The heat balance in the coolant is given by the following equation:

$$\frac{2mc_c \delta T_c}{L} + (C_c + C_s) \frac{d(\delta T_c)}{dt} = \frac{1}{R_{Fc}} (\delta T_F - \delta T_c) \quad . \tag{C-2}$$

Separating the lumped heat capacity C_F into its components, C_f of the fuel, C_b of the bonding, and C_{cl} of the cladding, the first equation becomes

$$\delta q_q - C_f \frac{d(\delta T_f)}{dt} - C_b \frac{d(\delta T_b)}{dt} - C_{cl} \frac{d(\delta T_{cl})}{dt} = \frac{1}{R_{Fc}} (\delta T_F - \delta T_c) \quad . \tag{C-3}$$

The relations between the temperature in the fuel, bonding, cladding, and coolant, and the corresponding heat transfer resistance are as follows:

$$\frac{1}{R_{bc}} (\delta T_b - \delta T_c) = \frac{1}{R_{fc}} (\delta T_f - \delta T_c) \quad ; \tag{C-4}$$

$$\frac{1}{R_{ccl}} (\delta T_{cl} - \delta T_c) = \frac{1}{R_{fc}} (\delta T_f - \delta T_c) \quad ; \tag{C-5}$$

$$\frac{1}{R_{Fc}} (\delta T_F - \delta T_c) = \frac{1}{R_{fc}} (\delta T_f - \delta T_c) \quad . \tag{C-6}$$

By means of the Laplace transform and elimination of δT_b, δT_{cl}, δT_F, and R_{Fc} between Equations (C-2) through (C-6), and making

$$\overline{F} = R_{fc}C_f + R_{bc}C_b + R_{ccl}C_{cl} \quad ,$$

the following transfer functions are obtained:

$$\frac{\delta T_f(S)}{\delta q_q(S)} = \frac{(L + 2mcR_{fc})}{L\overline{F}(C_c + C_s)} \cdot \frac{\left(1 + \frac{R_{fc}(C_c + C_s)L}{L + 2mcR_{fc}} S\right)}{S^2 + \left[\frac{2mc}{L(C_c + C_s)} + \frac{C_t}{\overline{F}(C_s + C_c)}\right] S + \frac{2mc}{L\overline{F}(C_s + C_c)}} \quad ; \tag{C-7}$$

$$\frac{\delta T_c(S)}{\delta T_f(S)} = \frac{L}{(R_{fc}2mc + L)} \times \frac{1}{\left(1 + \frac{L(C_c + C_s)R_{fc}}{2mcR_{fc} + L} S\right)} \quad . \tag{C-8}$$

The following constants are given per foot of averaged fuel element:

1. Heat transfer resistance equations are from Reference C-5.

   a. Fuel resistance:

      $R_f = 1/8\pi\overline{K}$, for a cylinder with internal heat generation;

$\overline{K}$ = 18.8 BTU/hr-ft-°F, for fuel alloy;

R_f = 0.00212 hr-ft-°F/BTU.

b. Bonding film resistance:

$R_b = 1/\pi \overline{D}_1 \overline{h}$; $\overline{h}$ = 100,000 BTU/hr-ft²-°F;

$\overline{D}_1$ = 0.144 in. = fuel pin diameter.

c. Bonding conductivity resistance, hollow cylinder, no heat generation:

$$R_b \text{ conductivity} = \frac{1}{2\pi \overline{K}} \ln\left(\frac{\overline{D}_2}{\overline{D}_1}\right); \quad \overline{K} = 40.3 \frac{\text{BTU}}{\text{hr-ft-°F}};$$

$$R_b \text{ conductivity} = 0.000316 \frac{\text{hr-ft-°F}}{\text{BTU}}; \quad \overline{D}_1 = 0.144 \text{ in.};$$

$\overline{D}_2$ = 0.144 + 0.012 = 0.156 in.,

where $\overline{D}_2$ is the diameter of fuel pin and sodium bonding thickness.

d. Cladding conductivity resistance:

$$R_{cl} = \frac{1}{2\pi \overline{K}} \ln \frac{\overline{D}_3}{\overline{D}_2}; \quad \overline{K} = 11.5 \frac{\text{BTU}}{\text{hr-ft-°F}} \text{(stainless steel)};$$

$$R_{cl} \text{ conductivity} = 0.00151 \frac{\text{hr-ft-°F}}{\text{BTU}}; \quad \overline{D}_3 = 0.174 \text{ in.};$$

$\overline{D}_2$ = 0.144 + 0.012 = 0.156 in.,

where $\overline{D}_3 = \overline{D}_2$ + stainless steel cladding thickness.

e. Cladding film resistance:

$$R_{film} = \frac{1}{\pi \overline{D}_3 \overline{h}} = 0.00088 \frac{\text{hr-ft-°F}}{\text{BTU}}; \quad \overline{D}_3 = 0.174 \text{ in.};$$

$$\overline{h} = 25{,}000 \frac{\text{BTU}}{\text{hr-ft}^2\text{-°F}}.$$

f. Composite resistance: hr-ft-°F/BTU

$R_{fc} = R_f + 2R_{b\ film} + R_b \text{ conductivity} + R_{cl} + R_{film}$;

R_{fc} = 0.00536; R_{bc} = 0.00297; R_{clc} = 0.00239.

2. Heat capacities: BTU/ft-°F

   a. Fuel $C_f = 0.00462$;

   b. Bonding $C_b = 0.000309$;

   c. Cladding $C_{cl} = 0.00215$;

   d. Coolant $C_c = 0.00222$;

   e. Structure $C_s = 0.00260$;

   f. $C_t = C_f + C_b + C_{cl} + C_c + C_s = 0.0119$;

   $\overline{F} = R_{fc} C_f + R_{bc} C_b + R_{clc} C_{cl} = 0.111$ sec.

3. Average coolant flow rate for each fuel pin.

   $m = 0.147$ lb/sec; $2mc_c = 0.0887$ BTU/sec-°F;

   $c_c = 0.302$ BTU/lb-°F.

4. Fuel pin length.

   $L = 1.185$ ft.

5. Heat produced per foot at 100% power in each core fuel pin.

   $\overline{\alpha} = 8.53$ BTU/sec-ft.

6. Fuel temperature reactivity coefficient:

Axial growth of the fuel	-0.39×10^{-5}	
Radial growth of the fuel	-0.09×10^{-5}	$\delta k/k/°C$
Doppler effect of the fuel	$+0.04 \times 10^{-5}$	
Total	-0.44×10^{-5}	$\delta k/k/°C$

or

$K_f = 0.333 \times 10^{-3}\ \delta k/k\beta/°F$.

7. Coolant temperature reactivity coefficient:

Since the structure is only 0.030 in. thick, it can be assumed that the structure temperature T_s is equal to the coolant temperature T_c and that the structure reactivity coefficient can be included with the coolant temperature coefficient. This assumes that the delay between δT_c and δT_s is not important.

It was found that the total reactivity contribution from the coolant and structure was:

$$K_c \simeq 1.74 \times 10^{-3} \delta k/k\beta/°F = 2.29 \times 10^{-5} \delta k/k/°C.$$

In the dynamic model of the feedback transfer function during transients, several values will be changing at the same time.

a. The value of $\overline{\alpha}$ changes directly as the power level, and its value at any particular time will be the value at 100% power (8.53 BTU/sec-ft) multiplied by the fraction of power level of operation, A:

$$\overline{\alpha} = 8.53 \text{ A}.$$

b. From Reference A-3, it will be noted that the desired flow rate through the reactor is not a linear function of the power level. As an example, the flow rate is $\frac{1}{8}$ of the maximum at 10% power. The value of m for any particular power level will be B, the fraction of maximum flow rate.

c. The values of R_{fc} and R_{film} will change with a change in power level due to the change in flow, but these changes are not of sufficient magnitude to cause a disturbance in the value of F. R_f, $R_{b\,film}$, $R_{c\,cond}$, and R_{cl} remain constant.

Pezuela substituted numerical values into the equations and calculated the numerical transfer function at 10% power and 100% power, but in the following derivations, the values of A and B remain undesignated and the general transfer function is calculated in terms of A and B.

The derived transfer functions are as follows:

$$G_1 = \frac{\delta T_f}{\delta q_q} = \frac{L + 2mcBR_{fc}}{2mcB} \frac{(1 + T_1 S)}{(1 + \hat{K}_1 S + \hat{K}_2 S^2)} \quad , \qquad \text{(C-9)}$$

where

$$T_1 = \frac{L(C_c + C_s)R_{fc}}{L + 2mcR_{fc}B} \quad ; \qquad \text{(C-10b)}$$

$$\hat{K}_2 = \frac{LF(C_s + C_c)}{2mcB} \quad ; \tag{C-10c}$$

$$G_2 = \frac{L}{(L + 2mcR_{fc}B)(1 + T_1S)} \quad . \tag{C-11}$$

The combined transfer function for the feedback becomes

$$\frac{\delta k/k\beta}{\Delta n/n} = A\bar{\alpha}\left(\frac{L + 2mcBR_{fc}}{2mcB}\right)\left[\frac{1 + T_1S}{(1 + T_3S)(1 + T_4S)}\right]$$

$$\left[K_f + \frac{LK_c}{(L + 2mcR_{fc}B)(1 + T_1S)}\right] \quad . \tag{C-12}$$

Rearrangement of this equation and simplification gives

$$\frac{\delta k/k\beta}{\Delta n/n} = A\bar{\alpha}\left[K_fR_{fc} + \frac{L(K_f + K_c)}{2mcB}\right]\left[\frac{1 + T_2S}{(1 + T_3S)(1 + T_4S)}\right] \quad ; \tag{C-13}$$

$$T_2 = \frac{K_f(2mcBR_{fc} + L)T_1}{K_f(2mcBR_{fc} + L) + K_cL} \quad ; \tag{C-14a}$$

$$T_3 = \frac{L\bar{F}(C_c + C_s)}{B\bar{F}mc + \frac{C_tL}{2} + mc\sqrt{\left(B\bar{F} + \frac{C_tL}{2mc}\right)^2 - \frac{2BL\bar{F}(C_c + C_s)}{mc}}} \quad ; \tag{C-14b}$$

$$T_4 = \frac{L\bar{F}(C_c + C_s)}{B\bar{F}mc + \frac{C_tL}{2} - mc\sqrt{\left(B\bar{F} + \frac{C_tL}{2mc}\right)^2 - \frac{2BL\bar{F}(C_c + C_s)}{mc}}} \quad . \tag{C-14c}$$

It can be seen that the gain constant of the transfer function has the following form:

$$\text{Gain Constant} = AK_1^*\left[\frac{1}{B} + K_2^*\right] = K^*(A,B) \quad , \tag{C-15a}$$

where

$$K_1^* = \frac{\bar{\alpha}L(K_f + K_c)}{2mc} \quad ; \tag{C-15b}$$

$$K_2^* = \frac{K_fR_{fc}2mc}{L(K_p + K_T)} \tag{C-15c}$$

By use of the values of the constants developed in the previous paragraphs, the values of the constants K_1^*, K_2^*, T_2, T_3, and T_4 were evaluated. The values of K_1^* and K_2^* were found to be

$$K_1^* = 0.236 \quad ; \quad K_2^* = 0.232 \quad .$$

By means of these values of K_1^* and K_2^*, and two sets of flow-rate data (B-values), two plots of the feedback gain constant were made (see Figure C-2). Curve number (1) was obtained by use of the primary flow rate data of the original hazards report.[A-3] Curve number (2) was obtained from the results of a re-evaluation study performed during the latter stages of actual construction. At this time, it was decided to operate the primary flow system at a constant rate for all power levels below 20%. Tabulated values of the flow rates can be found in Table C-1.

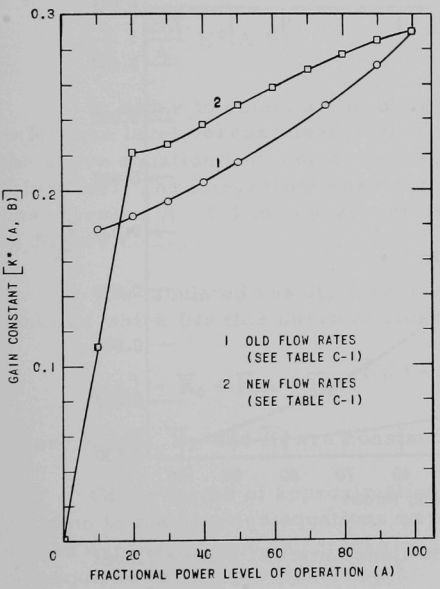

Fig. C-2. Feedback Gain Curve Vs. Power Level

Table C-1

PRIMARY SYSTEM FLOW RATES

A	B(old)*	B(new)**
0	0	0.224
0.10	0.136	0.224
0.20	0.269	0.224
0.30	0.400	0.338
0.40	0.514	0.438
0.50	0.625	0.535
0.60		0.629
0.70		0.718
0.75	0.856	
0.80		0.809
0.90	0.955	0.903
0.100	1.00	1.00

*Reference A-3
**Reference C-8

The values of T_2, T_3, and T_4 were evaluated over the range from 10% to 100% of power. The values of T_2 were found to remain relatively constant, as can be seen from Table C-2.

Table C-2

CALCULATED VALUES OF T_2

A	B(old)	T_2
100%	1	0.0113
50%	0.625	0.0121
10%	0.125	0.0133

The calculated values of T_3 and T_4, the denominator time constants, are plotted in Figure C-3. It will be noted that the values of the time constants depend on the flow rate only and that their values do not exceed 1.0 sec in the range of interest, 10% to 100% power. It can also be noted from the figures that, as the flow rate increases, the time delays become smaller. Because of the indicated short delay times and the low rate of reactivity insertion, these delays could be neglected and the negative feedback considered as prompt.

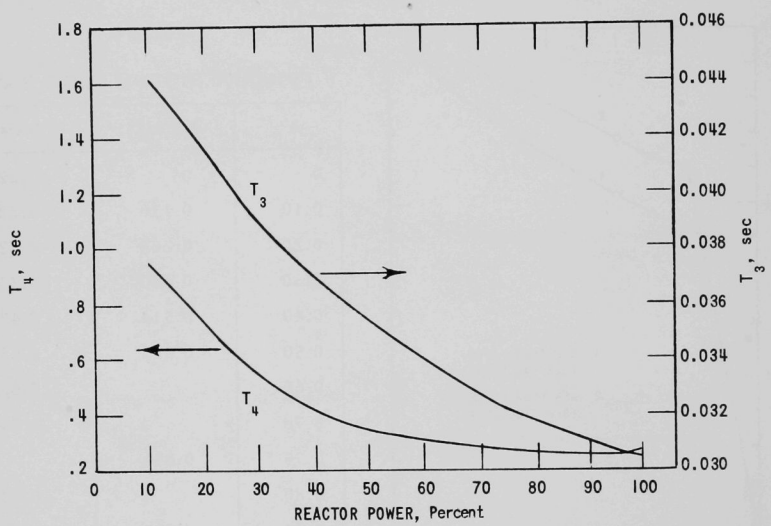

Fig. C-3. Feedback Delay Time Constants Vs. Power Level

Since the only interest is thus in the gain constant, it is necessary to take a good look at what it represents and how it can be modified to be used in an analytical analysis.

The transfer function (neglecting time constants) has the following simplified form, where δk is in "dollars" and where the value of k depends on the value of the particular power level of operation:

$$\frac{\delta k/k}{\Delta n/n} = K^*(A,B) \quad . \qquad \text{(C-17)}$$

For studies involving a disturbance of the steady state, this form of equation would be satisfactory, but for the purpose of defining a switching point, it would be desirable to have the power level as a function of the reactivity input above a desired reference point.

Since the power level of operation is directly dependent on the neutron density, it is possible to divide the neutron density at a particular power level by that at 100% power and obtain the fraction power of operation, A: i.e.,

$$A = \frac{n}{n_{100\%}} \quad . \tag{C-18}$$

The equation then has the following form:

$$\frac{\delta k}{k\beta} = \frac{\Delta A}{A_0} K^*(A,B) \quad . \tag{C-19}$$

In order to obtain a plot of reactivity inserted, $\rho(A)$, above a fixed reference level versus steady-state power, it is necessary to integrate the above equation with use of the various K* values along the normal operating line. The integration was done numerically in 1% increments above a base level of A = 0.1 for curve number 1 and of A = 0.2 for curve number 2 of Figure C-2.

The tabulated results (see Table C-3) are plotted in Figure C-4. A function which fits this curve to close tolerances was of the following form:

$$\rho(A) = \overline{K}_0 + \overline{K}_1 A + \overline{K}_2 e^{-\overline{K}_3(A - A_0)} \quad , \tag{C-20}$$

where $\overline{K}_0$, $\overline{K}_1$, $\overline{K}_2$, and $\overline{K}_3$ are constants (see Table C-4).

Other forms of approximation which might be more conducive to a solution to the kinetics equations were tried. One was a simple power series expansion in A, but it was noted that approximately 17 terms would be required for proper accuracy.†

The values of the constants used in the exponential approximation are:

$$\overline{K}_0 = 0.179 \quad ; \quad \overline{K}_1 = 0.3 \quad ; \quad \overline{K}_2 = 0.209 \quad ; \quad \overline{K}_3 = 5.53 \quad .$$

---

†A power-series expansion of this type transformed the first-order approximation of the kinetics equation into a type of Abel's Differential Equation, a treatment of which can be found in Reference C-7.

Table C-3

INTEGRATED FEEDBACK REACTIVITY

Curve 1		Curve 2	
Power Level	Integrated Feedback Reactivity, cents	Power Level	Integrated Feedback Reactivity, cents*
0.15	7.261		
0.20	12.526	0.20	0
0.25	16.710	0.25	4.9612
0.30	20.200	0.30	9.0497
0.35	23.22	0.35	12.589
0.40	25.92	0.40	15.715
0.45	28.36	0.45	18.540
0.50	30.60	0.50	21.122
0.55	32.69	0.55	23.498
0.60	34.64	0.60	25.725
0.65	36.49	0.65	27.813
0.70	38.25	0.70	29.784
0.75	39.94	0.75	31.650
0.80	41.56	0.80	33.424
0.85	43.12	0.85	35.117
0.90	44.64	0.90	36.734
0.95	46.13	0.95	38.281
1.00	47.59	1.00	39.76

*Reactivity A_0 = 0.1 to 0.2 = 0.111

Total at 100% from 10% = 50.86 cents

The reactivity base used for curve (2) was a base level of 0.20. The calculated value of the reactivity necessary to raise the reactor power from 0.10 to 0.20 was $0.111. Thus, the total reactivity representing the change from a power level of 0.10 to a power level of 1.00 was 50.86 cents.

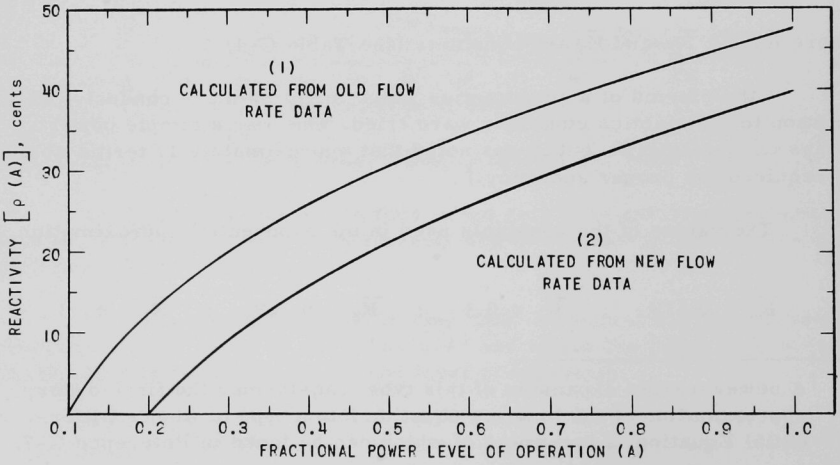

Fig. C-4. Feedback Reactivity as a Function of Power Level

Table C-4

EXPONENTIAL APPROXIMATION
TO REACTIVITY FEEDBACK

Approximate Value	Value from Table C-2	Error
0.119	0.1252	0.006
0.200	0.202	0.002
0.259	0.259	-
0.306	0.306	-
0.346	0.346	-
0.3815	0.382	-
0.415	0.416	0.001
0.4465	0.4464	-
0.478	0.4759	0.002

All values measured in dollars

Another form was suggested by an adaptation of Equations (C-15a) and (C-19). The adaptation proceeds as follows: Since the gain constant is a function of coolant flow rate and power level, and since the flow rate is almost a linear function of power level, a substitution of $B = \overline{K}_4 A$ will produce a feedback gain constant which is linear in A:

$$K^*(A,B) = \overline{C}_1 + \overline{C}_2 A \quad . \tag{C-22}$$

If small intervals of ΔA in Equation (19) are used, the process becomes close to a continuous integration of the forms:

$$\rho(A) = \Sigma\, K^*(A)\frac{\Delta A}{A} = \int (\overline{C}_1 + \overline{C}_2 A)\,\frac{dA}{A} \quad ; \tag{C-23}$$

$$\rho(A) = \overline{C}_1 \ln \overline{C}_3 A + \overline{C}_2 A \quad , \tag{C-24}$$

where $\overline{C}_3$ is the constant of integration.

If the value of $\overline{C}_2$ is such that the linear term could be neglected, the resultant feedback-reactivity expression has the form of a simple log function. Thus, it was decided to try a log approximation to the curve.

To evaluate the two constants involved in the log approximation, the type error and the maximum deviation from the given curve had to be considered. One approach was to specify that the error should be zero at the two ends of the interval of interest. Thus, $\overline{C}_4$ would be determined by establishing the base reference level A_{ref}, i.e., the point at which

$$\rho(A) = \overline{C}_1 \ln \overline{C}_4 A_{ref} = 0 \quad \text{or} \quad \overline{C}_4 A_{ref} = 1 \quad . \tag{C-25}$$

The value of $\overline{C}_1$ is determined by the total reactivity input corresponding to 100% power. From use of this type of approximation to curves 1 and 2 in Figure C-2, the values established for $\overline{C}_1$ and $\overline{C}_4$ and the respective values of $\rho(A)$ for various power levels are tabulated in Table C-5.

Table C-5*

NATURAL LOGARITHM APPROXIMATION TO REACTIVITY FEEDBACK USING "NO INTEGRAL ERROR" CRITERIA

	Curve 1		Curve 2	
	$\overline{C}_1 = 0.2067$ $\overline{C}_4 = 10$		$\overline{C}_1 = 0.2470$ $\overline{C}_4 = 5$	
Power Level	Reactivity	Error	Reactivity	Error
0.1	0	0		
0.2	0.1433	0.0180	0	0
0.3	0.2271	0.0251	0.1002	0.0097
0.4	0.2865	0.0273	0.1712	0.0141
0.5	0.3326	0.0266	0.2264	0.0152
0.6	0.3703	0.0239	0.2714	0.0142
0.7	0.4022	0.0197	0.3095	0.0117
0.8	0.4298	0.0142	0.3425	0.0083
0.9	0.4541	0.0077	0.3716	0.0043
1.0	0.4759	0	0.3976	0

*All reactivity values are in dollars.

Since all the errors were positive, a closer approximation could be achieved by using a criterion of minimum absolute deviation for the curve fitting. The constants and values for various power levels can be found in Table C-6.

Since the actual operating feedback gain constants were unknown at this date, the values of the constants used in comparing the results of the different analysis methods were $\overline{C}_1$ = \$0.20 and $\overline{C}_4$ = 10 for curve 1, and $\overline{C}_1$ = \$0.279 and $\overline{C}_4$ = 5 for curve 2.

Table C-6*

MINIMUM ABSOLUTE DEVIATION APPROXIMATION

	Curve 1		Curve 2	
	$\overline{C}_4 = 10$ $\overline{C}_1 = 0.1993$		$\overline{C}_4 = 5$ $\overline{C}_1 = 0.241$	
Power Level	Reactivity	Error	Reactivity	Error
0.1	0	0		
0.2	0.1381	+0.0128	0	0
0.3	0.2189	+0.0169	0.0977	0.0072
0.4	0.2762	+0.0170	0.1671	0.0099
0.5	0.3207	+0.0147	0.2207	0.0095
0.6	0.3570	+0.0106	0.2646	0.0074
0.7	0.3878	+0.0053	0.3018	0.0040
0.8	0.4144	-0.0012	0.3339	-0.0003
0.9	0.4379	-0.0085	0.3623	-0.0050
1.0	0.4589	-0.0170	0.3877	-0.0099

*All reactivity values are in dollars.

APPENDIX D

REACTOR ANALOG COMPUTER SIMULATION

1. Introduction

This section contains a brief description of each of the components of the analog computer simulation and the description of the entire system, with representative voltages for each of the various variables.

2. Components

Reactor Kinetics Analog Simulator

There are many methods to simulate the reactor kinetics. One of the two most popular is the use of a simulator developed by Pagel;(D-1) the other is the direct use of a common analog computer. The first method listed usually has a drift problem, and the second one requires a large number of amplifiers.

The method employed in this experiment was developed by following the same principles as a simulator, but using the operational amplifiers of a Modified Donner Analog Computer. This approach allows the use of a minimum number of amplifiers, but still gives the same performance as an analog computer simulator.

The elements used are a transistorized function multiplier, an operational amplifier on the computer, and a passive R-C network. The R-C network is placed in the feedback path of the amplifier to provide the effect of the six groups of delayed neutrons, and the function multiplier provides the nonlinear effect. A schematic representation of the kinetics simulator is illustrated in Figure D-1.

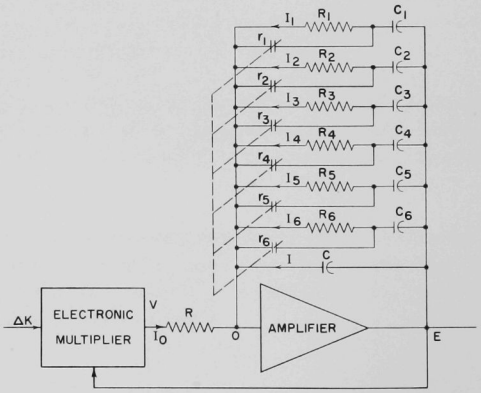

Fig. D-1. Kinetics Simulator

In order to facilitate the use of this circuit with the analog computer, it was necessary to place a relay so as to reduce the resistance, and hence the time constant, in the R-C network while the computer is in the reset position. The relay coil is operated by the reset switch on the computer and thus allows the capacitors to be charged to the initial conditions at a very rapid rate compared with the long time constant associated with the R-C network. The six-contact relay used to perform this task is wired as shown in Figure D-1. The reset time with the resistors shorted is determined by the total capacitance in the network and the computer reset potentiometer resistance of 80,000 ohms. The derivation and the scaling calculations for the R-C network are as follows:

Let the current flow through each branch be I_i ($i = 1, 2, 3$, etc). As the gain in the amplifier is high, the potential at the summing junction of the amplifier can be assumed to be negligible compared with the output potential. If the output voltage be denoted by E, the following equation can be obtained:

$$E = \frac{Q_i}{C_i} + R_i \frac{dQ_i}{dt} \quad , \tag{D-1}$$

where Q_i is the charge in i^{th} capacitance; R_i and C_i are the resistance and capacitance in i^{th} branch, respectively.

According to Kirchoff's Law, the resultant current at the summing junction is zero, that is,

$$I_0 = \sum_i I_i + I \quad . \tag{D-2}$$

The current through the i^{th} branch can be written as

$$I_i = \frac{dQ_i}{dt} = \frac{E}{R_i} - \frac{Q_i}{C_i R_i} \quad , \tag{D-3}$$

and the current through the capacitor as

$$I = C \frac{dE}{dt} \quad . \tag{D-4}$$

If the input voltage and resistance are denoted as V and R, respectively,

$$I_0 = V/R \quad . \tag{D-5}$$

Substitution of Equations D-3, D-4, and D-5 into D-2 gives

$$C \frac{dE}{dt} = \frac{V}{R} - \sum_i \left(\frac{E}{R_i} + \frac{Q_i}{C_i R_i} \right) \quad . \tag{D-6}$$

In Figure D-1, if the input to the multiplier is called Δk, then

$$V = -E \, \Delta k \quad . \tag{D-7}$$

The development of the kinetics equations of the reactor is as follows:

$$\frac{dn}{dt} = \frac{\delta K}{\ell^*} n - \frac{\beta}{\ell^*} n + \sum \lambda_i D_i \tag{D-8}$$

and

$$\frac{dD_i}{dt} = \frac{\beta_i}{\ell^*} n - \lambda_i D_i \quad . \tag{D-9}$$

Equations D-8 and D-9 are the same as Equations 1 and 2 in the Analytical Derivation section, where D_i has been substituted for C_i in representing the concentration of the i^{th} delayed-neutron group. The substitution is necessary to eliminate conflict in the use of the symbol C, which now stands for capacitance.

$$E = A_n n \quad ; \tag{D-10}$$

$$\Delta K = A_{\delta k} \delta k \quad ; \tag{D-11}$$

$$Q_i = \frac{\ell^*}{\beta_i R_i} A_n D_i \quad . \tag{D-12}$$

A_n, $A_{\delta k}$, and A_{D_i} are in V/n, $V/\delta k$, V/D_i, respectively.

Substitution of Equations D-7, D-10, D-11, and D-12 into D-1 and D-6 gives

$$A_n n = \frac{\ell^*}{\beta_i R_i C_i} A_{D_i} D_i + \frac{\ell^*}{\beta_i} A_{D_i} \frac{dD_i}{dt} \tag{D-13}$$

and

$$C A_n \frac{dn}{dt} = -A_n A_{\delta k} \frac{n \delta k}{R} - \sum \left(\frac{A_n n}{R_i} + \frac{\ell^*}{\beta_i R_i^2 C_i} A_{D_i} D_i \right) \quad . \tag{D-14}$$

Rearrange and compare Equations D-13 and D-14 with D-8 and D-9. If they are going to be identical, the following relations should hold:

$$A_n = \frac{A_{D_i}}{R_i C_i \lambda_i} = A_{D_i} \tag{D-15}$$

and

$$CA_n = \frac{A_n A_{\delta k} \ell^*}{R} = \frac{\ell^* A_n}{\beta_i R_i} = \frac{\ell^* A_{D_i}}{\lambda_i C_i R_i^2 \beta_i} \quad ; \tag{D-16}$$

$$A_n = A_{D_i} \quad ; \tag{D-17a}$$

$$\lambda_i = 1/R_i C_i \quad ; \tag{D-17b}$$

$$C = \frac{-A \delta k \ell^*}{R} = \frac{\ell^*}{\beta_i R_i} \quad . \tag{D-18}$$

Assume

$$A_n = A_{D_i} = 50 \quad ; \quad A_{\delta k} = 10^5 \quad .$$

Then we have

$$C = 10^5 \ell^*/R = \ell^*/\beta_i R_i \quad ; \tag{D-19a}$$

$$\lambda_i = 1/R_i C_i \quad . \tag{D-19b}$$

There now exists 13 equations and 14 unknowns. Thus, one unknown can arbitrarily be chosen. By assuming C_1 = 2mf*, the other thirteen unknowns are found as listed in Table D-1.

Table D-1

RESISTANCE AND CAPACITANCE VALUES FOR THE KINETICS SIMULATOR

No. i	R_i(MΩ)	C_i(mmf)
none	9.1	7.68
1	39.3	2
2	6.4	4.9
3	6.8	1.27
4	3.1	1.05
5	8.1	0.088
6	32.3	0.008

*mf = microfarad

Examine Equations D-8 and D-9 when t = 0:

$$\frac{dn}{dt} = 0 \quad ; \quad \delta k = 0 \quad ; \quad n = n_0 \quad ; \quad D_i = D_{i_0} \quad ; \quad \frac{\beta_i}{\ell^*} n_0 = \lambda_i D_{i_0} \quad ,$$

or

$$\frac{E_0}{A_n} \frac{\beta_i}{\ell^*} = \frac{1}{C_i R_i} \frac{Q_{i_0}}{\ell^*} \frac{\beta_i R_i}{A_{D_i}} \quad ; \tag{D-20}$$

$$E_0 = Q_{i_0}/C_i \quad , \tag{D-21}$$

The scaling factors just calculated required a large voltage to reactivity ratio for input. As a result, the analog computer amplifiers would become overloaded. At this point it was decided to change the gain through the kinetics simulator by decreasing R to a value below 500,000 ohms. To facilitate the changing of the reactivity input to valves other than the 3×10^{-5} $\Delta k/k/sec$ used as a comparison point between the different methods of analysis, a 500,000-ohm potentiometer was placed in the R position and wired as a variable resistor.

Function Multiplier (Solid State) Model 3732P

The function multiplier is a standard Donner component available for use with the analog computer, and requiring the use of three of the operational amplifiers and the computer B+ and B- voltages. The advantage of this multiplier over another self-contained Donner unit that was tried is the freedom from drift.

Reactivity Input Generator

In order to obtain ramp rate of reactivity changes, a 115-volt AC, 1-rpm Bodine motor was geared down to turn a potentiometer one revolution in approximately $4\frac{1}{2}$ min. Neglecting the dead zone and initial condition setting errors, this allows a continuous ramp input to occur for at least 240 sec. With the actual expected value of control rod worth rate to be 2.35×10^{-5} $\Delta k/k/sec$ or less in the EBR-II, "one direction" control rod motion times may run over 200 sec.

The Bodine motor is wired to a three-position switch which governs the direction of rotation of the motor. The end positions cause the motor to run in reverse directions from each other and the center position connects a DC potential across the motor for dynamic braking. The dynamic braking eliminates any coasting after the second switch time (time when rod motion should be zero).

The similarity between the operation of the Bodine motor and the actual control rod motors is very close. The actual control rod motors are three-phase synchronous machines equipped with dynamic braking. The main difference in operation is that the time constant of the Bodine motor is slightly longer than the 40-ms time constant of the control rod motor. But the effect of this difference is very small and may be neglected

Recorder

To record the results of the analog computer study, an Electro-Instruments, X-Y recorder was used. This recorder was equipped with a variable time base, but this base was inconsistent. As a result, a majority of the results obtained from the analog study had 10-sec marker points consisting of blank spaces in the trajectories. The space began at the 10-sec point.

Auxiliary Power Supplies

During practice runs with the analog computer, the voltages necessary for the activation of the R-C network relay and voltage applied to the potentiometer of the reactivity generator were taken from the computer power supply. The variations in computer voltages due to this slight overload were sufficient to disturb the system. To eliminate this disturbance, two New Jersey Electronics power supplies, Model S-200-C, were incorporated into the system. The voltages available ranged continuously from about 90 to 200 V. The reduction in loading was sufficient to permit normal operation.

Analog Computer

The analog computer used in this simulation consisted of a modified Donner Computer Model 3400. The modification consisted in using the basic Donner control with Berkley Amplifiers. The unit had ten operational amplifiers, five of which could be used as integrators with preset initial conditions.

Voltmeter (Hewlett-Packard Model 410B)

A vacuum tube voltmeter was used to monitor the excess reactivity and to determine the second switch point, i.e., the point at which the excess reactivity was zero.

Log Voltage Amplifier

Two different log voltage amplifiers were tried as the feedback function generator. The first one consisted of a 9004 diode in the feedback path of an operational amplifier. It was found that the use of a high input resistance, greater than 100 Mohms, gave a good log curve over three decades of input voltage, 0.1 V to 100 V, but that this arrangement when used in the system was sensitive to other circuit parameters. As a result, a second log amplifier was tried.

The second log amplifier was purchased from the Kane Engineering Corp., and is called a Log Voltage Compressor, Model C-7A. This amplifier is transistorized and only requires two batteries used for biasing. As a result, the output, although small, is quite stable.

The maximum output voltage with a 100-V input is about 0.4 V, thus necessitating the use of additional operational amplifiers to bring the voltage back up to a value usable with the function multiplier. This log amplifier was calibrated and found to give a good log representation over almost three decades.

3. Analog System Simulation

The analog computer system was synthesized from its components as shown in Figure D-2, where only the basic elements are shown. All of the ten operational amplifiers were utilized, although they are not all shown in the schematic. For example, the three amplifiers used by the function multiplier are included as part of the function multiplier on the schematic and hence are not shown separately. It was necessary to include extra amplifiers in the system to split up the gain of one section into two in order to reduce overloading of a particular stage.

Analog Computer Reactivity Voltage Relationships

To establish a proper relationship between the voltages used on the analog computer and the reactivity changes associated with the EBR-II primary system, the following computations were made:

The value of the reactivity feedback at 10 V = 10% power (and at 100 V = 100% power) was measured by the null-balance method with the analog computer; the values obtained were 27.14 and 39.75 V, respectively. Thus, the difference of 12.6 V represents the change necessary to go from 10% to 100% power.

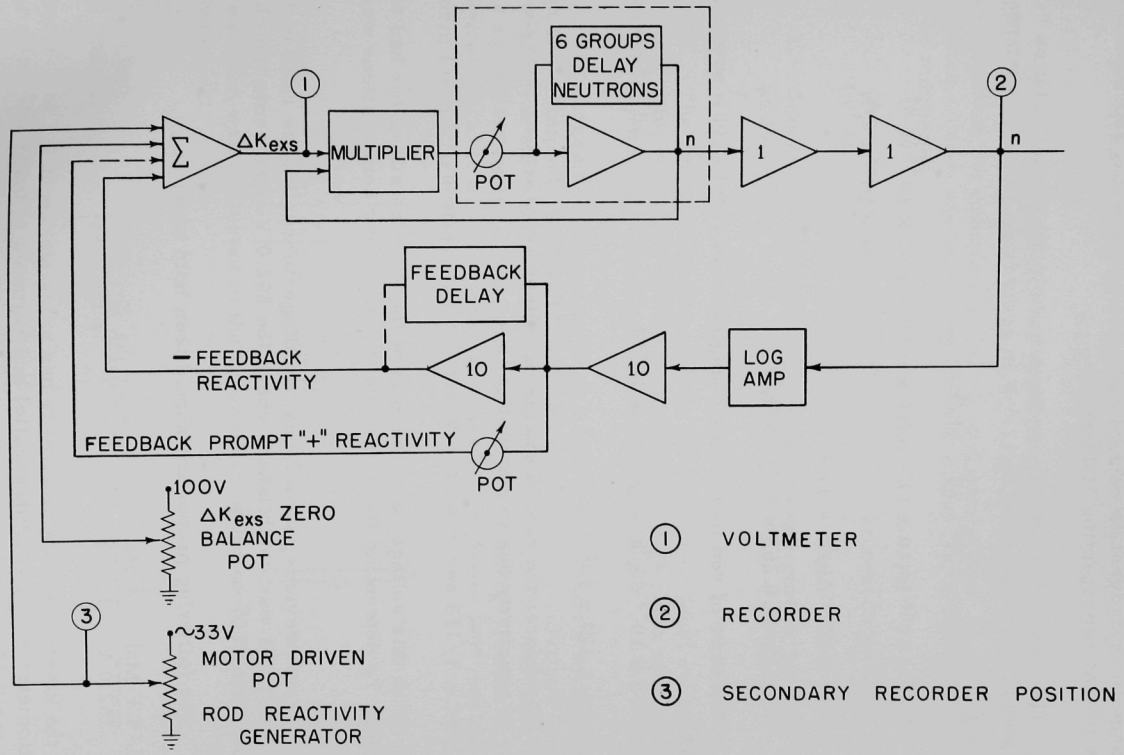

Fig. D-2. Analog Computer System Simulation

To obtain the voltage relation for the rate of increase of reactivity due to control rod motion, it was necessary to determine the time of motion to change the steady-state control rod position from that representing 10% power to that representing 100% power.

The value of reactivity feedback used in the digital solution "$\hat{C}$ ln 10A" should correspond to the 12.6 V in going from 10% to 100% power.

$$\hat{C} = 0.2\beta = 1.47 \times 10^{-3}\ \Delta k/k \quad ;$$

$$1.47 \times 10^{-3} \ln(10 \times 1) - \ln(10 \times 0.1) = 1.47 \times 10^{-3}\,(2.3)$$

$$= 3.38 \times 10^{-3}\ \Delta k/k$$

$$3.38 \times 10^{-3}\ \Delta k/k = 12.6\ V.$$

This gives $0.268 \times 10^{-3}\ \Delta k/k/V$.

The time of rod motion for changing from 10% to 100% power is as follows:

$$3.38 \times 10^{-3}\ \Delta k/k = \gamma t = 3 \times 10^{-5}\, t \quad ; \quad \gamma = 3 \times 10^{-5}\ \Delta k/k/sec \quad ;$$

$$t = 1.127 \times 10^{2} = 113\ sec \quad .$$

Therefore, the rate of change of voltage representing the rate of change of reactivity due to rod motion is

$$12.6\ V/113\ sec = 0.1115\ V/sec \text{ or } 6.68\ V/min \quad .$$

With this voltage rate, the gain of the kinetics simulator had to be adjusted. To determine the new value, the following computations were made:

From previous calculations, a voltage-to-resistance ratio of 352.0 V/9.1 MΩ was established, where the 352.0 V represents the change of power from 10% to 100%.

The following proportion should then hold true:

$$\frac{9.1\ M\Omega}{352.0\ V} = \frac{X\ M\Omega}{12.6\ V} \quad ; \quad X = 0.326\ M\Omega \quad .$$

Since the kinetics simulator already has a resistance of 9.1 MΩ, a 500-kΩ potentiometer was placed in parallel and adjusted to 0.338 MΩ so as to obtain the 0.326-MΩ input resistance.

APPENDIX E

KINETICS EQUATIONS EVALUATION PROGRAM WITH OPPOSING LOGARITHM FEEDBACK (KEEPWOLF)*

This appendix contains the LGP-30 digital program written for the evaluation of the analytical results of Case II. The purpose of this program was to eliminate the tedious process of hand computation of power-level trajectories. There are some restrictions in the use of this program that might be mentioned.

1. Computer memory overflow occurs for reactivity input rates (γ) of 1.1×10^{-4} $\Delta k/k/sec$.

2. Convergence is slow and sometimes nonexistent for high reactivity input rates and times below 5 sec, i.e., for $\gamma = 3 \times 10^{-3}$ $\Delta k/k/sec$.

3. The program section written for the power-level evaluation after switching does not converge for high rates of reactivity input. This problem was not investigated.

The program as traced through a flow sheet is fairly straightforward, except for statements "S3" and "S4," where iterative calculations are made. These iterative calculations become necessary because the variable "A" cannot be solved for explicitly. In order to develop a looping process to perform the convergence, it was necessary to rearrange Equation (40) into the following form for the first time zone:

$$A_{k+1} = A_0 \exp\left\{\frac{\gamma}{c}\left[t - \hat{\xi} + \left(\frac{K_{Z_1}}{A_k} e^{-\lambda t}\right)^{\frac{1}{1 + \lambda \hat{\xi}}}\right]\right\} .$$

This equation was evaluated in the program in two steps to facilitate the programming:

$$\text{Step 1.} \quad q = \left[(K_0/A_k)\, e^{-\lambda t}\right]^{\frac{1}{1 + \lambda \hat{\xi}}} ;$$

$$\text{Step 2.} \quad A_{k+1} = A_0 \exp\left\{\frac{\gamma}{c}\left[t - \hat{\xi} + q\right]\right\} .$$

---

* In the actual program (Keepwolf), a phonetic symbology was used to express the variables.

In the program, an initial value of A_k was postulated and then A_{k+1} was calculated; the values of A_k and A_{k+1} were then compared. If there was no difference, the value of A_k was then passed out of the loop and printed; if there was a difference, the calculated value of A_{k+1} was placed into A_k and another value of A_{k+1} was calculated. This continued until A_k and A_{k+1} were close to the same value; the program then proceeded and A_k was printed.

The same technique was used for the values of A in the second time zone, and the convergence equations were

$$q = \left[(K Z_2 / A_k) \exp(-\lambda t)\right]^{\frac{1}{1 + \lambda \bar{\xi}}}$$

and

$$A_{k+2} = A_0 \exp\left\{-\frac{\gamma}{c}\left[t - 2t_1 - \bar{\xi} + q\right]\right\} .$$

The symbols used in this program differ from the rest of the text. For the symbol correspondence, see the definitions of symbols in the "Program Identification" section.

```
                PROGRAM IDENTIFICATION:  "KEEP WOLF"
                TITLE:  EBR II KINETICS EQUATIONS WITH SWITCHING
                AUTHOR: THOMAS P. MULCAHEY
                TAPE  12
                DATE:  APRIL 1962

                PARAMETER IDENTIFICATION:
 azero      = INITIAL FRACTIONAL POWER LEVEL OF OPERATION
*a one      = FRACTIONAL POWER LEVEL OF OPERATION AT SWITCHING TIME
 akay       = VALUE OF POWER LEVEL AT ANY INSTANT IN TIME
*akay1      = PROGRAM VARIABLE USED IN  CONVERGENCE PROCEDURE
*akay2      =    "        "    "  "       "          "
 tzero      = INITIAL TIME-FOR CALCULATING FIRST POINT
 t one      = TIME OF SWITCHING
*t          = TIME VARIABLE
*tf         = TIME VARIABLE IN FLOATING-POINT
*tfone      = TIME OF SWITCHING IN FLOATING-POINT
 beta       = FRACTION OF DELAYED NEUTRONS
 gamma      = TIME RATE OF CHANGE OF REACTIVITY
 lamda      = DECAY TIME CONSTANT FOR DELAYED NEUTRONS
*ka si      = PROGRAM VARIABLE ( BEFORE SWITCHING )
*kasip      = PROGRAM VARIABLE ( AFTER SWITCHING )
*kzero      =     "     "      ( BEFORE SWITCHING )
*k one      =     "     "      ( AFTER SWITCHING )
*kexs       =     "     "    VALUE OF THE EXCESS MULTIPLICATION FACTOR (ΔK EXS )
 del 1      = CONVERGENCE FACTOR FOR THE CONVERGENCE OF akay and akay1,AND akay and akay2
*del 2      =       "        "   USED IN DETERMINING FINAL SHUT OFF TIME (ΔK EXS = 0)
 c          = COEFFICIENT OF THE LOG TERM IN THE REACTIVITY FEEDBACK
 c1         = TIME ADVANCE INCREMENT ( BEFORE SWITCHING )
 c2         = TIME ADVANCE INCREMENT ( AFTER SWITCHING )
 c3         = TIME DECREMENT  ( AFTER SWITCHING )
 c4         = MAXIMUM VALUE OF akay OF INTEREST
 c5         = MAXIMUM VALUE OF azero OF INTEREST
 c6         = TIME INCREMENT OF ADVANCE FOR THE SWITCHING TIME t one
 c7         = TIME INCREMENT OF DECREASE FOR t  AFTER A CHANGE IN t one
```

```
        c8          = INCREMENT OF INCREASE IN  azero
        c9          = RESET VALUE OF  t  AFTER A CHANGE IN  azero
        c10         = RESET VALUE OF  t one  AFTER A CHANGE IN azero
        c11         = MINIMUM VALUE OF akay OF INTEREST
        c12         = MINIMUM VALUE OF azero OF INTEREST

                        OUTPUT:  azero,   akay,   t,   t one, kexs, AS WILL BE INDICATED AT PRINT-OUT TIME

                        BREAKPOINT OPTIONS:
        bkp4  DOWN POSITION     ADVANCES  azero BY AMOUNT  c8
        bkp8    "       "         "       t one "    "    c6
        bkp16   MUST BE IN THE DOWN POSITION FOR PROGRAM OPERATION TO INCREASE POWER LEVEL FROM azero TO A
                                        HIGHER VALUE.
                MUST BE IN THE UP POSITION FOR PROGRAM OPERATION TO DECREASE POWER LEVEL FROM azero TO A
                                        LOWER VALUE.

                        INPUT:
        ALL TIME VARIABLES ON INPUT TAPE SHOULD BE IN INTERGER FORM IN SECONDS.
        ALL OTHERS SHOULD BE IN FLOATING POINT FORM.
        THE USUAL RANGE OF INTEREST FOR ALL " POWER LEVEL " VARIABLES AND CONSTANTS IS 0.1 to 1.0.

             *  VARIABLES MARKED IN THIS MANNER ARE CALCULATED IN THE PROGRAM AND NO VALUE NEED BE INSERTED
                             IN THE DATA TAPE'


                        STATEMENTS:
TAPE 12
MULCAHEY AUTHOR'
EBR II KINETICS EQUATIONS PROGRAM WITH SWITCHING'
daprt'cr4'uc2'M'U'L'C'A'H'E'Y' 'E'B'R' 'I'I' 'lcl' 'k'i'n'e't'i'c's'cr4''
s1'read'azero'read'akay'iread'tzero'iread't one'read'beta'read'gamma'read'lamda'read'del 1'
       read'c'iread'c1'iread'c2'iread'c3'read'c4'read'c5'iread'c6'iread'c7'read'c8'
       iread'c9'iread'c10'read'c11'read'c12''
s32'tzero':'t''
       .75''e'0'x'abs'gamma':'del 2''
s2'beta'/'['gamma'+'lamda'x'c']':'ka si''
       azero'x'ka si'pwr'['.1''e'1'+'lamda'x'ka si']':'kzero''
s42'4'reprt'cr4''
       daprt'a'z'e'r'o' ' ' 'uc2'='lcl''
       804'dprt'azero''
s43'daprt'cr4'cr4't' 'o'n'e' ' ' 'uc2'='lcl''
       800'iprt't one''
       daprt'cr4'cr4' ' ' ' ' ' 't' ' ' ' ' ' ' 'a'k'a'y' ' ' ' ' ' ' 'k'e'x's'cr4''
s33'0'flo't':'tf''
s3'['['kzero'/'akay']'x'exp'['0'-'lamda'x'tf']']'pwr'['.1''e'1'/'['.1''e'1'+'lamda'x'ka si']']':'q''
       azero'x'exp'['gamma'x'['tf'-'ka si'+'q']'/'c']':'akayl''
s10'if'['abs'['akayl'-'akay']'-'del 1']'neg'sl8'zero'sl8''
       akayl':'akay''
       use's3''
sl8'gamma'x'tf'-'c'x'ln'['akay'/'azero']':'kexs''
s29'set'sl9'to'sl2''
sll'cr'800'iprt't''
       1105'dprt'akay''
       1404'print'kexs''
sl9'go to's0''
sl2'bkp4'use's6''
       bkp8'use's7''
sl3'if'['t'i-'t one']'zero'sl6'pos'sl5''
sl4't'i+'cl':'t''
       use's33''
sl5't one':'t''
       use's33''
sl6'akay':'a one''
       daprt'cr4'uc2'S'W'I'T'C'H' 'T'I'M'E' 'R'E'A'C'H'E'D'lcl'cr4''
s9'0'flo't one':'tfone''
       beta'/'['lamda'x'c'-'gamma']':'kasip''
       ['a one'x'exp'['lamda'x'tfone']']'x'['kasip'+'tfone'-'['c'/'gamma']'x'
       ln'['a one'/'azero']']'pwr'['.1''e'1'+'lamda'x'kasip']':'k one''
s23't'i+'c2':'t''
s34'0'flo't':'tf''
```

```
s4'['['k one'x'exp'['0'-'lamda'x'tf']']'/'akay']'pwr'['.1''e'1'/'['.1''e'1'+'lamda'x'kasip']']':'q''
      azero'x'exp'['0'-'['gamma'/'c']'x'['tf'-'.2''e'1'x'tfone'-'kasip'+'q']']':'akay2''
s5'if'['abs'['akay2'-'akay']'-'del 1']'neg's8'zero's8''
      akay2':'akay''
      use's4''
s8'gamma'x'['.2''e'1'x'tfone'-'tf']'-'c'x'ln'['akay'/'azero']':'kexs''
s17'ret's19'use's11''
s20'if'['abs'kexs'-'del 2']'pos's21''
s31'if'['azero'-'c12']'neg's28''
s30'if'['akay'-'c11']'neg's26''
s25'if'['akay'-'c4']'zero's6'pos's6''
s7't one'i+'c6':'t one''
s27't one'i-'c7':'t''
      cr'daprt'uc2'C'H'A'N'G'E' 'lcl't' 'o'n'e''
      use's43''
s6'if'['azero'-'c5']'zero's28'pos's28''
s26'azero'+'c8':'azero''
      c9':'t''
      c10':'t one''
      daprt'uc2'cr4'C'H'A'N'G'E' 'lcl'a'z'e'r'o''
      use's2''
s21'bkp4'use's6''
      bkp8'use's7''
      bkp16'use's22''
      0'-'kexs':'kexs''
s22'if'kexs'pos's23''
      t'i-'c3':'t''
use's34''
s28'stop'''
```

LIST OF SYMBOLS

A	Fraction of power level of operation
$\overline{A}$	Area
A_n	Constant relating analog voltage and neutron density
$A_{\delta k}$	Constant relating analog voltage and reactivity
A_{D_i}	Constant relating analog voltage and delayed neutrons
A_0	Initial value of A
A_1	Value of A at first reactivity reversal time t_1
A_2	Value of A at t_2
b	Subscript indicating a relation to bonding material
B	Fractional flow rate
C	Capacitance, electrical or thermal (thermal capacitance per unit length)
$\hat{C}$	Coefficient of the log feedback term
c	Heat capacitance of coolant per pound
c	Subscript indicating relation to coolant
cl	Subscript indicating relation to cladding
C_0	Constant (see Equation 38a) for Case I
C_1	Constant (see Equation 29) of integration
C_2	Constant (see Equation 29) of integration
C_3	Constant (see Equation 39)
C_4	Constant (see Equation 40)
$\overline{C}_1$	Constant (see Equation C-22)
$\overline{C}_2$	Constant (see Equation C-22)
$\overline{C}_3$	Constant (see Equation C-24)
$\overline{C}_4$	Constant (see Equation C-25)
D_i	Concentration of delayed neutron precursors
$\overline{D}_1$	Diameter of fuel pin
$\overline{D}_2$	Diameter of fuel pin plus sodium bonding
$\overline{D}_3$	Diameter of fuel pin plus sodium bonding plus stainless steel cladding
E	Voltage

F	Subscript referring to fuel subassembly
$\overline{F}$	See Appendix C, Section 2.f.
f	Subscript indicating relation to fuel
$f_0(x)$	A particular function of x (see Equation 14)
$f_1(x)$	A particular function of x (see Equation 15)
$g(x)$	A particular function of x (see Equation 16)
G_1	Transfer functions (see Equation C-9)
G_2	Transfer functions (see Equation C-11)
$\overline{h}$	Convection heat transfer coefficient
$h_2(x)$	Particular function of x (see Equation 20a)
$h_3(x)$	Particular function of x (see Equation 20b)
i	Subscript indicating ith group
I	Current Equation D-2
K	Constant (general)
K_1	Constant Case I (see Equation 30)
K_2	Constant Case II (see Equation 31)
K_c	Coolant feedback reactivity coefficient
K_f	Fuel feedback reactivity coefficient
K_i	Constant defined Equation 28
K_1^*	Constant defined in Equation C-15b
K_2^*	Constant defined in Equation C-15c
$K^*(A,B)$	Constant defined in Equation C-15a
$\overline{K}$	Heat conductance
$\overline{K}_0$	Constant (see Equation C-20)
$\overline{K}_1$	Constant (see Equation C-20)
$\overline{K}_2$	Constant (see Equation C-20)
$\overline{K}_3$	Constant (see Equation C-20)
$\overline{K}_4$	Constant (see page 99)
$\hat{K}_1$	See Equation C-10b
$\hat{K}_2$	See Equation C-10c
k_{eff}	Ratio of neutrons produced in one generation to previous generation

k_{exs} =	$k_{eff} - 1$
Δk	Voltage relationship (see Equation D-9)
δk, δk_f, δk_c	Small changes in reactivity
ℓ	Prompt neutron lifetime
ℓ^*	ℓ / k_{eff}
L	Length
M	Mass in slugs
m	Mass in pounds
n	Neutron density
n_0	Particular or initial neutron density
δn	Change in neutron density
Q	Charge (electrical)
δq_q	Heat generation in average fuel element
R	Resistance, thermal or electrical
s	Subscript referring to structure
S	Laplace transform variable
t	Time
t	As subscript indicates total
$\hat{t}$	Substitution variable (see Footnote, Equation 24)
t_1	Time at first reactivity reversal
t_2	Time at second reactivity reversal
T_1	Feedback time constant (see Equation C-10a)
T_2	Feedback time constant (see Equation C-14a)
T_3	Feedback time constant (see Equation C-14b)
T_4	Feedback time constant (see Equation C-14c)
δT_f	Change in fuel temperature
δT_c	Change in coolant temperature
U(x)	Substitution variable (see Equation 18)
$\overline{U}$	Over-all heat transfer coefficient
V	Voltage (see Equation D-5)
v	Velocity

x	Substitution variable for fractional reactor power (see Equation 12)
y	Substitution variable for time (see Equation 12)
Z	Subscript indicating a zone
Z_1	Subscript indicating a relation to first time zone
Z_2	Subscript indicating a relation to second time zone
Z_3	Subscript indicating a relation to third time zone
exp	Symbol indicating e to a power
ln	Symbol indicating natural logarithm
α	Constant-relation to step change of reactivity
$\bar{\alpha}$	Relation of neutron density to power
β	Delayed neutron fraction
γ	Reactivity change rate
δ	Constant which sets the zero reactivity point in "log feedback" expression
ρ	Reactivity above base power level k/k_{eff}
ρ_1	Reactivity input to reactor
ρ_2	Reactivity feedback
$\eta(\xi)$	Substitution variable (see Equation 21)
ξ	Substitution variable (see Equation 22)
$\hat{\xi}$	Constant used to simplify switching equation (see Equation 71)
$\bar{\hat{\xi}}$	Constant used to simplify switching equation (see Equation 75)
λ	Decay constant for delayed neutron group
\$	Measurement of reactivity - dollars

BIBLIOGRAPHY

1. L. W. Nordheim, Pile Kinetics, MDD-35 (1946).

2. H. Soodak, "Problems of Reactor Kinetics," Proceedings of Symposia in Applied Mathematics, (Rhode Island, American Mathematical Society, 1961), Vol. XI: Nuclear Reactor Theory, pp 233-255.

3. D. J. Hughes et al., Delayed Neutrons from Fission of U^{235}, Phys. Rev. 73, 111-124 (1948).

4. G. R. Keepin and T. F. Wimett, Reactor Kinetic Functions: A New Evaluation, Nucleonics 16, 86-90 (Oct 1958).

5. R. L. Murray, Nuclear Reactor Physics,(Prentice-Hall, Inc., New Jersey, 1957), p. 148.

6. J. A. Thie, Dynamic Behavior of Boiling Reactors, ANL-5849 (1959).

7. H. B. Smets, "Non-linear Analytical Methods in Nuclear Power Reactor Kinetics," Paper presented at the European Atomic Energy Society Symposium on Reactivity Feedback Mechanisms and Nuclear Reactor Stability, Zurich, Sept, 1961, NP-10722.

8. H. Soodak, Pile Kinetics, Science and Engineering of Nuclear Power, Addison-Wesley Press, Inc., Massachusetts (1949), Vol. II.

9. J. Chernick, The Dependence of Reactor Kinetics on Temperature, BNL-173 (T-30) (Dec 1951).

10. R. S. Margulies, The Combined Effect of Delayed Neutrons and Temperature on Reactor Kinetics, BNL-280 (T-47) (July 1954).

11. W. K. Ergen, Current Status of the Theory of Reactor Dynamics, CF-53-7-137 (July 1953).

12. J. MacPhee, The Kinetics of Circulating Fuel Reactors, Nuclear Science and Engineering, 4, 588 (1958).

13. J. M. Stein, Homogeneous Reactor Experiment Quarterly Report, ORNL-630 (April 1950), p. 23. See also Homogeneous Reactor Experiment Quarterly Report, ORNL-925 (Jan 1951), p. 78 and Homogeneous Reactor Experiment Feasibility Report, ORNL-730 (July 1950), p. 66.

14. H. B. Smets, The Response of a Nuclear Power Reactor to a Linear Reactivity Variation, Nukleonik 1, 351-357 (Dec 1959).

15. H. B. Smets and E. P. Gyftopoulos, The Application of Topological Methods to the Kinetics of Homogeneous Reactors, Nuclear Science and Engineering 6, 341-349 (1959).

16. C. R. Bingham, Kinetics Analysis by Inverse Method Using Reactivity Transform of Power Function, TID-15646 (1961).

17. J. Chernick, A Review of Nonlinear Reactor Dynamics Problems, BNL-6302 (1962).

18. J. J. Syrett, The Variation of Power in a Fast Reactor for a Linear Increase of Reactivity, AERE RP/M47 (1954).

19. E. Kamke, Differentialgleichungen, Edwards Brothers, Inc., (1945), Michigan 2nd ed., Vol. I, p. 26.

20. Reactor Physics Constants, ANL-5800 (1st Edition), p. 29.

A-1. T. R. Bump and H. O. Monson, Some Steady-state Thermal Characteristic of a Three-loop Reactor Power System, ANL-6137 (March 1960).

A-2. Reactor Development Program Progress Report, ANL-6343 (March 1961).

A-3. L. J. Koch, Hazard Summary Report Experimental Breeder Reactor II, ANL-5719 (May 1957).

B-1. L. J. Koch et al., Construction Design of EBR-II: An Integrated, Unmoderated Nuclear Power Plant, Proceedings of the Second International Conference for the Peaceful Uses of Atomic Energy, Geneva, Switzerland, 9, 323 (1958).

B-2. H. A. Bethe, Reactor Safety and Oscillator Tests, APDA-117 (1956).

B-3. L. J. Koch et al., Hazards Summary Report for EBR-II, ANL-5719 (1957).

B-4. J. B. Nims and P. F. Zweifel, Preliminary Report on Sodium Temperature Coefficients in Large Fast Reactors, APDA-135 (Nov 1959).

B-5. S. Yiftah and D. Okrent, Some Physics Calculations on the Performance of Large Fast Breeder Reactors, ANL-6212 (Dec 1960).

B-6. L. J. Koch, EBR-II Dry Critical Experiments (Program), ANL-6299 (Feb 1961).

B-7. R. L. McVean, EBR-II Dry Critical Experiments (Results), ANL-6462 (Feb 1962).

C-1. P. Pezuela, internal memorandum dated Feb 1960.

C-2. T. R. Bump and H. O. Monson, Predicted Dynamic Behavior of EBR-II, Proceedings of the Second United Nations International Conference on Peaceful Uses of Atomic Energy, Geneva, Switzerland, 11, 404 (1958).

C-3. T. R. Bump, Predicted Transfer Functions for EBR-II, internal memorandum dated November 26, 1958.

C-4. H. H. Hummel and L. T. Bryant, Stability of EBR-II, ANL-6484 (Jan 1962).

C-5. T. R. Bump and R. F. Seidensticker, Analysis of Temperatures and Expansion Resulting from Exponential Power Changes in a Reactor, Nuclear Science and Engineering, 4, 44-64 (1958).

C-6. F. Storrer, Temperature Response to Power, Inlet Coolant Temperature and Flow Transients in Solid Fuel Reactors, APDA-132.

C-7. M. P. Appell, Sur les invariants de quelques equations differentielles, Journal de Mathematiques 5, 4 (Serie, 1889).

C-8. L. J. Koch, W. B. Loewenstein, and H. O. Monson, Addendum to Hazard Summary Report Experimental Breeder Reactor II, ANL-5719 (Addendum) p. 134, (June 1962).

D-1. W. Pagel, A Portable Electronic Pile Kinetic Simulator, AIEE Paper No. 51-262, AIEE Transactions 70 (1951).

ACKNOWLEDGMENT

I wish to gratefully acknowledge the help, encouragement, and guidance given to me by the people listed below:

Dr. Philip N. Powers, who was my main thesis advisor.

Drs. Alexander Sesonske, Edward Gamble, Calvin Putnam, and W. G. Smith, who were the Advisory Committee members.

Walter C. Lipinski, the ex-officio ANL member of my advisory committee, for the time and effort spent in discussions and advice associated with this thesis.

Chun Hsu, for the hours spent in discussions dealing with work previously done in the fields of reactor kinetics and reactor kinetics simulation.

William Kann, Charles Michels, and Martin Glass, for their advice and construction of components.

Dr. Henry Thacher and Dorothy Bingaman, for their help with the construction and modifications of the digital programs involved in this analysis.

Irene Tkaczyk, for the care and perseverance in the typing of this manuscript.

Dr. B. I. Spinrad and all other Argonne and AMU employees who have helped make this project possible.